The Thesis Committee for Pável Zuloaga Molero
Certifies that this is the approved version of the following thesis:

Performance Evaluation of CO_2 EOR in Tight Oil Formations with Complex Fracture Geometries

APPROVED BY
SUPERVISING COMMITTEE:

Supervisor:

Kamy Sepehrnoori

Wei Yu

Performance Evaluation of CO_2 EOR in Tight Oil Formations with Complex Fracture Geometries

by

Pável Zuloaga Molero, B.S.E.

Thesis

Presented to the Faculty of the Graduate School of

The University of Texas at Austin

in Partial Fulfillment

of the Requirements

for the Degree of

Master of Science in Engineering

The University of Texas at Austin

May 2016

Dedication

A mis abuelos Eva Báez Peña y Federico Molero Villar

Acknowledgements

I would like to express my sincere gratitude and appreciation to Dr. Kamy Sepehrnoori for his guidance and encouragement during my studies and research at The University of Texas. My deepest gratitude goes also to Dr. Wei Yu for his invaluable support and countless hours of dedication throughout this two years. It was a great privilege for me to receive their mentorship and friendship.

I would also like to thank to Yifei Xu, Dr. Sergio Cavalcante Filho, Dr. Hamid Lashgari and Marut Wantawin for their collaboration and advices during my research. I am especially thankful to all my friends and officemates for the memorable experiences we enjoyed together. I sincerely appreciate their kindness and companionship.

I am extremely grateful to my parents and my family for their encouragement and support in all of my pursuits and for motivating me with their actions.

Finally, I would send my thanks to Pluspetrol Peru Corporation for providing the financial support to attain this degree. I extend my appreciation to my colleagues Marcelo Pomeraniec, Francisco Herrero, Ebert Coronado, David Quispe and William Navarro.

Abstract

Performance Evaluation of CO_2 EOR in Tight Oil Formations with Complex Fracture Geometries

Pável Zuloaga Molero, M.S.E.

The University of Texas at Austin, 2016

Supervisor: Kamy Sepehrnoori

The recent development of tight oil reservoirs has led to an increase in oil production in the past several years due to the progress in horizontal drilling and hydraulic fracturing. However, the oil recovery factor expected is still very low even after the wells have been fractured and therefore, tight formations are considered good candidates for enhanced oil recovery (EOR). One of the most suitable solutions to improve the oil recovery is the carbon dioxide (CO_2)-based EOR. Although the injection of CO_2 is not new for conventional oil reservoirs, its practice in tight oil formations is still a relatively novel idea. Two injection-production strategies are often employed: continuous CO_2 injection or flooding and CO_2 Huff-n-Puff. However, it is not clear which scenario is the best strategy to achieve an optimal recovery, which highly depends on many uncertain reservoir and fracture parameters and it is not clearly understood until recently.

Another challenge of the estimation of the incremental recovery of these injection approaches is to properly model the hydraulic fractures and CO_2 transport mechanism. The actual hydraulic fracturing process often creates complex fracture networks, especially

when the fracture propagates in a formation with a large amount of pre-existing natural fractures.

In this study, the CO_2-EOR effectiveness is simulated and analyzed by comparing the Huff-n-Puff and the continuous injection scenarios. The effect of matrix permeability on the comparison of well performance of these two scenarios was investigated. Subsequently, Design of Experiment and Response Surface Methodology is used to perform sensitivity studies with four uncertain parameters including matrix permeability, number of wells, well pattern, and fracture half-length to determine the best injection approach. In addition, an efficient methodology of embedded discrete fracture model (EDFM) is introduced to explicitly model complex fracture geometries. The effects of complex fracture geometries on well performance of CO_2 Huff-n-Puff and CO_2 continuous injection were also investigated as well as the effect of natural fractures. The analysis of the CO_2-EOR effectiveness confirms that the appropriate modelling of the complex fractures geometry plays a critical role in estimation of the incremental oil recovery. This study provides new insights into a better understanding of the impacts of reservoir permeability, complex hydraulic fractures and natural fractures on well performance during CO_2-EOR process in tight oil reservoirs and in the determination and design of the optimal injection-production scheme to maximize the oil recovery factor for multi-fractured horizontal wells.

Table of Contents

List of Tables

List of Figures

Chapter 1: Introduction

1.1. MOTIVATION

In recent years, the development of unconventional oil reservoirs has played a critical role in the rapid increase in oil production in the United States. As shown in **Figure 1.1**, the tight oil production has constantly increased during the last decade and this trend is expected to continue during the next decades, since most of these resources are still not fully exploited. According to the U.S. Department of Energy, the proved reserves from tight oil reservoirs at the end of year 2014 were 13,365 million of barrels, which represented a 37% of the total oil proved reserves in US (EIA, 2015). Similarly, **Figure 1.2** shows that around the world there is also a significant amount of resources from tight formations.

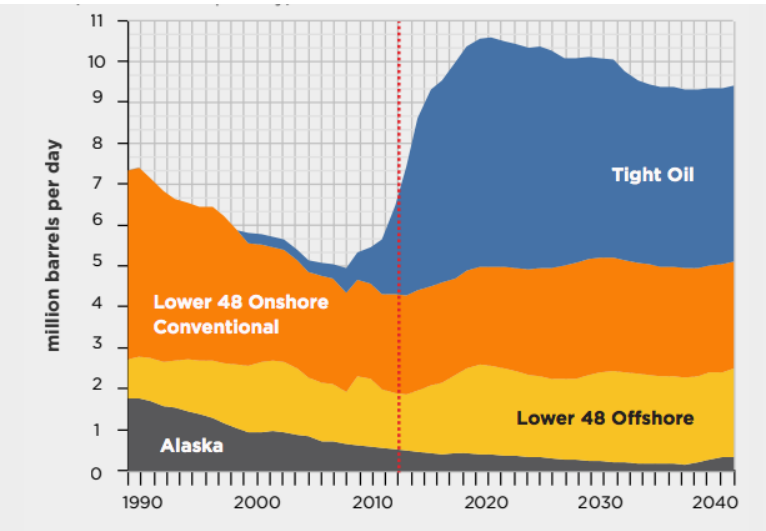

Figure 1.1: US crude oil production in million barrels per day. (EIA Annual Energy Outlook, 2015). http://www.api.org/~/media/apiwebsite/oil-and-natural-gas/primers/us-crude-and-gas-production-by-source.png?la=en

Figure 1.2: Low and high estimates of total shale and tight resources in billions of barrel of oil equivalent (BOE) (Schlumberger Business Consulting, 2013). https://www.sbc.slb.com/~/media/Images/Our%20Ideas/Energy_Perspectives/1st%20Semester%202013/Global/originalsize/Global-Fig-2.ashx

Typically, the tight oil reservoirs are characterized by very low porosity (<10%) and low permeability (<0.1 md) (Sorensen et al., 2015), which are difficult to economically produce without the recent two enabling technologies such as horizontal drilling and hydraulic fracturing. One of the biggest challenges in production of tight oil reservoirs is to achieve an economical operation, maximizing the hydrocarbon recovery and optimizing the production strategy. The primary oil recovery factor is typically below 10% due to the low matrix permeability (Sorensen et al., 2015), resulting in substantial volumes of oil still remain in the underground. It has been reported that a small improvement in oil recovery factor could yield several billion barrels of incremental oil (Hawthorne et al., 2013). This makes these tight-oil wells become good candidates for investigation of enhanced oil recovery (EOR) methods to improve the long-term well productivity.

Carbon dioxide (CO_2) injection has proven to be a feasible method to improve the oil recovery in tight oil reservoirs. It performs better than water flooding due to its favorable injectivity

and the possibility to develop miscible displacement when the injection pressure is larger than the minimum miscibility pressure (MMP). In conventional oil reservoirs, the main physical mechanisms for improving oil recovery by CO_2 injection include oil swelling, oil viscosity reduction, the formation of multiple contact, and miscible mixed CO_2-oil phases (Jarrell et al., 2002).

However, in tight formations, there are many challenges with respect to CO_2 injection due to the nature of low permeability and the complex fracture system, which provides the main path for movement of injected fluid. Two common injection-production scenarios are often utilized in the field to implement the CO_2 injection: continuous CO_2 injection (which will be also referred to as CO_2 flooding in this study) and CO_2 Huff-n-Puff. In the Huff-n-Puff scenario, also known as cyclic injection, the producers are converted temporarily to CO_2 injectors to stimulate the surrounding area of the fractures, after a shut-in period for soaking, these wells are reverted to the producers. This cycle is repeated periodically. In the flooding scenario, or continuous injection, the injectors remain as injectors until the end of production lifetime and the stimulation effect is observed in the surrounding wells. The continuous injection requires to assure the conductive paths between injectors and producers during the lifetime of the project in order to achieve effective flooding process. In tight oil reservoirs, it is challenging to determine the best injection-production strategy, which depends on many uncertain parameters such as matrix permeability, fracture half-length, and well spacing.

Additionally, another challenge in tight oil reservoir simulation is to properly model complex hydraulic fractures. The actual hydraulic fracturing process often creates complex fracture networks, especially when the fracture propagates in a formation with pre-existing natural fractures. However, this complex geometry is not usually captured in the simulation models. Often the fractures are assumed to be planar or orthogonal due to the limitation of local grid refinement (LGR) approach. More flexible methods like the use of unstructured grids can significantly increase the computational demand. However, the embedded discrete fracture model (EDFM) can

efficiently handle complex fracture geometry and it can be used to investigate the effect of the complex fracture geometry on well performance of CO_2 Huff-n-Puff and CO_2 continuous injection for a system of hydraulic fractures. Furthermore, the EDFM approach permits to explicitly model not only complex fracture geometries but also it allows to model the effect of natural fractures on the production performance.

Accordingly, further investigation is required to quantify the best injection-production strategy, i.e. Huff-n-Puff or flooding, to optimize the oil recovery for multi-fractured horizontal wells, and also to evaluate the effects of different fracture geometries and natural fractures on these scenarios.

This study takes the typical reservoir, fluid, and fracture properties from the Bakken Formation in the Williston Basin as reference since it is the largest tight oil play in the United States, with proved reserves of 5,962 million of barrels at December of 2014 (EIA, 2015).

1.2. RESEARCH OBJECTIVES

The general objective of this study is to perform a systematical investigation of multiple uncertain parameters that affect the production performance of the CO_2-based EOR (continuous flooding and Huff-n-Puff) in tight oil formations. The parameters considered in the study were grouped into two sets. The first set includes parameters such as matrix permeability, number of wells, well pattern, and fracture half-length. The second set includes different hydraulic fracture geometries and the presence of natural fractures. The specific objectives of this study can be summarized as follows:

- Develop a compositional numerical model with multiple hydraulic fractures based on the typical fluid and reservoir properties from the Middle Bakken Formation, with an optimum refinement for the modeling of the fractures.

- Use Design of Experiment (DOE) and Response Surface Methodology (RSM) to systematically perform sensitivity studies with four uncertain parameters, including matrix permeability, number of wells, well pattern, and fracture half-length, to investigate the order of influence of each parameter on the comparison between CO_2 flooding scenario and CO_2 Huff-n-Puff scenario.
- Generate diagnostic plots to conveniently identify whether CO_2 flooding or CO_2 Huff-n-Puff has the higher CO_2-EOR effectiveness under different reservoir and fracture conditions.
- Investigate the effects of the complex fracture geometry and the presence of natural fractures on the performance of CO_2 flooding and CO_2 Huff-n-Puff.

1.3. THESIS OUTLINE

This thesis consists of six chapters. The first chapter introduces the research, explains its motivation and presents its objectives. Chapter 2 discusses the literature review related to this study. It reviews both experimental and simulation studies for investigation of well performance using continuous CO_2 injection and CO_2 Huff-n-Puff.

Chapter 3 presents the implementation of the simulation model, the description of both CO_2 injection scenarios, the Design of Experiment, the Sensitivity Analysis to the parameters affecting the performance of both scenarios aforementioned and the assessment of the Response Surface for the comparison of the best injection approach.

Chapter 4 describes the modelling of complex fracture geometries using EDFM and the study of the effects of the fracture geometry and the natural fractures on the performance of the CO_2-based EOR.

Finally, Chapter 5 summarizes the results for this research and presents the conclusions as well as recommendations for the future work.

Chapter 2: Literature Review

Recently, the CO_2 Huff-n-Puff process has received more attention in the literature, because it is considered as one of the most effective treatments for low permeability formations. The CO_2 Huff-n-Puff is a single-well process, so well-to-well connectivity is not required as the hydraulic and natural fractures provide a large contact area for CO_2 to diffuse into the low-permeability matrix to increase the oil recovery. In addition, many experimental works have been conducted to evaluate the performance of CO_2 injection in the core plugs.

Kovscek et al. (2008) performed a series of experiments with CO_2 injection in shale core samples with permeability values in the range of 0.02 to 1.3 md. The experiments were performed for immiscible and near miscible conditions and two gas injection modes were used: in the first one, described as countercurrent flow, only one face is used to inject the CO_2 and to produce the oil, simulating the diffusive process that happens in the fracture face. In the second mode (cocurrent injection), the CO_2 is injected in one face and the oil is collected in the opposite face, simulating the continuous flooding process. The results have shown a higher total recovery for the near miscible test, which achieves an incremental oil recovery of 25% for the countercurrent injection and 10% for the cocurrent injection.

Song and Yang (2013) used core plugs with permeability ranging from 0.27 to 0.83 md to reproduce the Huff-n-Puff process for immiscible conditions, near miscible and miscible conditions. The authors concluded that the miscible and near miscible injection produce almost the same incremental oil recovery, illustrating that injection at a pressure above the MMP does not significantly improve the oil recovery. In addition, they found that the soaking time will not further increase the ultimate recovery after a critical time.

Alharthy et al. (2015) conducted the laboratory experiments to evaluate the incremental oil recovery using the Huff-n-Puff process. The cores are from Middle Bakken and Lower Bakken Formation with permeability in the range of 0.002 to 0.04 md. The experimental results reached a

total recovery of 95% for the Middle Bakken while 32% for the Lower Bakken. The results show that the primary physical production mechanism of CO_2 injection is the miscible oil extraction through the matrix-fracture interface.

On the other hand, several simulation studies have been done to evaluate the potential of CO_2 injection at the field scale. Song and Yang (2013) built a numerical model for a tight oil formation to evaluate the water-alternating-gas (WAG) flooding and the CO_2 Huff-n-Puff scheme, which includes one month of CO_2 injection, 15 days of CO_2 soaking, and six months of back production. The simulation results show that the WAG scheme produces a higher oil recovery than the Huff-n-Puff scheme because the Huff-n-Puff process only affects a limited region nearby the wellbore. However, the physical mechanism of CO_2 molecular diffusion was not considered in the numerical model.

Yu et al. (2014, 2015) built a numerical reservoir model by including multiple hydraulic fractures for the Bakken Formation to simulate the CO_2 Huff-n-Puff process. The authors concluded that the CO_2 molecular diffusion effect is an important physical mechanism to improve oil recovery in the formation with low permeability and pointed out that this effect should be correctly implemented in the numerical model.

Sánchez Rivera (2014) developed a simulation model to extensively study the main parameters that affect the CO_2 Huff-n-Puff process for the Bakken Formation. This study analyzed several values of CO_2 molecular diffusion coefficient and concluded that the values proposed by Yu et al. (2014) are the most suitable. However, the continuous injection was not studied because it was thought that it might not be the best approach to enhance recovery from tight reservoirs due to the long propagation time of the injection fluid caused by the low permeability.

Alharthy et al. (2015) also performed simulation studies to evaluate the CO_2 Huff-n-Puff process in the Bakken Formation. The model uses matrix permeability of 0.0005 md, fracture half-length of 180 ft and fracture conductivity of 100 md-ft. The incremental recovery was in the range

of 3.3% to 5.1%. The authors concluded that long soaking time yields only a small additional oil recovery and the soaking process is more effective when fracture spacing is shorter since closer fracture spacing creates more macro fractures and a greater total surface area. However, the effect of uncertainties in matrix permeability and fracture half-length on well performance of CO_2 injection was not investigated.

Regarding the simulation studies that attempted to compare the different CO_2 injection scenarios, Wang et al. (2010) built a numerical model with a unique set of permeability in the range of 0.04 md and 2.5 md to compare CO_2 flooding and Huff-n-Puff scenarios and presented that CO_2 flooding has a better performance. However, the model did not consider the CO_2 molecular diffusion mechanism and no further sensitivity analysis was performed to study the influences of well and fracture configurations. Another limitation of the model is that it did not explicitly model multiple transverse hydraulic fractures.

Hoffman and Shoaib (2014) used a numerical reservoir simulation to evaluate different EOR strategies to develop the Middle Bakken Formation, including CO_2 flooding and cyclic injection. The range of permeability in the evaluated zone was between 0.01 to 0.04 md. The study indicates that the CO_2 flooding using horizontal wells is the best method to increase the production and can lead to an incremental oil recovery of 16% after 18 years, while the cyclic injection only leads to an incremental recovery of 1%. Nonetheless, the model did not explicitly handle hydraulic fractures and ignored CO_2 molecular diffusion effect.

Wan et al. (2014) performed comparative studies of both injection approaches using a compositional simulation under the same pore volume injected. The model used a matrix permeability of 0.0003 md and the results show that the Huff-n-Puff scenario performs better than the flooding scenario because there is no good communication between multiple wells. However, the authors did not provide an effective range of matrix permeability and well spacing to make a reliable comparison between two injection scenarios. To date, the comparison of well performance

between these two approaches has not been investigated clearly and systematically. In addition, most of these studies do not comprehensively consider the influences of many uncertain reservoir and fracture properties. Consequently, the goal of this study is to determine which CO_2 injection scenario is more suitable under what reservoir and fracture properties for enhanced oil recovery in tight oil reservoirs.

The accurate modeling CO_2-EOR process in tight oil reservoirs is also very challenging. The actual hydraulic fracturing treatment often creates complex fracture networks through opening and interconnecting the pre-existing natural fractures. The fracture diagnostic technologies like microseismic (Fisher et al. 2004; Warpinski et al. 2009; Maxwell, et al., 2013) and the recent developed fracture propagation models (Wu et al., 2012; Xu and Wong, 2013; Wu and Olson, 2015) indicate that the fracture geometry is complex and non-planar.

Although many efforts in the literature are dedicated to modeling CO_2-EOR in tight oil reservoirs (Hoffman and Shoaib, 2014; Wan et al., 2014; Sánchez Rivera, 2014; Alharthy et al., 2015), they made an assumption of simple bi-wing planar fracture geometry without considering the more-realistic complex fracture geometry. Even though the complex fracture networks provide the primary conduits for oil production, they might be detrimental to CO_2-EOR effectiveness (Jarrell et al., 2002). This is because of early CO_2 breakthrough and poor sweep efficiency during CO_2 flooding. CO_2 Huff-n-Puff operation might overcome this issue. Hence, more studies are required to understand this operation in detail. Based on our knowledge, there are no published studies to date that focused on modeling complex fracture networks and natural fractures explicitly and investigating their effects on the CO_2-EOR effectiveness in multiple horizontal wells.

Numerical modeling of well performance from tight oil reservoirs based on explicitly handling the complex fracture networks remains a challenging topic. Although significant attempts have been focused on developing unstructured grids method to model the complex fracture networks (Hoteit and Firoozabadi 2006; Hui et al. 2013), it is still limited in field-scale application

due to its complexity in gridding and large computational demand, especially in simulation of CO_2-EOR process using compositional numerical model with multiple components.

Accordingly, an efficient approach to simulate CO_2-EOR process from tight oil reservoir with complex fracture geometry is still lacking in the petroleum industry. In this study, we introduced an embedded discrete fracture model (EDFM), which was originally proposed by Li and Lee (2008). Further extensions have been done by Moinfar et al. (2014) and Cavalcante Filho et al. (2015). Based on the EDFM, we can modify compositional reservoir simulator in a non-intrusive manner to accurately and efficiently handle the complex fracture geometry (Xu, 2015).

Chapter 3: Performance Evaluation of CO_2 Huff-n-Puff and Continuous CO_2 Injection in Tight Oil Reservoirs

In this study, we built a field-scale numerical reservoir model including two horizontal wells with multiple hydraulic fractures based on the typical fluid and reservoir properties from the Middle Bakken Formation. First, we performed a sensitivity analysis to the number of local grid refinement (LGR) and the number of vertical layers to determine the optimum numbers of LGR cells and layers to accurately model hydraulic fractures without significantly increasing the computational cost. Then, we compared the well performance between CO_2 flooding scenario and CO_2 Huff-n-Puff scenario under the same total CO_2 injected volume. We examined the impact of matrix permeability from 0.001 md to 0.1 md. After that, we expanded the model size from half-section (1 mile × 0.5 mile) including 2 wells to full-section (1 mile × 1 mile) which can handle 4, 6, and 8 wells. Based on the expanded model, we employed Design of Experiment (DOE) and Response Surface Methodology (RSM) to systematically perform sensitivity studies with four uncertain parameters, including matrix permeability, number of wells, well pattern, and fracture half-length, to investigate the order of influence of each parameter on the comparison between CO_2 flooding scenario and CO_2 Huff-n-Puff scenario.

In addition, we built two response surface models in terms of the incremental oil recovery factor on the basis of variables of matrix permeability, number of wells, and fracture half-length. Finally, we generated diagnostic contour plots, which can easily identify which zone has a better well performance for different CO_2 injection scenarios in the short and long term. This work can provide a quantitative assessment of which CO_2 injection scenario is the most suitable for enhanced oil recovery in tight oil reservoirs under various conditions.

3.1. RESERVOIR MODEL

Based on the typical reservoir and fracture properties from the Middle Bakken Formation, we built a field-scale reservoir model using a numerical compositional reservoir simulator (CMG-GEM, 2015). The 3D Cartesian grid system was used, which consists of 262 grids in *x* direction,

134 grids in *y* direction, and 1 grid in *z* direction. Totally, the model has 35,108 grids. The dimension of the reservoir model is 5,240 ft × 2,680 ft × 40 ft, which corresponds to length, width, and thickness, respectively. It covered an area of approximately half section. Two horizontal wells with the lateral length of 4,140 ft and well spacing of 1,320 ft were incorporated in the model. Each horizontal well has 6 hydraulic fracturing stages and each stage has 4 perforation clusters. The total number of effective hydraulic fracture is 24 for each well. The local grid refinement (LGR) approach was utilized to model hydraulic fracture explicitly, which can accurately capture the fluid transport behavior from shale matrix to fracture (Rubin, 2010), as shown in **Figure 3.1**. The fracture grid has a small fracture width but a large permeability.

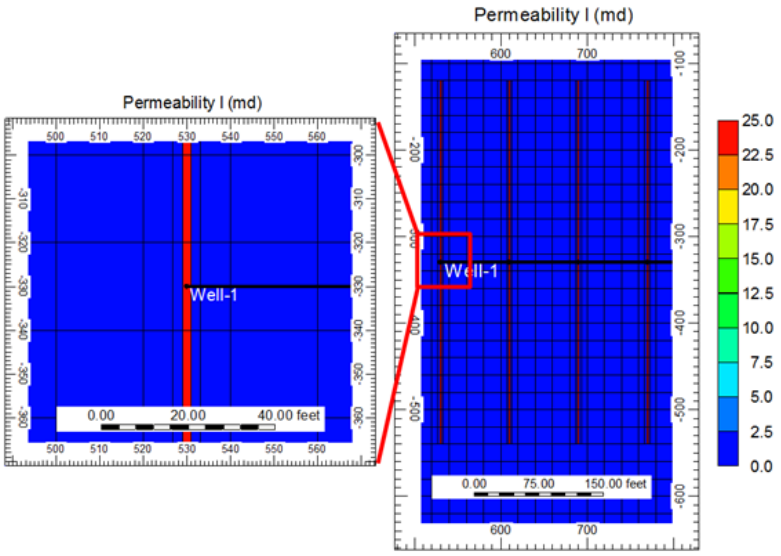

(a) Enlarged zone with LGR used to model hydraulic fracture

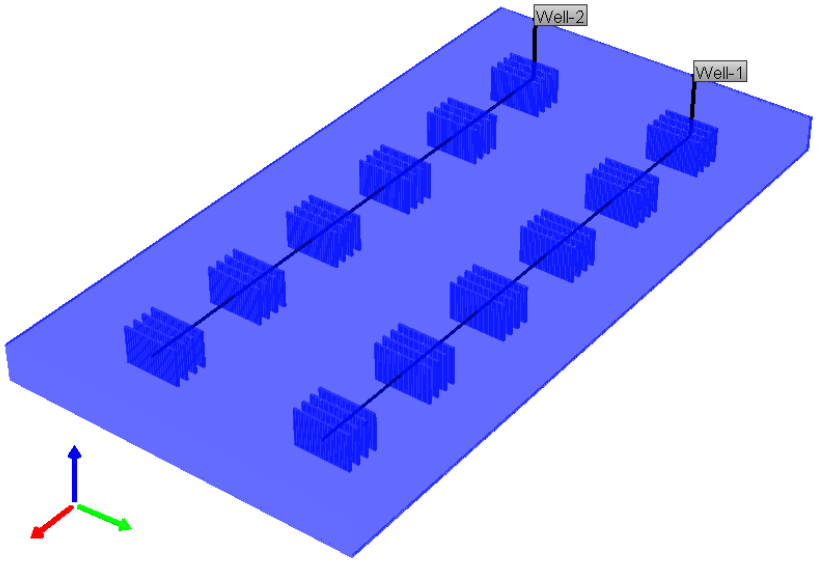

(b) A 3D model including two horizontal wells

Figure 3.1: A schematic of 3D reservoir model with two horizontal wells and multiple hydraulic fractures.

Table 3.1 summarizes a typical reservoir and fracture properties from the Middle Bakken Formation used in the numerical model. The bottomhole pressure (BHP) was set to above or close

to the MMP to achieve the miscible condition during the whole simulation period. If the miscible condition is not achieved, the CO_2 Huff-n-Puff scenario will show a poor performance because the presence of multiphase flow results in a decrease in relative permeability of oil. The relative permeability curves including the water-oil relative permeability and liquid-gas relative permeability are from our previous study (Yu et al., 2014), which were generated based on history matching with a field production well from the Middle Bakken Formation. The Sigmund method was used to model the important physical mechanism of CO_2 molecular diffusion (Sigmund, 1976; Sigmund et al., 1984). More details about the CO_2 molecular diffusion effect can be found in the work by Yu et al. (2015). The CO_2 molecular diffusion coefficient in the oil phase was set at 0.001 cm^2/s in this study.

Parameter	Value	Unit
Grid block dimensions ($x \times y \times z$)	20 × 20 × 40	ft
Initial reservoir pressure	8,000	psi
Reservoir temperature	240	°F
Reservoir thickness	40	ft
Matrix porosity	7%	-
Matrix permeability	0.1	md
Initial oil saturation	75%	-
Initial water saturation	25%	-
Fracture half-length	210	ft
Fracture conductivity	50	md-ft

Table 3.1: Typical reservoir and fracture properties from the Middle Bakken Formation.

3.1.1 Fluid properties and EOS model

There is less information available in the literature about the composition data for the Middle Bakken Formation. Hence, in this study, we divided the crude oil into seven pseudo components according to the study of crude oil composition for the Middle Bakken Formation by Yu et al. (2015), i.e., CO_2, N_2, CH_4, C_2-C_4, C_5-C_7, C_8-C_9, C_{10+}, and their corresponding molar

fractions are 0.02%, 0.04%, 25%, 22%, 20%, 13%, and 19.94%, respectively. The primary oil properties such as bubble point, oil gravity, oil viscosity, oil density, and oil formation factor were calculated using CMG-WinProp (CMG-WinProp, 2015) based on the above compositions and were listed in **Table 3.2**. It is important to point out that these oil properties are within the reasonable range of typical oil properties from the Middle Bakken Formation reported in the scientific literature (Nojabaei et al., 2013; Kurtoglu et al., 2013). In addition, the MMP was calculated as 2,400 psi.

Parameter	Value	Unit
Bubble point pressure	2,968	psi
Oil gravity	42	°API
Oil viscosity at 8,000 psi	1.4	cp
Oil viscosity at bubble point	0.36	cp
Oil density at bubble point	42.7	lb/ft3
Oil formation factor at bubble point	1.33	bbl/STB

Table 3.2: Primary oil properties calculated based on seven pseudo components for the Middle Bakken Formation.

3.1.2 Computational Domain

The reservoir model covers half section (0.5 mile × 1 mile). For the first part of the study 4 wells were considered, and all of them are horizontal wells with 24 fractures grouped in 6 stages of 4 fractures each one. **Figure 3.2** shows a scheme of the well and fractures used in this model.

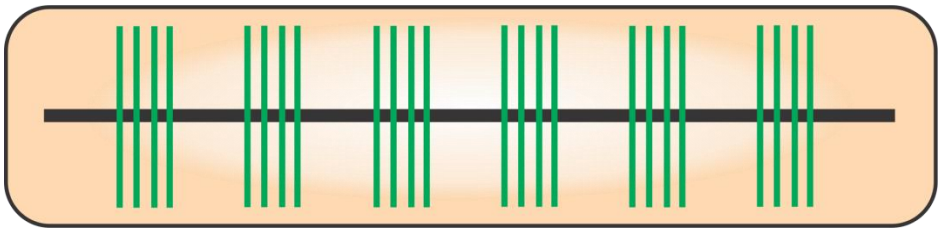

Figure 3.2: Well and fracture scheme.

The number of wells is always even, as half of them will be converted to injectors in the flooding cases.

Sensitivity analysis of LGR-grid size.

In order to avoid the numerical dispersion effect induced by modeling hydraulic fractures using the LGR approach, we performed sensitivity studies on the number of refined cells around the fracture ranging from 3 to 7 based on CO_2 Huff-n-Puff scenario, as shown in **Figure 3.3**. It can be seen that the LGR with 5 cells has the similar simulation results with the LGR with 7 cells, so the LGR-grid size with 5 cells is enough to mitigate the numerical dispersion effect, which was used in the following simulation studies.

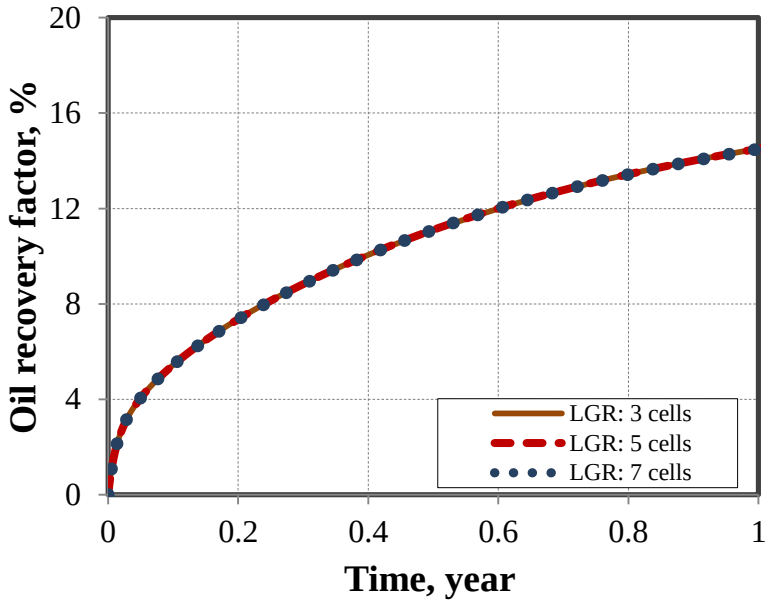

(a) First year of production

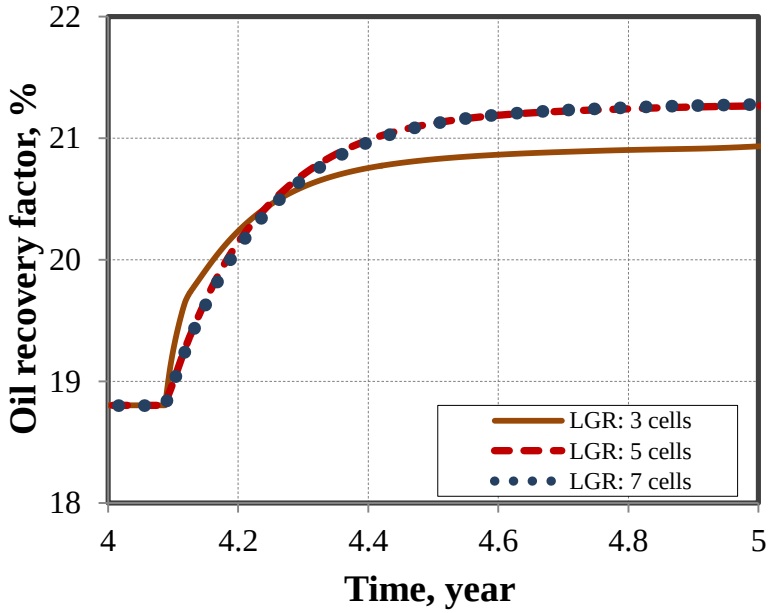

(b) Fifth year of production

Figure 3.3: Sensitivity analysis of the effect of LGR-grid size on well performance for CO_2 Huff-n-Puff scenario.

It is important to mention that a pseudo fracture with a width of 2 ft has been used to represent the actual fracture with a width of 0.01 ft. This pseudo fracture uses an effective fracture

permeability that has been reduced based on the ratio of the actual fracture width and the pseudo fracture width under the assumption of equal fracture conductivity.

Sensitivity analysis of vertical layering.

With respect to the vertical layering, Ghaderi et al. (2012) has pointed out that there is an important segregation effect when CO_2 is injected into an oil formation. To evaluate the impact of segregation, we performed two case studies based on the CO_2 flooding with different vertical layering: one with single layer and another one with five layers. **Figure 3.4** presents the comparison results of well performance, illustrating that there is a very small difference between the single layer and multiple layers in this study. Considering the lower computational efficiency of the multiple layer model, the single layer model is selected in the following simulation studies.

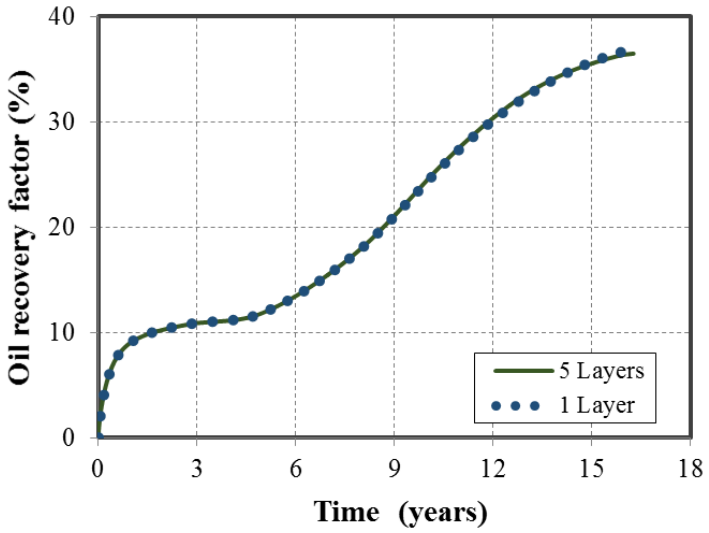

Figure 3.4: Sensitivity analysis of the number of vertical layers on well performance for the entire production lifetime.

CO_2 Diffusion

The CO_2 diffusion has been proved to have a high impact in the recovery of the process of CO_2 Huff-and-Puff, especially for low values of permeability, as it has been described by Yu (2015). **Figure 3.5** shows his results for the differences in Oil Recovery factor when the CO_2

diffusion coefficient is used. For this study a value of 0.001 cm^2/s has been used for the CO_2 diffusion in both gas and oil phases.

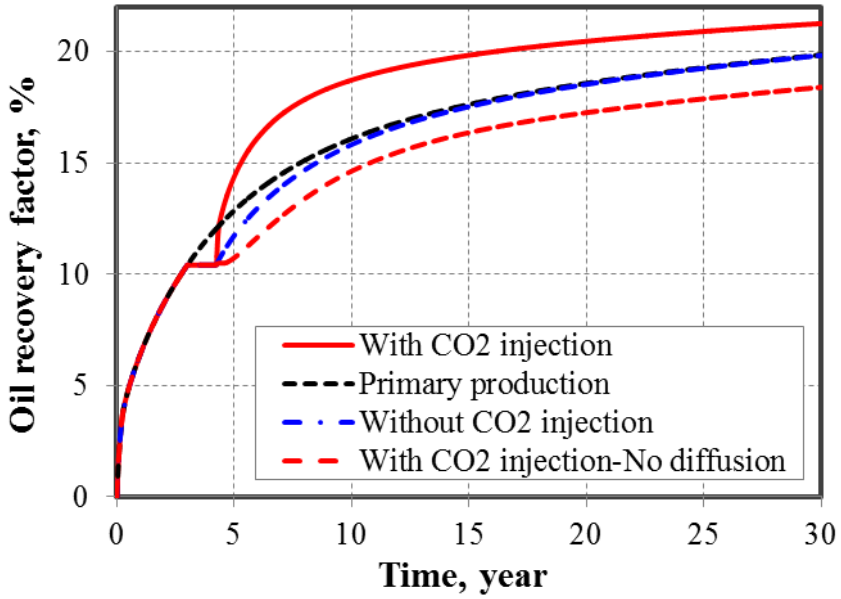

Figure 3.5: Effect of CO_2 diffusion in Oil Recovery Factor. (Yu, 2015)

3.1.3 Production and Injection Scenarios

We performed three case studies to compare the well performance between CO_2 flooding scenario and CO_2 Huff-n-Puff scenario:

- Base case: two wells are only under primary production without CO_2 injection.
- CO_2 flooding scenario: one well is converted to CO_2 injector after a period of primary production, as shown in **Figure 3.6**.
- CO_2 Huff-n-Puff scenario: two wells will experience three cycles of Huff-n-Puff and each cycle includes three stages after a period of primary production: CO_2 injection, followed by CO_2 soaking, and then back production, as shown in **Figure 3.7**.

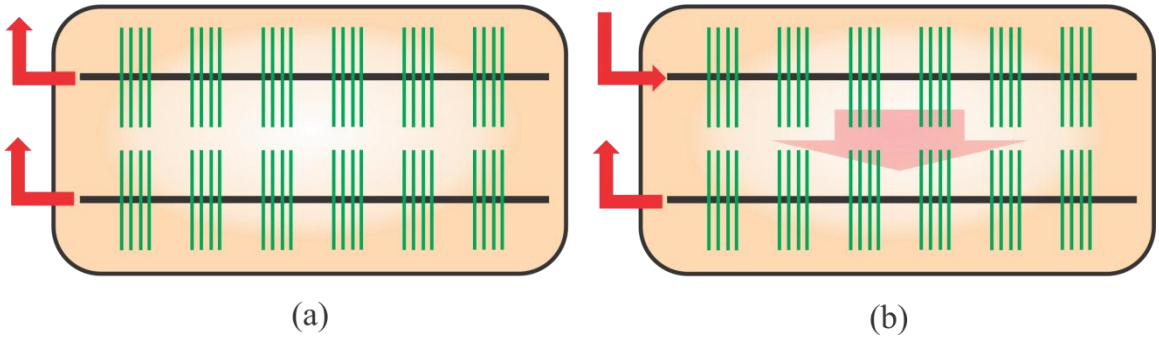

Figure 3.6: CO_2 flooding scenario with two horizontal wells and production sequence: Primary production: 3 years. CO_2 flooding and EOR production: 15 Years.

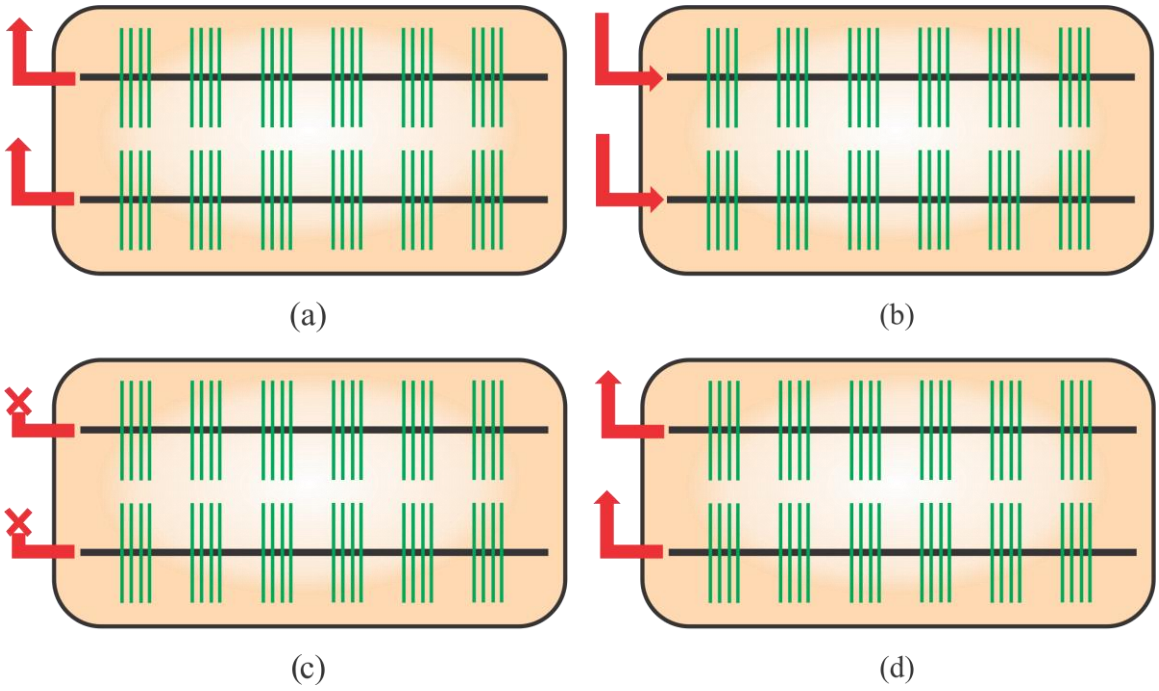

Figure 3.7: CO_2 Huff-n-Puff scenario with two horizontal wells and sequence of each cycle of Huff-n-Puff includes three stages, after the primary production: CO_2 injection, CO_2 soaking, and back production.

Figure 3.8 presents the detailed time schedule of primary production and CO_2 injection for two wells of these three cases. The total simulation time for each case is 18 years. The primary production time is 3 years for both CO_2 flooding and Huff-n-Puff scenarios. For the CO_2 flooding scenario, after the primary production period, one well is changed to CO_2 injector and another well remains producing until the end of simulation. For the CO_2 Huff-n-Puff scenario, after the primary

production period, three cycles of CO_2 injection, CO_2 soaking and back production are considered. Additionally, for each cycle, CO_2 injection time is one year, CO_2 soaking time is one month, and back production time is 47 months. Hence, the total time is 5 years for each cycle period.

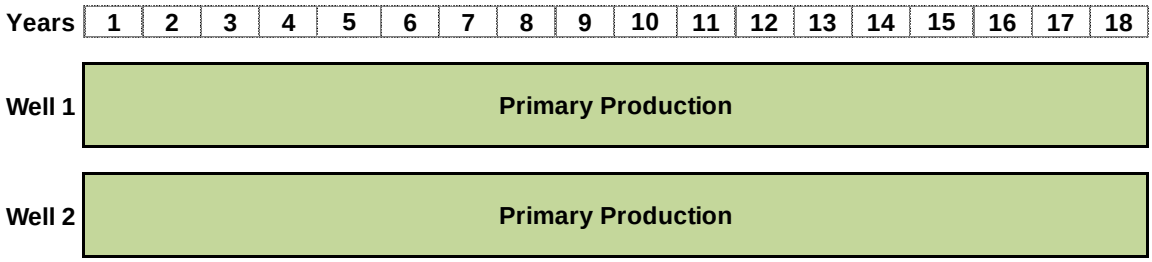

(a) Base case

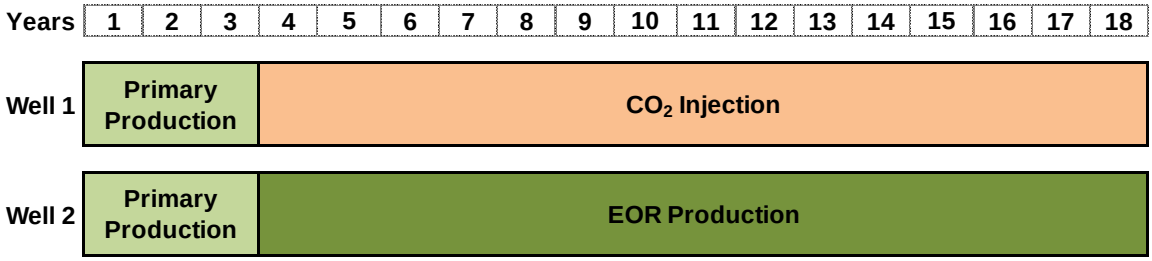

(b) CO_2 flooding scenario

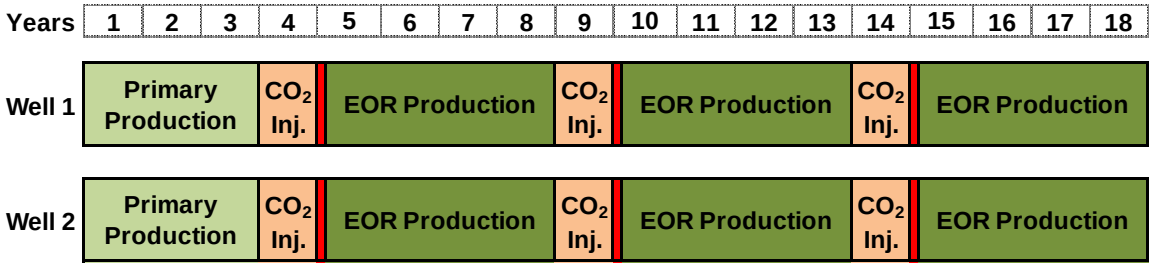

(c) CO_2 Huff-n-Puff scenario (the red bar represents CO_2 soaking)

Figure 3.8: Detailed time schedule for three case studies with the total simulation time of 18 years.

In order to make an appropriate comparison between the CO_2 flooding scenario and the CO_2 Huff-n-Puff scenario, we keep the total CO_2 injected volume the same, which is 5,475

MMSCF. Correspondingly, we have different CO_2 injection rate for each case due to the different injection time and injection wells, as shown in **Table 3.3**. **Figure 3.9** shows the path of cumulative CO_2 injected volume for both scenarios, illustrating that the final cumulative volume is exactly the same.

	Total Daily Injection Rate (MSCF/day)	
Year	CO_2 Huff-n-Puff	CO_2 Flooding
1	-	-
2	-	-
3	-	-
4	5,000	1,000
5	-	1,000
6	-	1,000
7	-	1,000
8	-	1,000
9	5,000	1,000
10	-	1,000
11	-	1,000
12	-	1,000
13	-	1,000
14	5,000	1,000
15	-	1,000
16	-	1,000
17	-	1,000
18		1,000
Injected Volume (MMSCF)	5,475	5,475

Table 3.3: Detailed CO_2 injection rate schedule for the CO_2 flooding and CO_2 Huff-n-Puff scenarios.

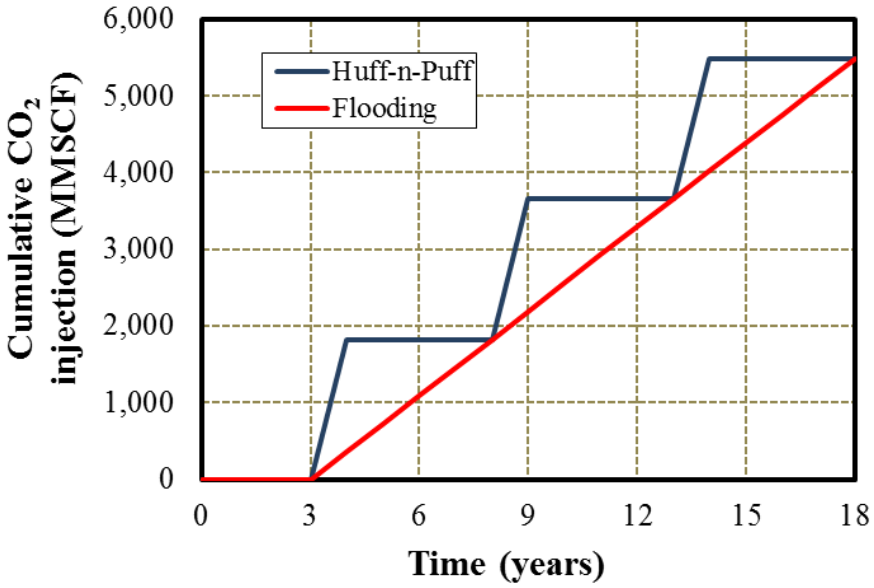

Figure 3.9: Comparison of cumulative CO_2 injection volume between the CO_2 flooding and CO_2 Huff-n-Puff scenarios, showing the same final cumulative injection volume after 18 years.

Production Constraints

The BHP was used as primary constraint for the production. The value of BHP was set based on the criteria of achieving the miscible CO_2 injection condition and also trying to reach a reasonable recovery factor. A high BHP pressure will not allow to reach recover enough oil during the primary production; but on the other hand a low value of BHP will not lead to an effective injection, especially for Huff-and-Puff, because the injection will be below the MMP and the flow will decrease because of two-phase flow effects.

The MMP calculated in this study is 2,400 psi. According to Dong et al. (2011), a pressure of 290 psi (2 MPa) lower than MMP is generally considered as the near-miscible condition. In addition, Song (2013) mentioned that the near-miscible CO_2 injection condition has a similar oil recovery as the miscible condition and a further increase in pressure does not result in an additional oil recovery. In this case study, the BHP of 1,800 psi was used as production constraint in the simulation model. Although it is less than the MMP, the miscible condition can be quickly achieved after a short period of CO_2 injection, i.e., between one and two months for both scenarios.

Soaking time

The soaking time has a small effect on the recovery factor in the long term. For this study, several length of soak phase has been tested for Huff-and-Puff cases. **Figure 3.10** shows the curves of oil recovery for periods of soaking time ranging from 2 weeks to 6 months. As can be seen, the results in the long term are practically the same. The case with 6 months of soaking time show higher production during the first months, but the recovery in general is the same because the well has no production during the months in soak phase.

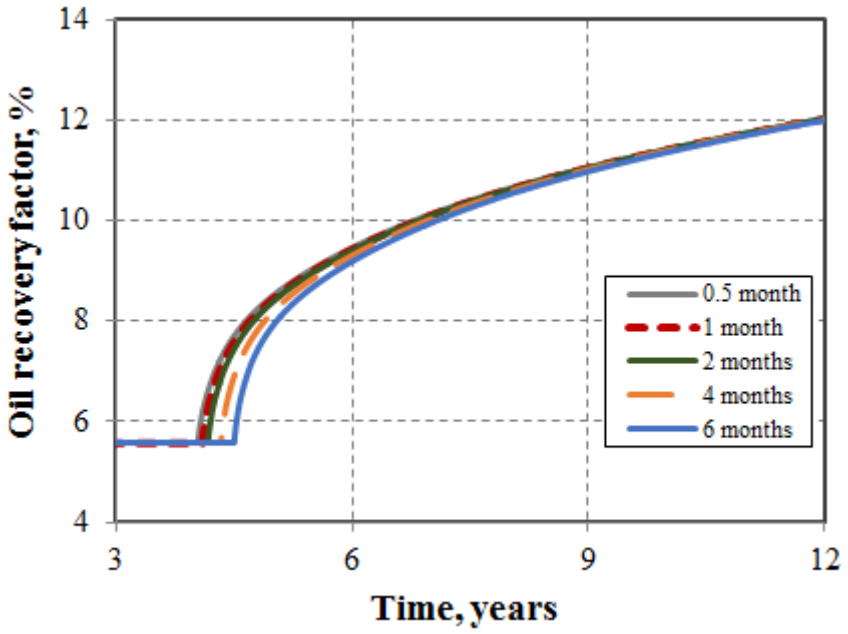

Figure 3.10: Effect of soaking time in Oil Recovery Factor for Huff-and-Puff

3.2. EFFECT OF MATRIX PERMEABILITY IN CO_2 HUFF-AND-PUFF AND CO_2 FLOODING.

In order to analyze the effect of matrix permeability on the performance of CO_2 Huff-and-Puff and CO_2 flooding, we used the model described in the previous sections to perform several simulations varying the values of permeability accordingly. Three scenarios were evaluated: (a) a base case with only primary production, (b) primary production followed by three cycles of CO_2 Huff-and-Puff, and (c) primary production followed by a CO_2 continuous flooding. These

scenarios were evaluated for three permeability values which are in the typical range of tight oil formations: 0.1 md (higher case), 0.01md (medium case) and 0.001md (lower case).

3.2.1 Simulation Results

Three different matrix permeabilities were studied to investigate the CO_2-EOR effectiveness: 0.001 md, 0.01 md, and 0.1 md, as shown in **Figures 3.11**, **3.12** and **3.14**, respectively.

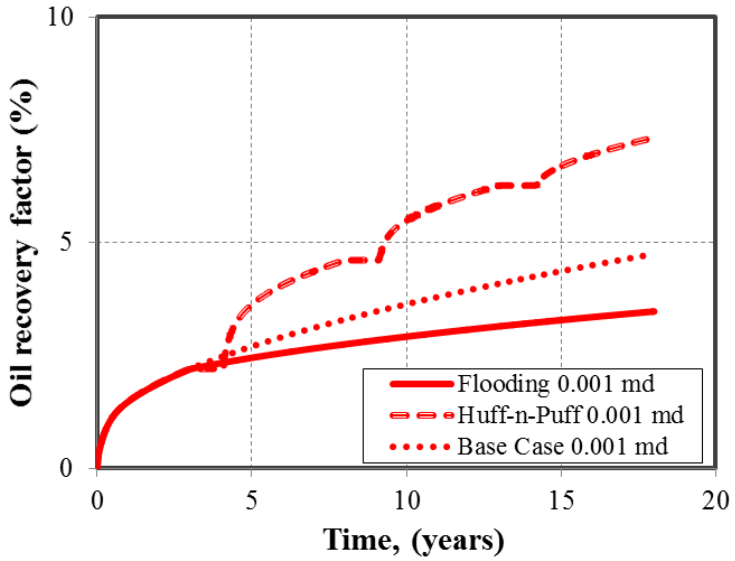

Figure 3.11: Effect of permeability on the comparison of CO_2-EOR effectiveness along the production lifetime for low permeability of 0.001 md.

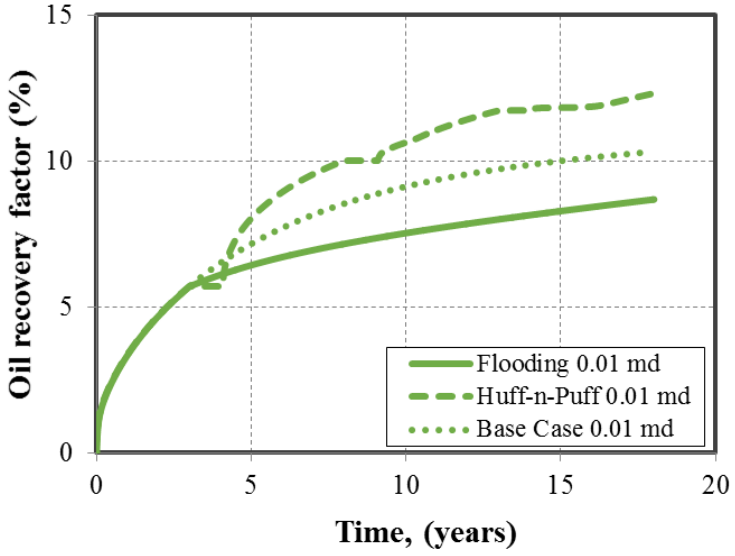

Figure 3.12: Effect of permeability on the comparison of CO_2-EOR effectiveness along the production lifetime for medium permeability of 0.01 md.

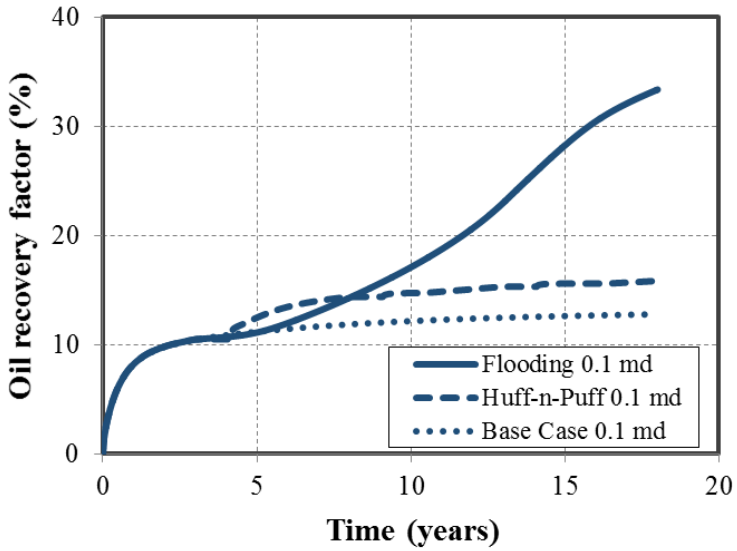

Figure 3.13: Effect of permeability on the comparison of CO_2-EOR effectiveness along the production lifetime for high permeability of 0.1 md.

3.2.2 Discussion

It can be seen that the CO_2 Huff-n-Puff scenario always increases the oil recovery factor compared to the base case and larger incremental recoveries are observed for the lower permeability cases. The incremental oil recovery factors are 3%, 2%, and 1.3% at the end of simulation corresponding to 0.1 md, 0.01 md, and 0.001 md, respectively. The CO_2 flooding scenario only increases the oil recovery factor for the high permeability of 0.1 md while decreases the oil recovery factor for the permeabilities of 0.01 md and 0.001 md. This is due to the fact that only one well is in production, and that the CO_2 injection did not reach the production well due to low permeability, even after 15 year of continuous injection. The injected CO_2 is only concentrated nearby the injection well. However, for the high permeability of 0.1 md, the CO_2 flooding scenario shows a significant increase of oil recovery factor in 20.5% at the end of simulation, which is much larger than the CO_2 Huff-n-Puff scenario.

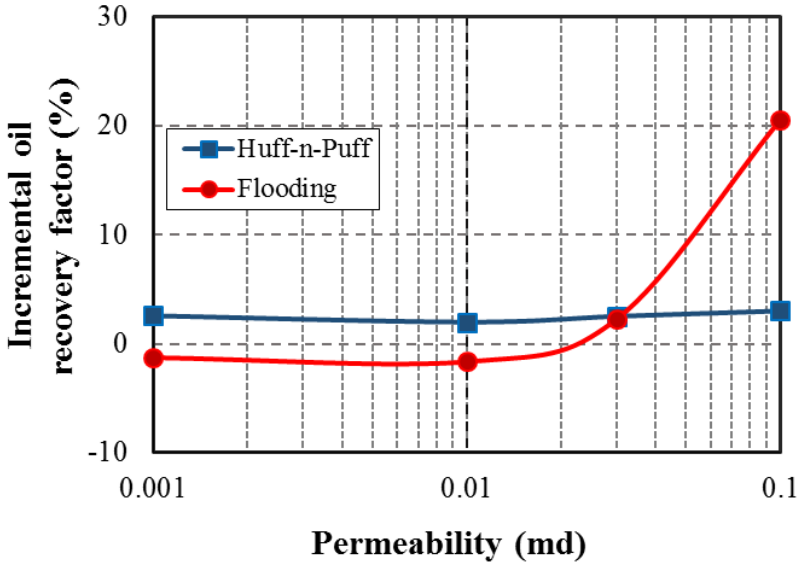

Figure 3.14: Comparison of incremental oil recovery factor between CO_2 flooding and CO_2 Huff-n-Puff for the range of permeability from 0.001 md to 0.1 md.

Figure 3.14 compares the incremental oil recovery factor between CO_2 flooding and Huff-n-Puff scenarios, which was calculated by subtracting the oil recovery factor of base case without CO_2 injection from that of CO_2-EOR scenarios. It is important to note that an additional intermediate case with permeability of 0.03 md was considered in order to identify the intersection point of both curves. As shown, the incremental recovery factor for CO_2 flooding is much more sensitive to the permeability change. The intersection of these two lines represents the critical value of permeability that leads to the same oil recovery factor for both scenarios of injection, which is around 0.03 md in this case study. The intersection point can also be regarded as the lower limit of permeability under which the CO_2 flooding scenario has a better CO_2-EOR effectiveness than the CO_2 Huff-n-Puff scenario. For the values of permeability lower than this critical value, the CO_2 Huff-n-Puff will always be a preferable choice for improving oil recovery.

The performance of CO_2 is strongly influenced by the breakthrough time of the CO_2 injected. This is a function of permeability but it is also affected by other parameters such as the distance between the wells and the fractures. Consequently, the next section in this study is intended to systematically analyze the effect of other parameters such as fracture half-length, well

spacing and pattern of fractures, on the incremental recovery and the performance of the two injection approaches.

3.3. SENSITIVITY STUDY USING DESIGN OF EXPERIMENT AND RESPONSE SURFACE METHODOLOGY

It is important to understand how the incremental oil recovery and the limits of good CO_2-EOR performance for both injections scenarios are affected by the uncertain parameters. In the following study, we employ Design of Experiment (DOE) and Response Surface Methodology (RSM) to perform a sensitivity study, which is a statistical and effective approach to determine the relationship between uncertain factors and the response function (Myers et al., 2008). It has been widely used in unconventional oil and gas reservoirs to quantify the key reservoir and fracture properties affecting the well performance (Yu and Sepehrnoori, 2014). In addition, the DOE is very flexible to deal with both continuous and categorical variables.

3.3.1 Parameters considered for the Design of Experiment

In order to systematically compare the well performance of two different CO_2 injection scenarios, four uncertain parameters including matrix permeability, number of wells, well pattern, and fracture half-length are considered.

Fracture pattern

Two patterns were considered for this part of the study. The first pattern considers the fractures stages in one well aligned with the fractures in the adjacent wells. The second considers a zipper pattern, as shown in **Figure 3.15**.

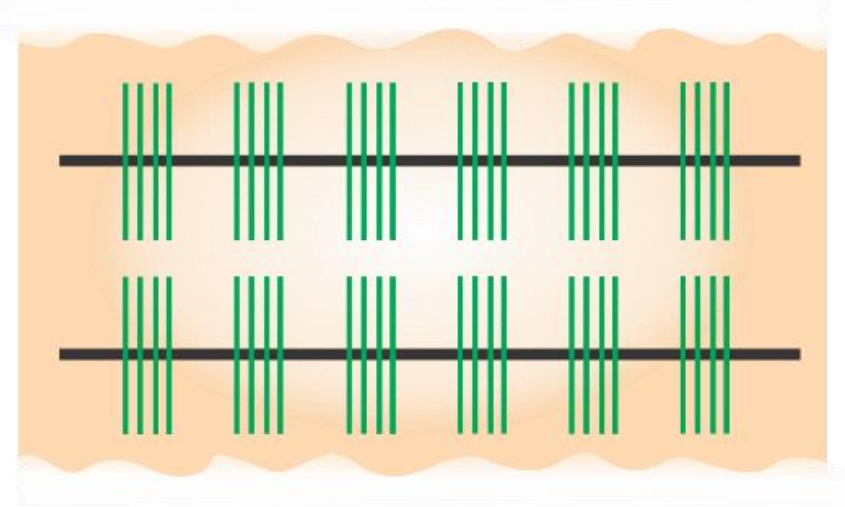

(a) Aligned well pattern

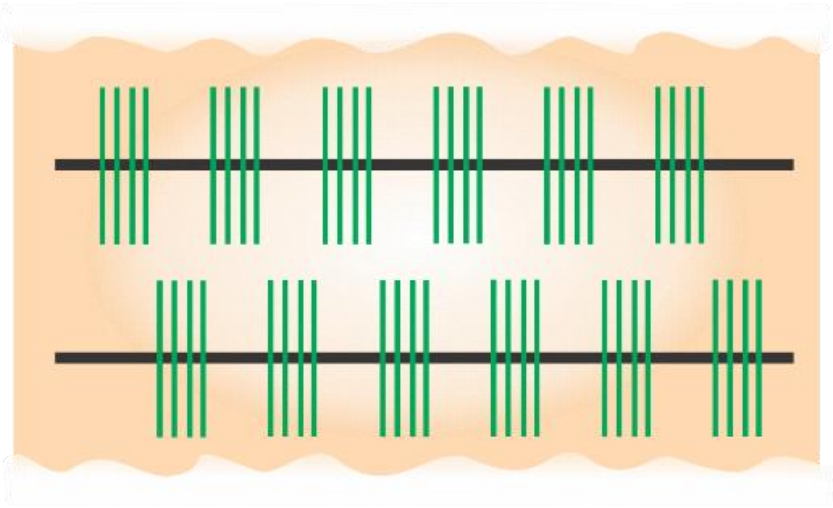

(b) Zipper well pattern

Figure 3.15: Schematic of two different well patterns considered in the simulation study.

Well spacing (number of wells per section)

Recent works in the Bakken Formation have considered the reduction of the spacing between wells especially for injection purposes (Baker et al., 2014). **Figure 3.16** shows the scheme of 4 wells per section and 8 wells per section (lower and higher case) considered in this study. In addition, it is important to point out that we expand the size of reservoir model from half section

(5,240 ft × 2,680 ft × 40 ft) to full section (10,480 ft × 2,680 ft × 40 ft) in order to cover the range of number of wells from 4 to 8.

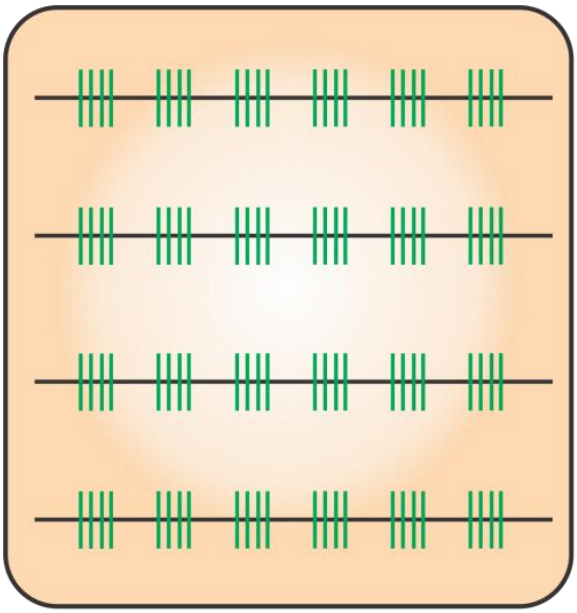

(a) 4 wells per section with well spacing of 1,320 ft between two neighboring wells

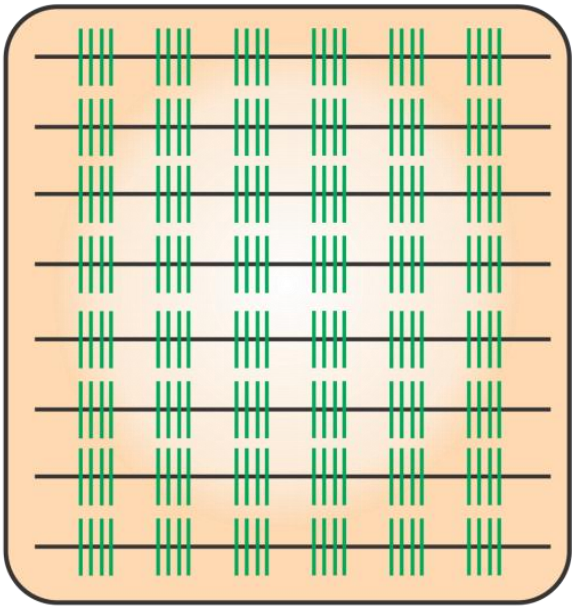

(b) 8 wells per section with well spacing of 610 ft between two neighboring wells

Figure 3.16: Schematic of the minimum and maximum number of wells per section considered in the study and corresponding well spacing.

Fracture half-length

Increasing the fracture half-length has been proved to have a positive effect in the performance of the CO_2 Huff-and-Puff, because it increases the area of contact between the CO_2 injected and oil. However, is not clear the effect of fracture half-length in the performance of CO_2 flooding. This study considers a fracture half-length in the range of 210 ft to 410 ft.

Permeability

Even though the permeability is not a parameter of design, this variable has been included in the design of experiment in order to evaluate its effect on the oil recovery together with the other parameters.

The actual minimum and maximum values are listed in **Table 3.4**. These ranges were determined based on field data, analogues, and history matching results (Yu et al., 2014, 2015).

Parameter	Units	Type	Subtype	Minimum	Maximum
Permeability	md	Numeric	Continuous	0.001	0.1
Fracture half-length	ft	Numeric	Continuous	210	410
Number of wells	-	Numeric	Discrete	4	8
Well pattern	-	Categorical	Nominal	Zipper	Aligned

Table 3.4: Four uncertain parameters with a reasonable range considered in this study.

3.3.2 SENSITIVITY ANALYSIS AND RESPONSE SURFACE

According to four uncertain parameters, 24 cases were generated based on the approach of D-optimal design, which was originated from the optimal design theory (Kiefer and Wolfowitz, 1959), as listed in **Table 3.5**. More details about the approach of D-optimal design can be found in the work by Myers et al. (2008). The objective function of incremental oil recovery factor was utilized to compare the well performance of CO_2 Huff-n-Puff and CO_2 flooding scenarios.

The software Design-Expert (Stat-Ease, 2015) was used to quantify the rank of important parameters and build the response surface model for each scenario. After numerical simulation of each case, the incremental oil recovery factor was obtained and listed in **Table 3.5**. It should be noted that another additional 24 cases without CO_2 injection were also simulated in order to calculate the incremental oil recovery factor. It can be seen that the range of incremental oil recovery factor is 2.56-14.34% and -1.79-30.06% for CO_2 Huff-n-Puff and CO_2 flooding scenarios, respectively.

The average incremental oil recovery factor corresponding to CO_2 Huff-n-Puff and CO_2 flooding scenarios is 7.67% and 14.13%, respectively. The Pareto chart for the ranking of significant parameters affecting the difference of oil recovery factor between two injection scenarios is shown in **Figure 3.17**. It shows that the matrix permeability is the most significant parameter and the second-most significant parameter is the well pattern. With respect to this parameter, the results show that the zipper well pattern performs always better than the aligned well pattern, which will be explained subsequently. The next important parameters in the rank are the interaction between fracture half-length and number of wells, followed by the fracture half-length, and the number of wells.

Case	Permeability (md)	Fracture half-length (ft)	Number of wells	Well pattern	Incremental oil recovery factor (Huff-n-Puff)	Incremental oil recovery factor (flooding)
1	0.1	410	6	Zipper	12.47	28.97
2	0.001	290	8	Zipper	8.30	-1.16
3	0.0505	310	6	Aligned	9.31	22.00
4	0.1	210	8	Aligned	9.67	25.07
5	0.1	210	8	Aligned	9.67	25.07
6	0.01882	350	6	Zipper	9.89	21.65
7	0.001	210	8	Aligned	5.78	-1.50
8	0.001	270	6	Aligned	5.22	-1.79
9	0.001	410	4	Aligned	5.11	-1.77
10	0.001	410	8	Zipper	12.22	0.89
11	0.03763	210	4	Aligned	2.69	6.63
12	0.04948	410	4	Zipper	7.08	21.57
13	0.06337	410	8	Aligned	11.85	14.61
14	0.03763	210	4	Aligned	2.69	6.63
15	0.1	210	4	Zipper	3.02	27.91
16	0.0505	210	8	Zipper	9.40	28.54
17	0.1	330	8	Zipper	14.34	30.06
18	0.1	410	4	Aligned	6.93	25.25
19	0.06337	410	8	Aligned	11.85	14.61
20	0.001	210	4	Zipper	2.56	-1.28
21	0.1	370	6	Aligned	10.96	21.63
22	0.001	210	4	Zipper	2.56	-1.28
23	0.001	410	4	Aligned	5.11	-1.77
24	0.1	330	4	Zipper	5.32	28.55

Table 3.5: 24 cases generate based on the D-optimal design and corresponding incremental oil recovery factor for CO_2 Huff-n-Puff and CO_2 flooding scenarios.

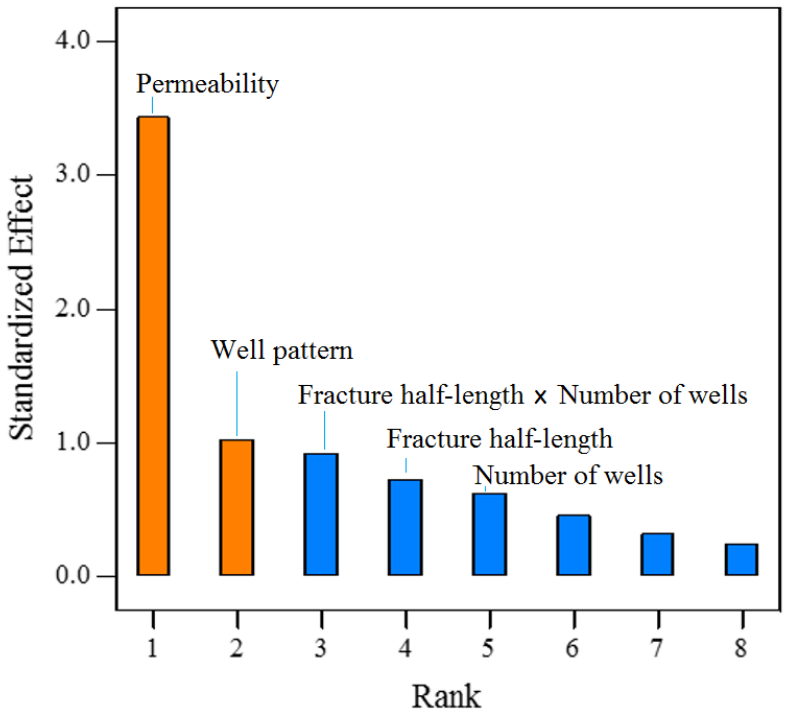

Figure 3.17: Pareto chart of all parameters affecting the difference of oil recovery factor between CO_2 Huff-n-Puff and CO_2 flooding scenarios.

Figures 3.18 and **3.19** present the comparison of contour plot of incremental oil recover factor between the zipper well pattern and the aligned well pattern for CO_2 Huff-n-Puff and CO_2 flooding scenarios with 8 horizontal wells, respectively. As shown, the zipper well pattern always produces a larger incremental oil recovery factor than the aligned well pattern regardless of CO_2 injection scenario. For the Huff-n-Puff scenario, the difference between two well patterns is not significant, which is around 2%. The reason is that the injected CO_2 is mainly concentrated nearby the fractures [see **Figure 3.20(a)**] and the contact fracture area of both well patterns is almost the same. For the flooding scenario, the difference becomes larger, which is around 10%, since the CO_2 drainage area is in contact between injectors and producers [see **Figure 3.20(b)**].

Hence, the well pattern plays an important role in CO_2 sweep efficiency. The zipper well pattern allows to increase the contact area and has a longer CO_2 breakthrough time, because the distance between the neighboring fractures under injectors and producers is larger than that of the

aligned well pattern. Accordingly, it is implied that the zipper well pattern should be designed to improve oil recovery through CO_2 injection.

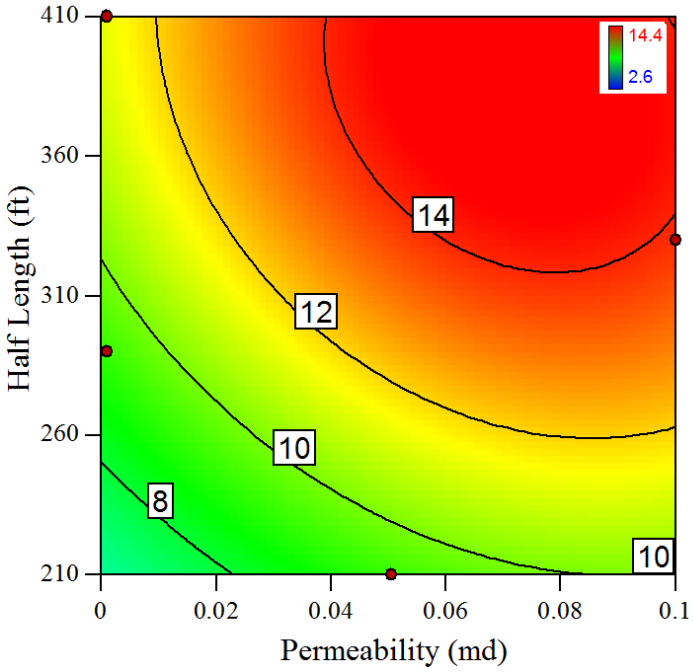

(a) Zipper well pattern

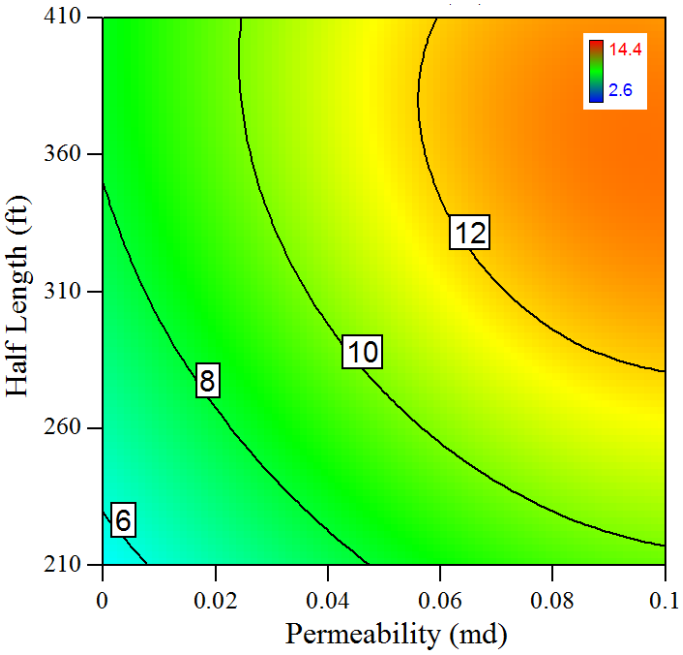

(b) Aligned well pattern

Figure 3.18: Comparison of contour plots of incremental oil recovery factor between zipper well pattern and aligned well pattern for CO_2 Huff-n-Puff scenario with 8 wells.

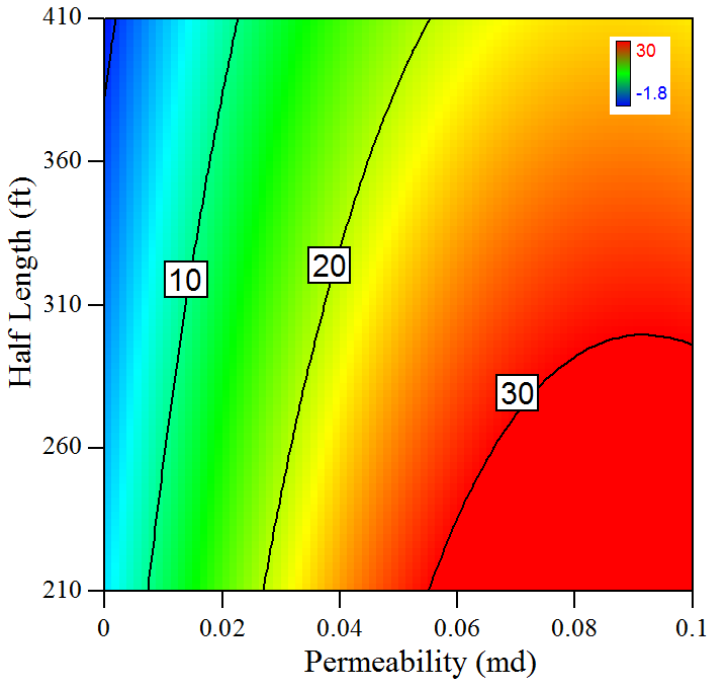

(a) Zipper well pattern

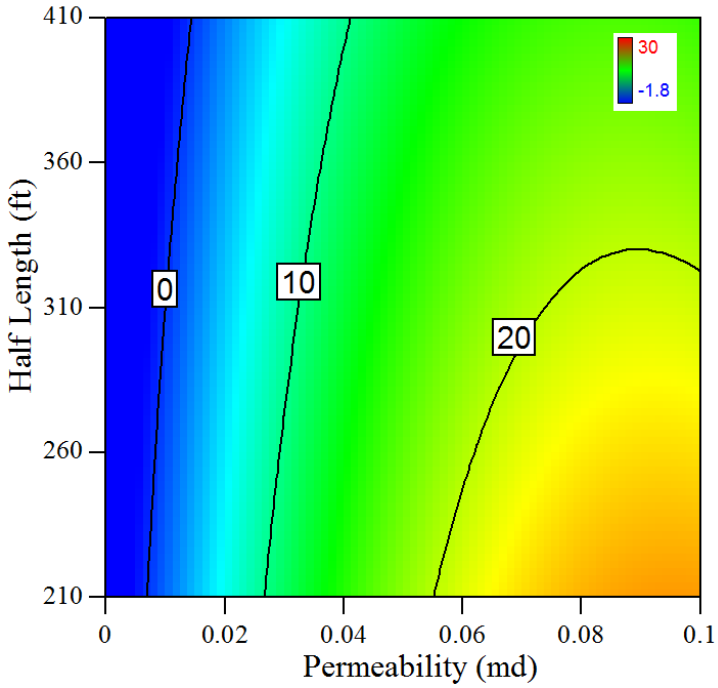

(b) Aligned well pattern

Figure 3.19: Comparison of contour plots of incremental oil recovery factor between zipper well pattern and aligned well pattern for CO_2 flooding scenario with 8 wells.

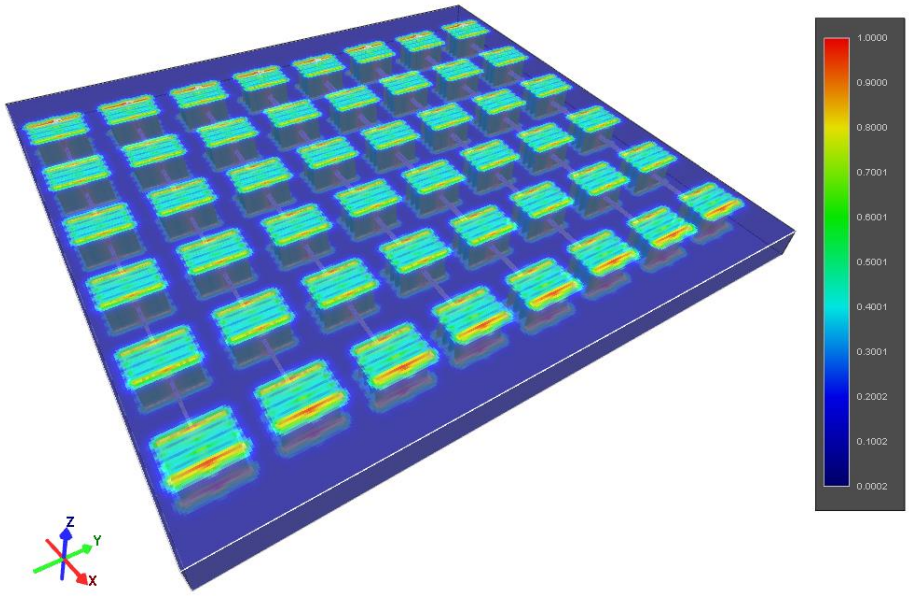

(a) CO_2 Huff-n-Puff scenario

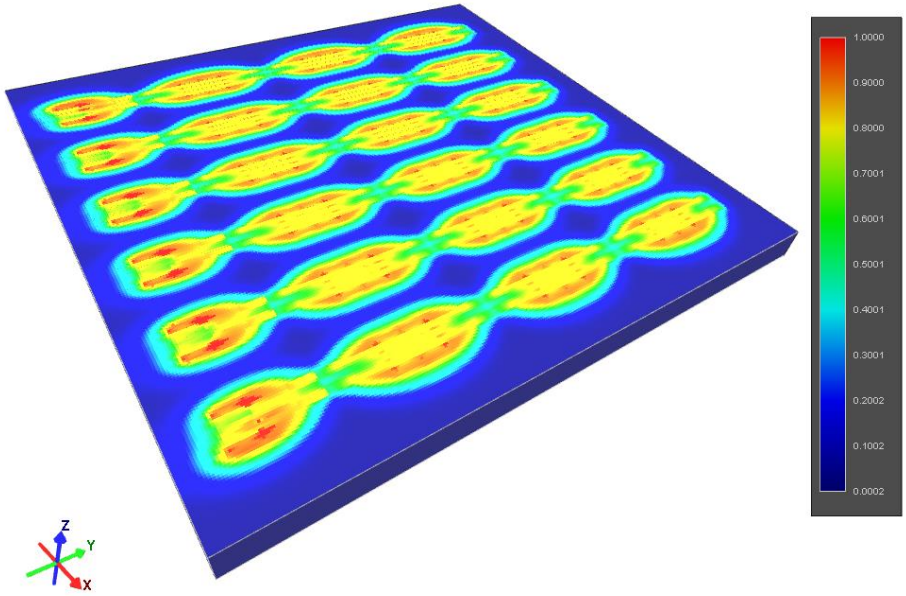

(b) CO_2 flooding scenario

Figure 3.20: 3D plot of CO_2 global mole fraction distribution after CO_2 injection under the zipper well pattern with fracture half-length of 210 ft and matrix permeability of 0.1 md, illustrating the different drainage areas between two CO_2 injection scenarios.

The fully quadratic model was selected to build the response surface model. **Figures 3.21** and **3.22** show the Box-Cox plot used to determine the most suitable power transform for the

response variable. As it can be see the values of λ are in the recommended range. The inverse quadratic root was selected for response variable corresponding to the Huff-n-Puff scenario.

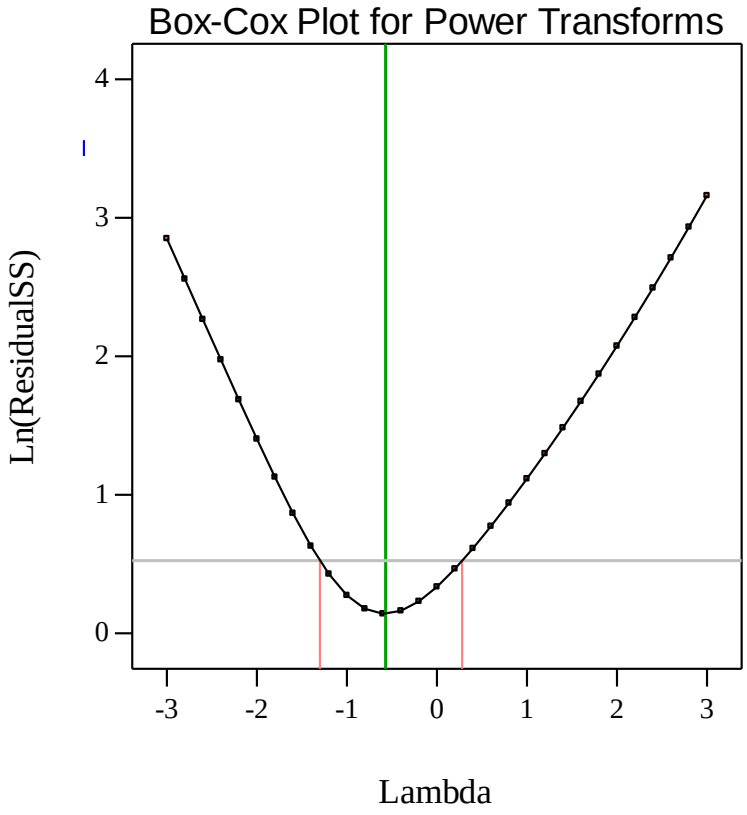

Figure 3.21: Box-Cox Plot for the variable response corresponding to the CO_2 Huff-n-Puff scenario.

The Box-Cox plot for the flooding scenario displayed in **Figure 3.22** shows that the value of λ is slightly outside the range required. However, the model was not transformed, because the resultant response surface model produces too optimistic results. The incremental recovery values using the suggested transform were above 40%.

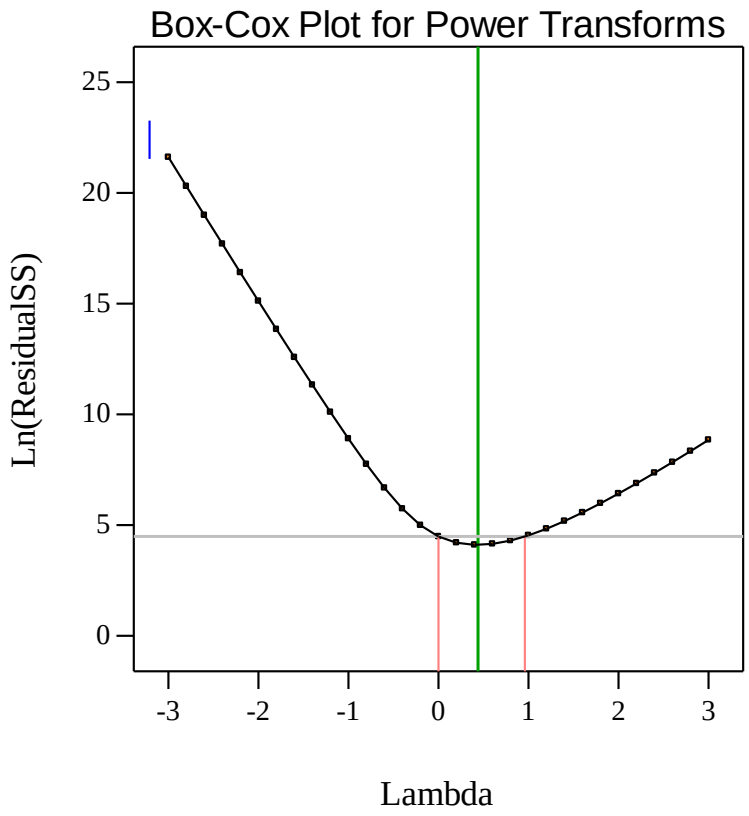

Figure 3.22. Box-Cox Plot for the variable response corresponding to the CO_2 flooding scenario.

The equations fitted to the response surface of incremental recovery factor corresponds to the zipper well pattern and 8 wells presented next.

For the CO_2 Huff-n-Puff scenario:

$$\text{Incremental oil recovery factor} = (1/(1.7988 - 1.6798\,k - 3.0608 \times 10^{-3} X_f - 0.2364\,N_w + 1.7849 \times 10^{-3} k\,X_f - 2.1357 \times 10^{-2} k\,N_w + 1.7885 \times 10^{-4} X_f\,N_w + 8.1129\,k^2 + 1.9481 \times 10^{-6} {X_f}^2 + 1.144 \times 10^{-2} {N_w}^2))^2 \quad (3.1)$$

For the CO_2 flooding scenario:

$$\text{Incremental oil recovery factor} = -75.1742 + 702.08\,k + 0.1064\,X_f + 21.587\,N_w - 0.3126\,k\,X_f - 1.8965\,k\,N_w - 1.6133 \times 10^{-2} X_f N_w - 3235.7\,k^2 - 1.6839 \times 10^{-5} {X_f}^2 - 1.35\,{N_w}^2 \quad (3.2)$$

where k is permeability (md), X_f is fracture half-length (ft), and N_W is number of wells.

Figure 3.23 shows the plot of "predicted vs. actual" for both injection scenarios, illustrating that there is a reasonable match between the generated response values and the actual response values. Hence, the generated response surface models are reliable.

The effects of fracture half-length and matrix permeability for the comparison of incremental oil recovery factor between two CO_2 injection scenarios with 8 wells are shown in **Figure 3.24**. The intersection curve between two response surfaces indicates the limit of better performance of CO_2 Huff-n-Puff compared to CO_2 flooding and vice versa.

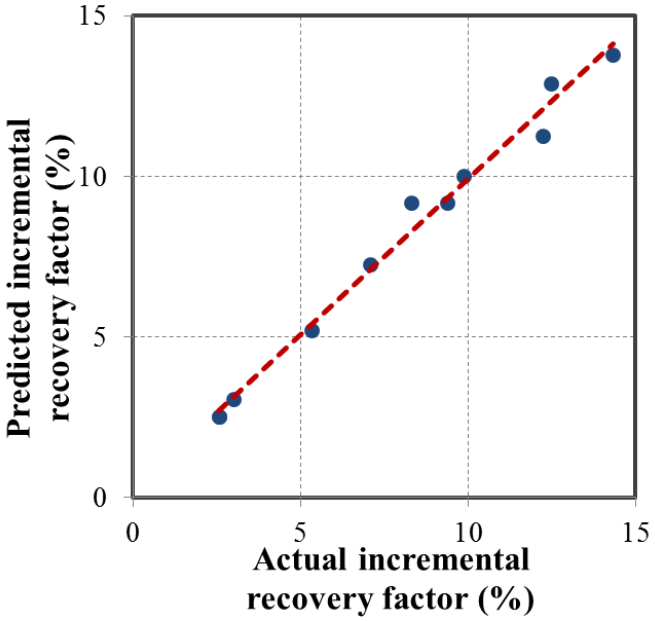

(a) CO_2 Huff-n-Puff scenario

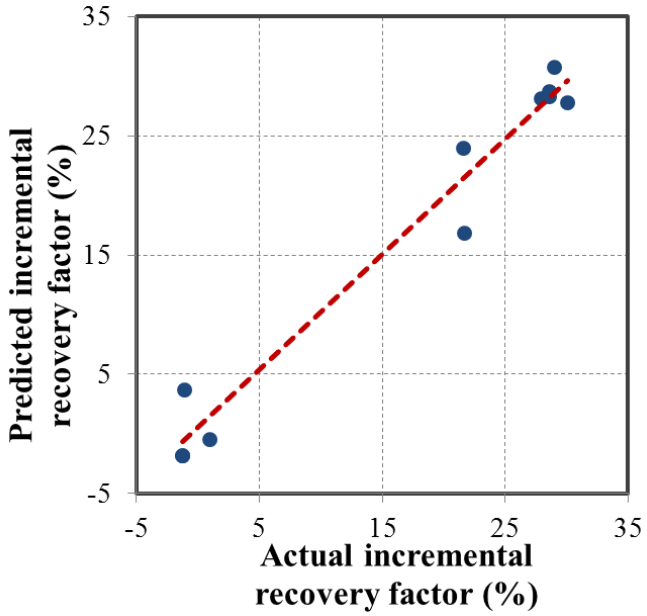

(b) CO_2 flooding scenario

Figure 3.23: Validation for two response surface models illustrating a reasonable match between predicted and actual values.

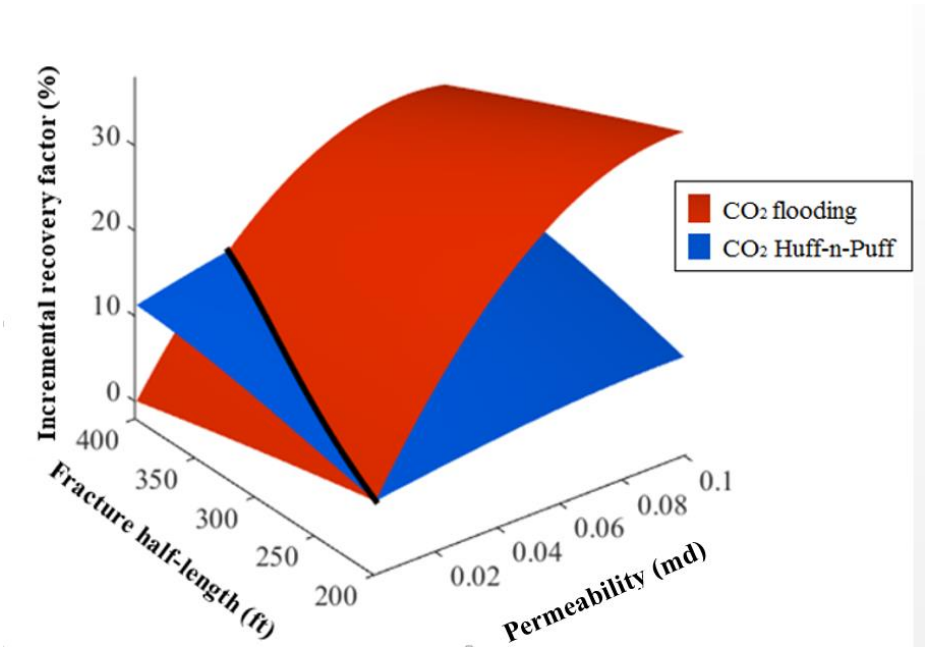

(a) Response Surfaces of injection scenarios with permeability in linear scale

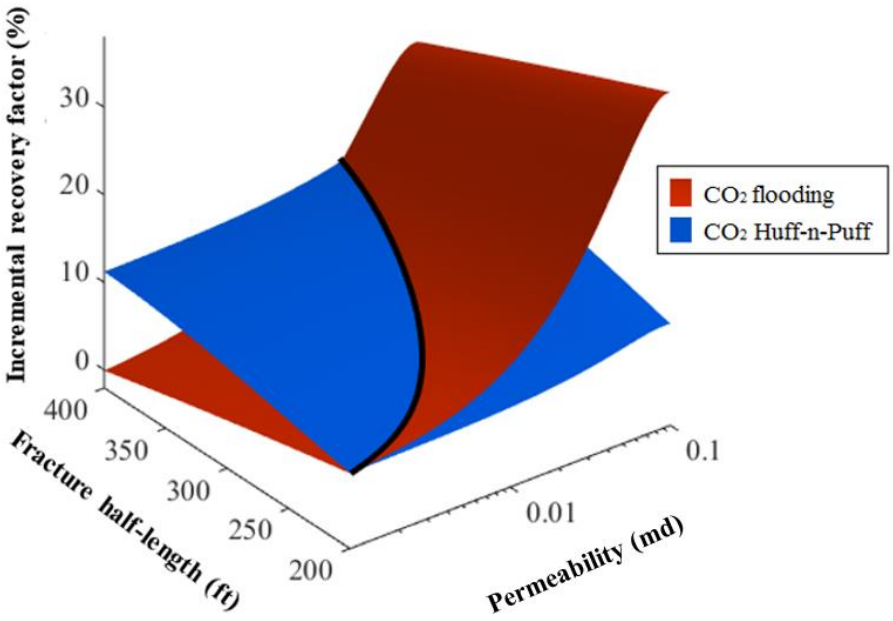

(b) Response Surfaces of injection scenarios with permeability in logarithmic scale

Figure 3.24: 3D response surfaces of incremental oil recovery factor for CO_2 Huff-n-Puff and CO_2 flooding with the zipper well patter and 8 horizontal wells.

Figure 3.25 presents the diagnostic contour plot of two response surfaces with 8 horizontal wells, clearly distinguishing the different zones with better well performance for each CO_2 injection scenario. In the zone of CO_2 Huff-n-Puff, the incremental oil recovery factor is larger than that of CO_2 flooding.

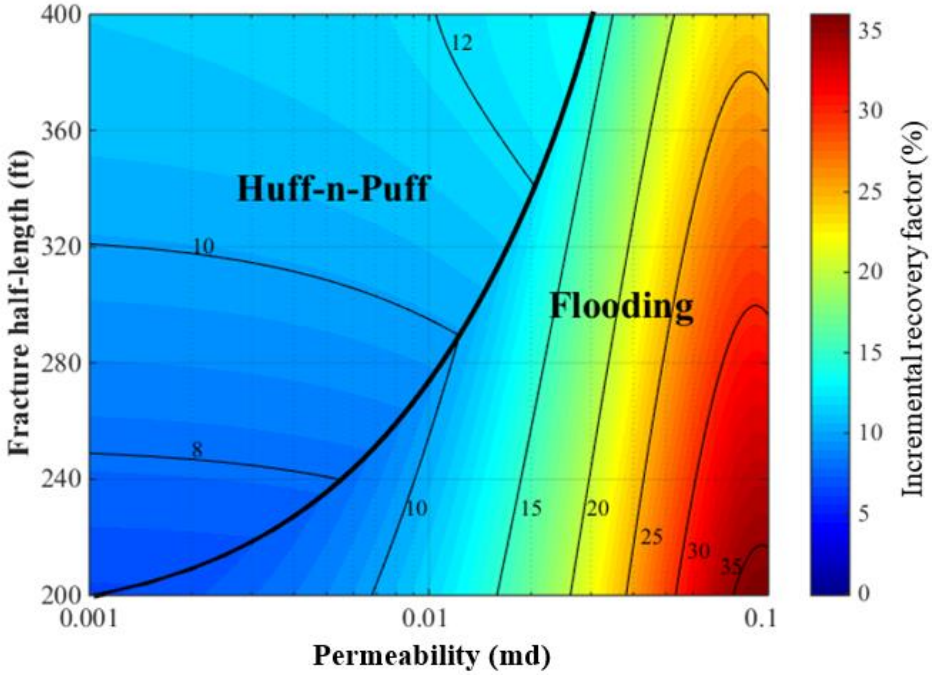

Figure 3.25: Contour plot of two response surfaces with 8 horizontal wells.

Figure 3.26 shows the diagnostic contour plot of two response surfaces with 6 horizontal wells. It can be seen that when the number of wells decreases from 8 to 6, the zone of flooding scenario increases significantly. The reason is that the CO_2 breakthrough time decreases with the increasing well spacing from 8 wells to 6 wells, resulting in a larger CO_2 sweep efficiency and higher incremental oil recovery factor.

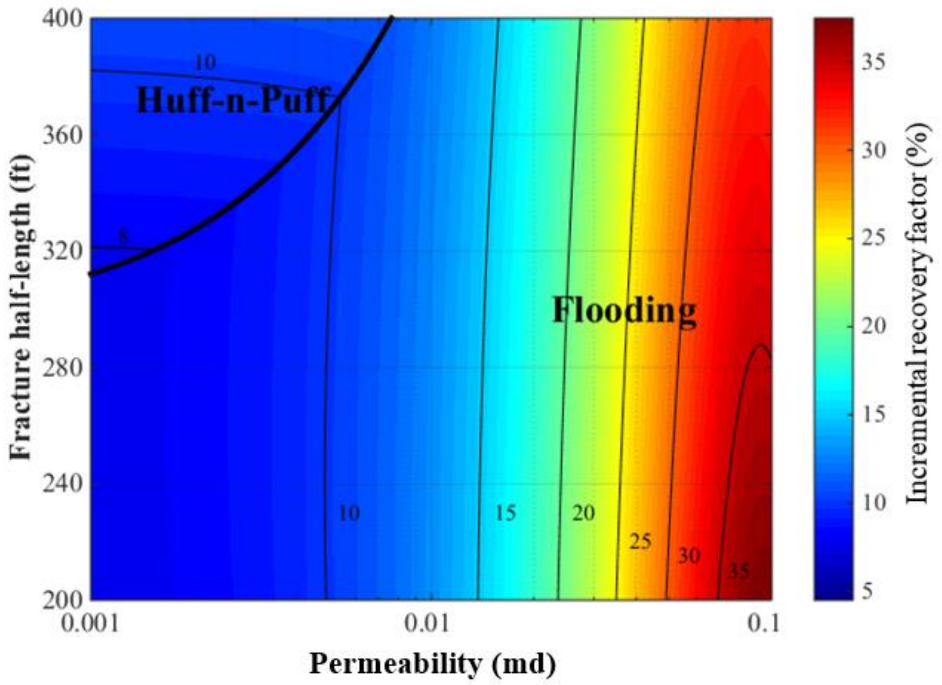

Figure 3.26: Contour plot of two response surfaces with 6 horizontal wells.

However, when the number of wells continuously decreases from 6 to 4, the zone of CO_2 flooding did not increase further while the zone of CO_2 Huff-n-Puff increases, as shown in **Figure 3.27**. For this case with 4 wells, CO_2 is difficult to reach the producers during the production time due to the larger distance between injectors and producers, especially for lower values of permeability. Hence, it can imply that well spacing plays an important role in the comparison of well performance of CO_2 Huff-n-Puff and CO_2 flooding scenarios.

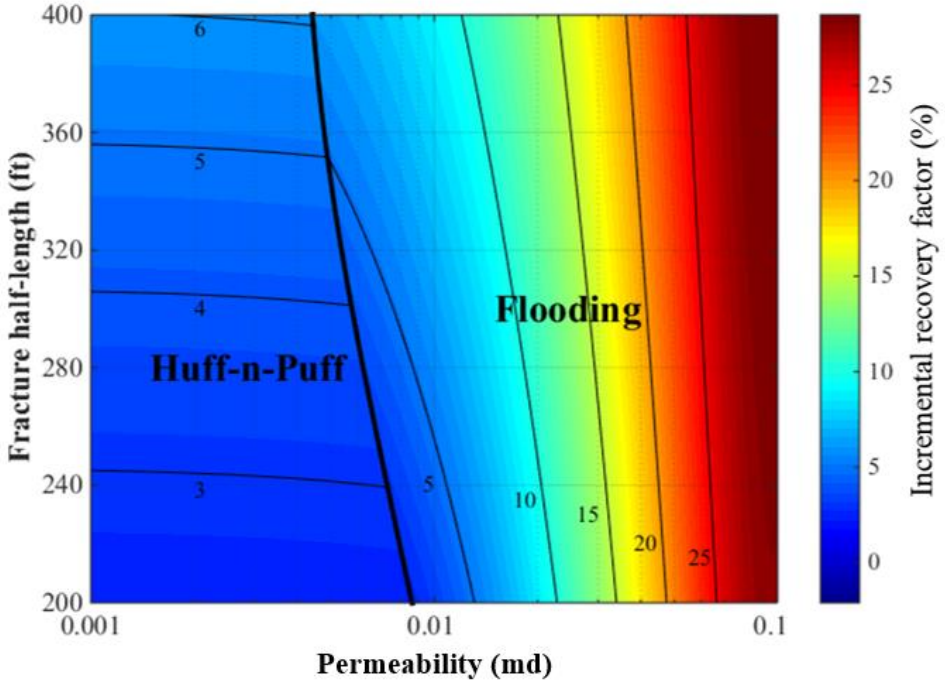

Figure 3.27: Contour plot of two response surfaces with 4 horizontal wells.

According to the analysis of results, it can be observed that in the range of permeability from 0.001 md to 0.01md, the CO_2 Huff-n-Puff scenario performs better than CO_2 flooding scenario under the situations of appropriate number of wells (4 and 8 wells) and fracture half-length. When the number of wells and fracture half-length increase, the incremental oil recovery factor of CO_2 Huff-n-Puff increases due to the increasing contact fracture area. In this case study, the highest incremental oil recovery factor of 13% was achieved for the CO_2 Huff-n-Puff scenario with permeability of 0.02 md, 8 wells, and fracture half-length of 400 ft, which is located in **Figure 25**.

On the other hand, when the permeability ranges from 0.01 md to 0.1 md, the CO_2 flooding scenario performs better than CO_2 Huff-n-Puff scenario for most situations, especially when the number of wells is 6. In addition, increasing the number of wells does not necessarily lead to the increasing incremental oil recovery factor due to the occurrence of early breakthrough of CO_2. In this case study, the highest incremental oil recovery factor of 37% was reached for the CO_2

flooding scenario with permeability of 0.1 md, 6 wells, and fracture half-length of 210 ft, which is located in **Figure 26**.

Additionally, the analysis performed for a production lifetime of 18 years has been repeated for a shorter production term of 8 years. This shorter period only takes into account 3 years of primary production and only one cycle of Huff-n-Puff of 5 years. The results of the cases with 8, 6, and 4 wells per section are shown in **Figures 3.28, 3.29** and **3.30**, respectively. The plots clearly show that there is a strong dependence on the production lifetime to determine the best injection strategy. In this case the Huff-n-Puff scenario is the most suitable for a largest range of permeability and the continuous flooding scenario only shows better results for permeability higher than 0.05 md. A similar result is observed when 6 wells per section are used. When 4 wells per section are considered Huff-n-Puff strategy is the most suitable for the whole range of permeability evaluated.

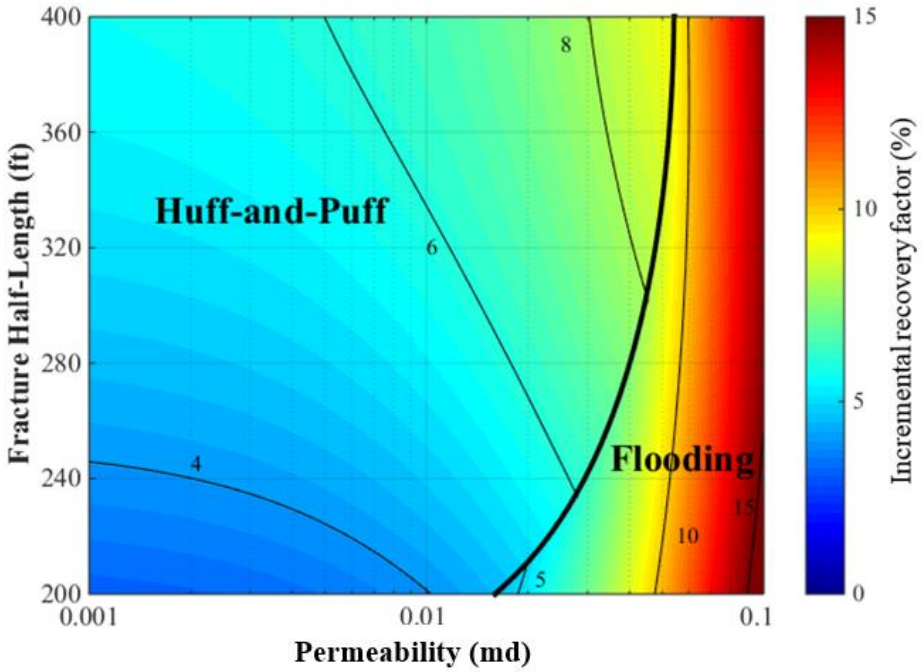

Figure 3.28: Contour plot of two response surfaces with 8 horizontal wells, for a production lifetime of 8 years.

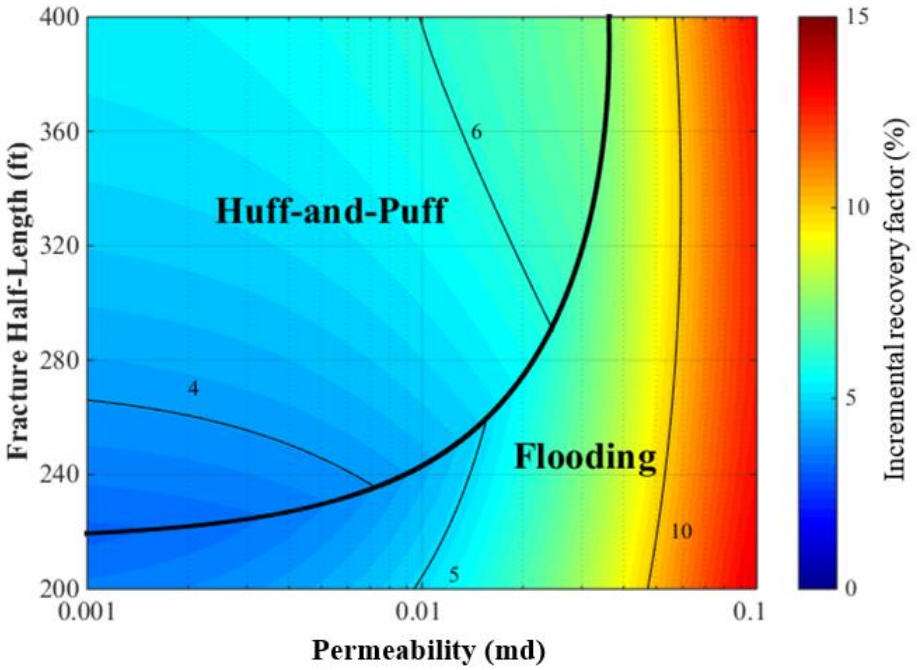

Figure 3.29: Contour plot of two response surfaces with 6 horizontal wells, for a production lifetime of 8 years.

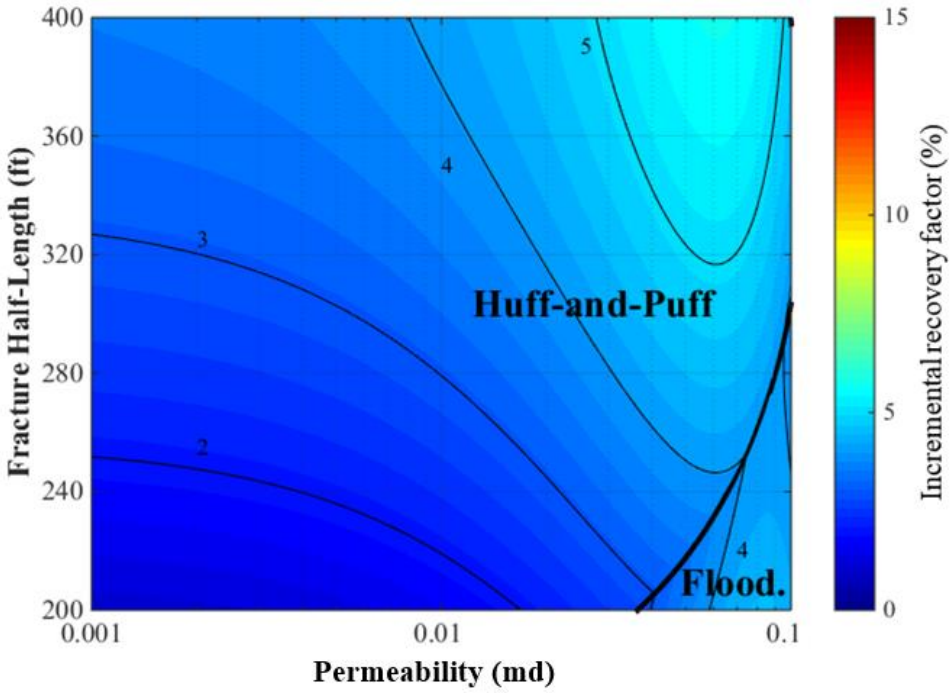

Figure 3.30: Contour plot of two response surfaces with 4 horizontal wells, for a production lifetime of 8 years.

Chapter 4: Simulation Study of CO_2-EOR in Tight Oil Reservoirs with Complex Hydraulic Fracture Geometries

In this section we first built a single-stage production model with multiple fractures based on typical fluid and reservoir properties from the Middle Bakken Formation. Four cases with different fracture geometries from simple to complex were modelled using the EDFM. We verified the EDFM methodology for simple bi-wing hydraulic fractures against the traditional local grid refinement (LGR) approach, which can accurately capture the fluid transport from shale matrix to fracture (Rubin, 2010), but it is difficult to handle complex non-planar fractures using LGR.

Afterward, we use the validated model to analyze the CO_2 Huff-n-Puff stimulation and to evaluate the effect of the fracture complexity on the production performance. The Huff-n-Puff stimulation consists of the three cycles of injection and production (1 year of injection, 1 month of soaking period, and 4 years of production), analogous to the Huff-n-Puff presented in Chapter 3, section 3.1.3. Subsequently, we extended the model to include two wells, each well has four fractures within single stage, to simulate CO_2 flooding. Finally, we built a field-scale reservoir model including two horizontal wells to study the effects of complex non-planar hydraulic fractures and natural fractures on well performance of both CO_2 injection scenarios under two different reservoir permeabilities of 0.01 md and 0.1 md. This work provides critical insights about the effect of fracture complexity on well performance of CO_2 Huff-n-Puff and CO_2 flooding in tight oil reservoirs.

4.1 Embedded Discrete Fracture Model

The Embedded Discrete Fracture Model (EDFM) is an efficient approach to simulate complex fractures using reservoir simulators. In this method, fractures are discretized into small segments with matrix cell boundaries and virtual cells are created to represent these fracture segments. This method can be applied in traditional simulators by appending cells in the grid domain and adding non-neighboring connections (NNCs) for these cells to account for the mass

transport associated with fractures, including the flow between matrix and fractures, flow inside an individual fracture, and flow between intersecting fractures. Through transmissibility factors between corresponding cells, the volume flow rate of phase l between cells in a NNC pair is

$$q = \lambda_l T_{NNC} \Delta P , \tag{4.1}$$

where λ_l is the relative mobility of phase l, T_{NNC} is the NNC transmissibility factor, and ΔP is the potential difference between the cells.

For the calculation of transmissibility factors, generally, T_{NNC} can be expressed as

$$T_{NNC} = \frac{k_{NNC} A_{NNC}}{d_{NNC}} , \tag{4.2}$$

where k_{NNC}, A_{NNC}, and d_{NNC} are the permeability, contact area, and distance associated with this connection, respectively.

For matrix-fracture connection, in **Equation 4.2**, k_{NNC} is the matrix permeability in the direction perpendicular to the fracture plane, A_{NNC} is the area of the fracture plane inside matrix block, and d_{NNC} is the average normal distance from matrix block to fracture plane.

For connections between fracture segments, k_{NNC} is calculated as an average of fracture permeability, A_{NNC} is the common area between fracture segments, and d_{NNC} is the distance between centroids of the fracture segments. More details of the calculation can be found in Xu et al. (2016).

In addition, the fracture-wellbore intersections are modeled as effective well indices in the EDFM. The effective well index in the EDFM can be calculated as (Xu, 2015)

$$WI_f = \frac{2\pi k_f w_f}{\ln(r_e / r_w)}, \tag{4.3}$$

$$r_e = 0.14\sqrt{L^2 + W^2}, \tag{4.4}$$

where k_f is the fracture permeability, w_f is the fracture aperture, L and W are the length and height of the fracture segment, respectively. **Equations 4.3** and **4.4** can be derived by replacing the dimensions and permeability of the gridblock in Peaceman's model with those of the fracture segments.

By discretizing large fractures into interconnected small fractures, the EDFM has been proven to be effective in modeling complex hydraulic fracture geometries such as non-planar fractures and fractures with variable width (Xu, 2015). Furthermore, the computational performance of the EDFM in traditional simulators was also verified through detailed comparison with LGR model. In this study, we first present a case study to verify the EDFM with LGR model, then for other cases, we apply the EDFM method in the compositional simulator (CMG-GEM, 2012) to simulate complex fractures.

4.2 Reservoir Simulation Model

A compositional numerical reservoir model with single fracture stage was built based on the model described in Chapter 3. A Cartesian grid system was also used, which consists of 70 grids in *x* direction, 51 grids in *y* direction, and 1 grid in *z* direction. The dimension of the reservoir model is 1,400 ft × 1,020 ft × 40 ft, which corresponds to length, width, and thickness, respectively. The reservoir and fracture properties are the same as **Table 3.1** in the previous chapter. Similarly, the oil properties listed in **Table 3.2** were used for this section.

4.2.1 Verification of Embedded Discrete Fracture Model.

For the verification purpose, we only model four simple planar hydraulic fractures. The comparison of grid blocks used to model hydraulic fractures between EDFM and LGR is displayed in **Figure 4.1**. As shown, the LGR approach has more grid blocks to handle fractures than the EDFM approach.

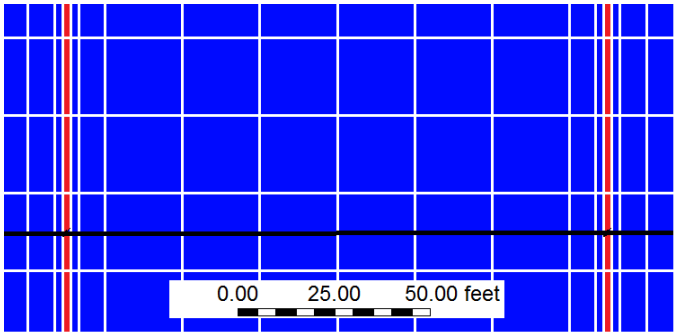

(a) Grid blocks to model fracture using LGR

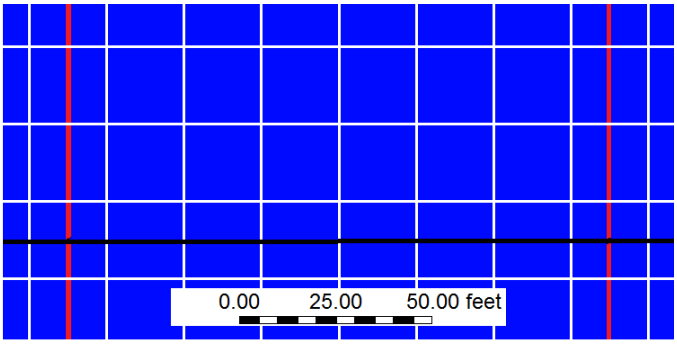

(b) Grid blocks to model fracture using EDFM

Figure 4.1: Comparison of grid blocks to model hydraulic fractures using the methodologies of LGR and EDFM (The red lines represent fractures).

Figure 4.2 presents the comparison of oil recovery factor using LGR and EDFM to model four hydraulic fractures in a single stage for a period of primary production (4 years) and three consecutive cycles of CO_2 Huff-n-Puff. Each cycle contains 1 year of injection, 1 month of soaking period, and 4 years of production. As it is observed, a good agreement was obtained and therefore the EDFM methodology can be applied to properly model the CO_2 injection in tight oil reservoirs with hydraulic fractures.

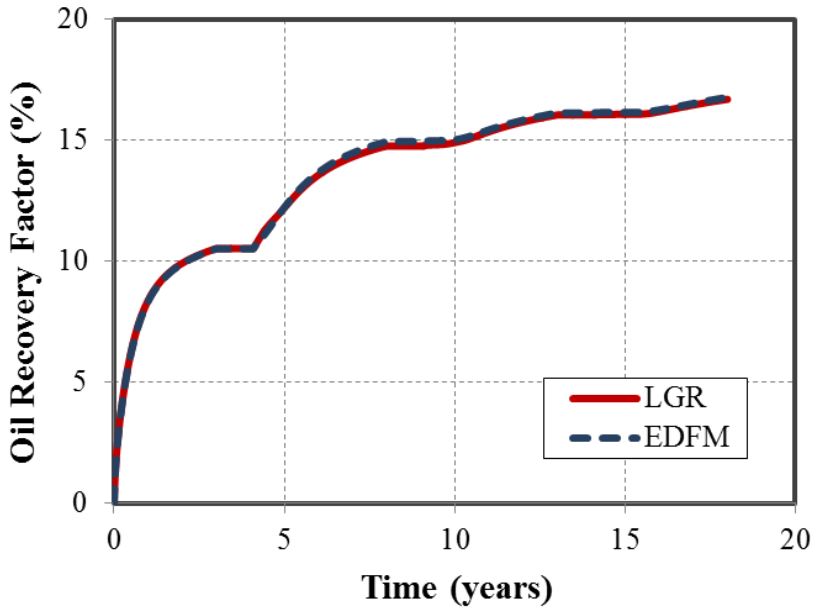

Figure 4.2: Comparison of oil recovery factor for three years of primary production and three cycles of Huff-n-Puff using LGR and EDFM methodologies.

4.2.2 Effect of CO_2 Molecular Diffusion Coefficient on Modelling of Huff-n-Puff

The validated model was then used to examine the effect of the CO_2 molecular diffusion in the simulation of the Huff-n-Puff process. Yu et al. (2014, 2015) pointed out the importance of CO_2 molecular diffusivity is a key physical mechanism for CO_2-EOR process in tight oil reservoirs, which must be taken into account correctly when building a numerical model. **Figure 4.3** presents the comparison of oil recovery factor with and without considering the CO_2 molecular diffusivity in the simulation. **Figure 4.3(a)** shows that there is no difference since there is no CO_2 injection. However, **Figure 4.3(b)** clearly displays that an important increase in the oil recovery factor is achieved when the CO_2 molecular diffusion is considered. The incremental oil recovery factor when compared to primary recovery factor is 3.89% and 0.41% with and without considering CO_2 molecular diffusion, respectively. Hence, in the following case studies, the physical mechanism of CO_2 molecular diffusivity is considered.

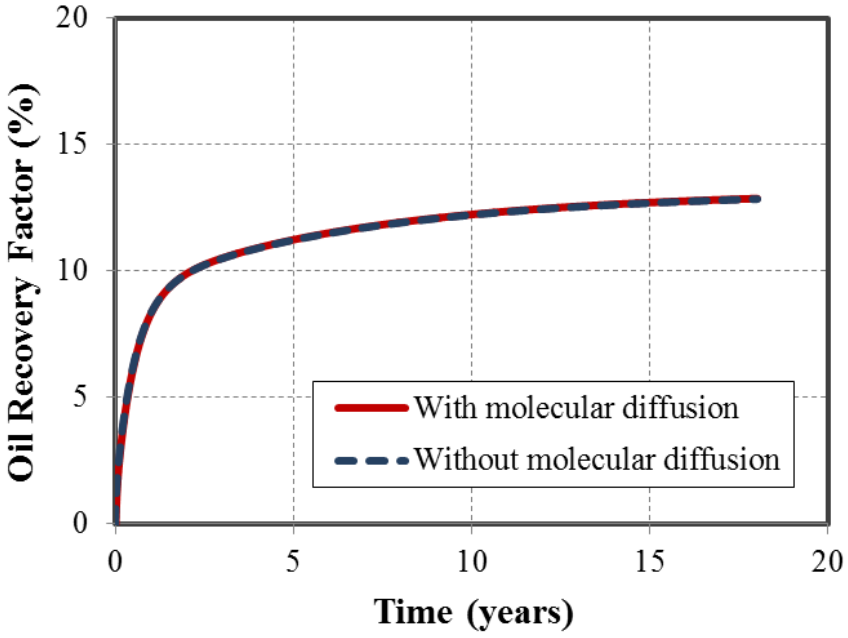

(a) Comparison of oil recovery factor for primary production

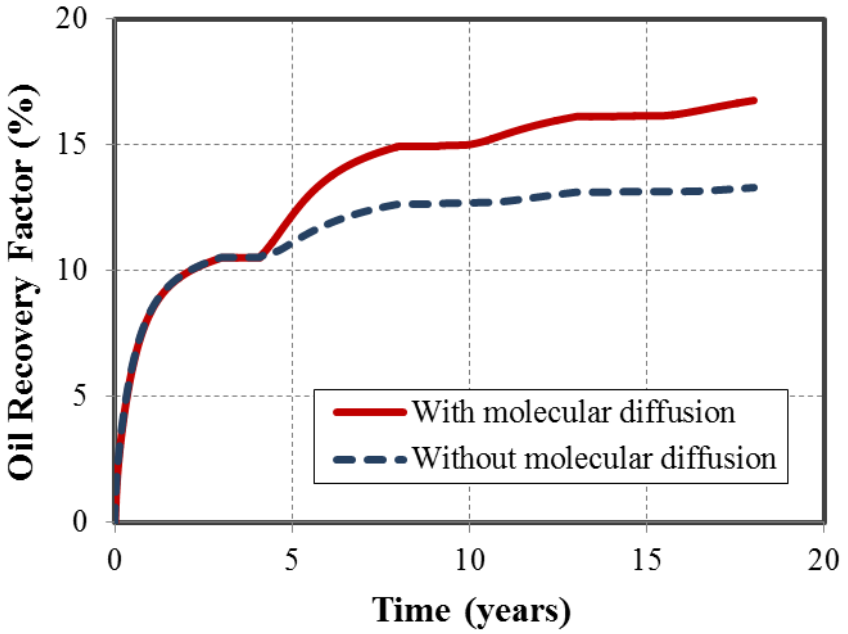

(b) Comparison of oil recovery factor for CO_2 Huff-n-Puff

Figure 4.3: Effect of CO_2 molecular diffusion on oil recovery factor for primary production and Huff-n-Puff.

4.3 CASE STUDIES FOR SINGLE STAGE

4.3.1 Case Studies of CO_2 Huff-n-Puff

We performed four case studies for CO_2 Huff-n-Puff simulation by considering different fracture geometries within single stage including four hydraulic fractures.

- Case 1: **Planar fractures** (Note that this scenario is considered as reference case).
- Case 2: **Diagonal fractures**
- Case 3: **Reoriented fractures**
- Case 4: **Fracture networks**.

These cases consider different fracture geometries with different degrees of complexity such as the striking angle between horizontal well and fractures, irregular fracture length of individual fracture, and the creation of fracture networks. These cases were used to quantify the effect of the increasing fracture complexity on well performance for primary production and Huff-n-Puff scenario.

Parameter	Value	Unit
Fracture half-length	210	ft
Fracture height	40	ft
Fracture conductivity	50	md-ft
Fracture spacing	140	ft

Table 4.1: Parameters of hydraulic fractures in single stage

Case 1: Planar fractures.

This case presents four simple planar fractures orthogonal to the horizontal wellbore. All fractures have the same properties, as shown in **Table 4.1**. **Figure 4.4(a)** shows the projection of

the aforementioned fractures. **Figure 4.4(b)** shows the comparison of oil recovery factor between the primary production and Huff-n-Puff scenario. It can be seen that the difference of oil recovery factor at end of simulation period is around 3.9%. As a reference case, this model was used to evaluate the impact of various cases on well performance.

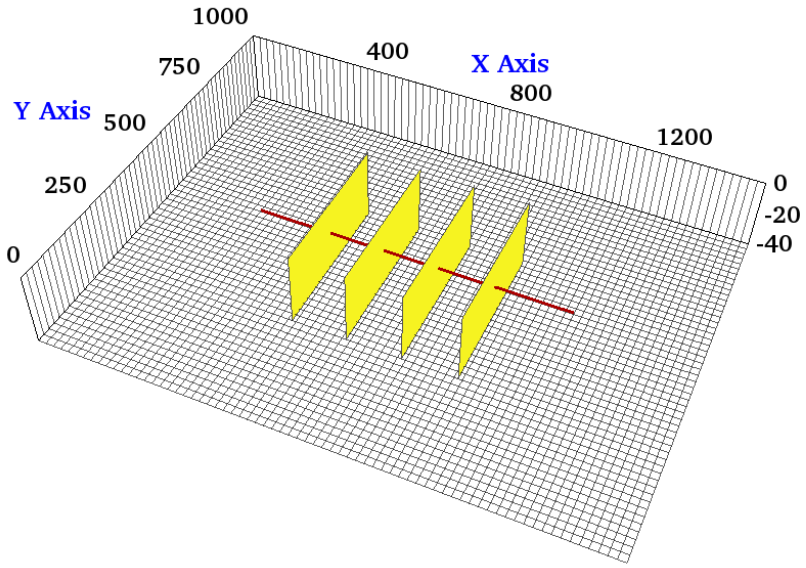

(a) Case 1: Planar fractures

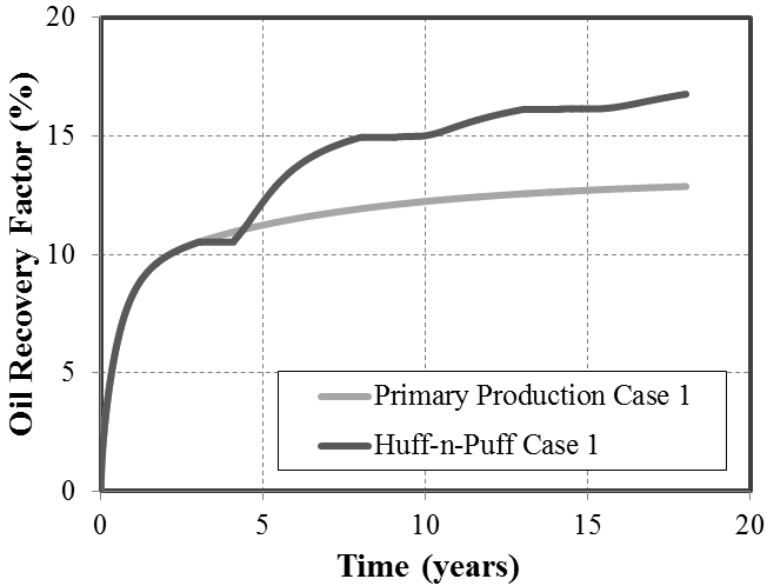

(b) Oil recovery factor for base case and Huff-n-Puff scenario

Figure 4.4: Illustration of four planar fractures for case 1 (The yellow plane represents fracture and the red line represents horizontal wellbore) and comparison of oil recovery factors for primary production and Huff-n-Puff.

Case 2: Diagonal fractures.

The first degree of complexity considered in this study was the orientation of the fractures with respect to the horizontal wellbore. For case 2, four fractures form an angle of 45° with the wellbore, as shown in **Figure 4.5(a)**. The other fracture properties are kept the same as case 1. Although the distance between perforation clusters is the same as case 1, the orthogonal fracture distance between two neighboring fractures was reduced to from 140 ft to 99 ft due to the change of fracture orientation. **Figure 4.5(b)** compares the difference of oil recovery factor between cases 1 and 2.

As shown, the primary oil recovery without CO_2 injection is almost the same. However, the incremental oil recovery factor of case 2, which is around 2.9%, is less than case 1 with 3.9%. This difference can be explained by analyzing the CO_2 molecule distribution maps, which are shown in **Figure 4.6**. The map clearly illustrates that there is a lower production interference between the fractures in case 1 [**Figure 4.6(a)**] than in case 2 [**Figure 4.6(b)**], resulting in CO_2 Huff-n-Puff is less effective for case 2. The increase in the interference between the fractures of case 2 is expected since the orthogonal distance between the fractures decreases from 140 ft to 99 ft.

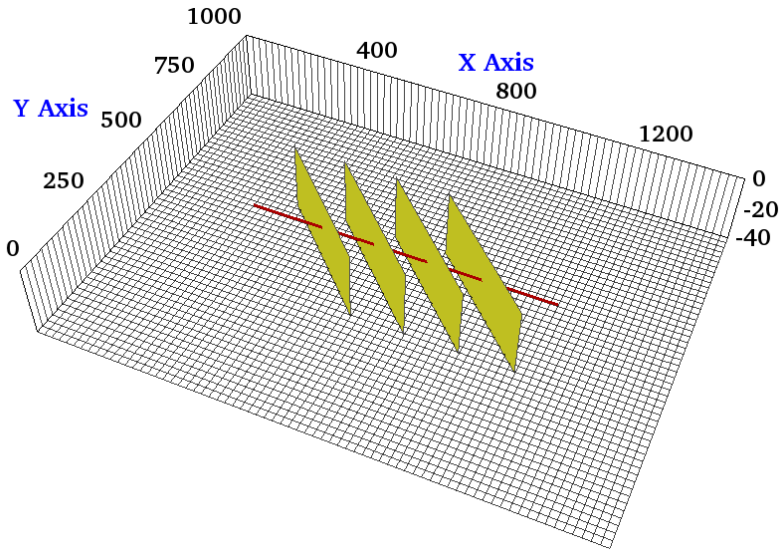

(a) Case 2: Diagonal fractures

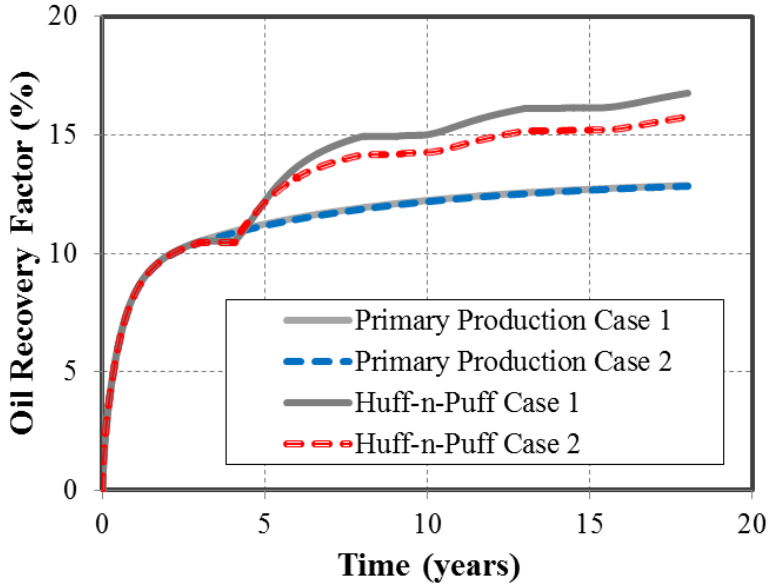

(b) Oil recovery factor curves for the primary production and Huff-n-Puff

Figure 4.5: Illustration of the fractures for case 2 and comparison of the oil recovery factors for case 1 and case 2.

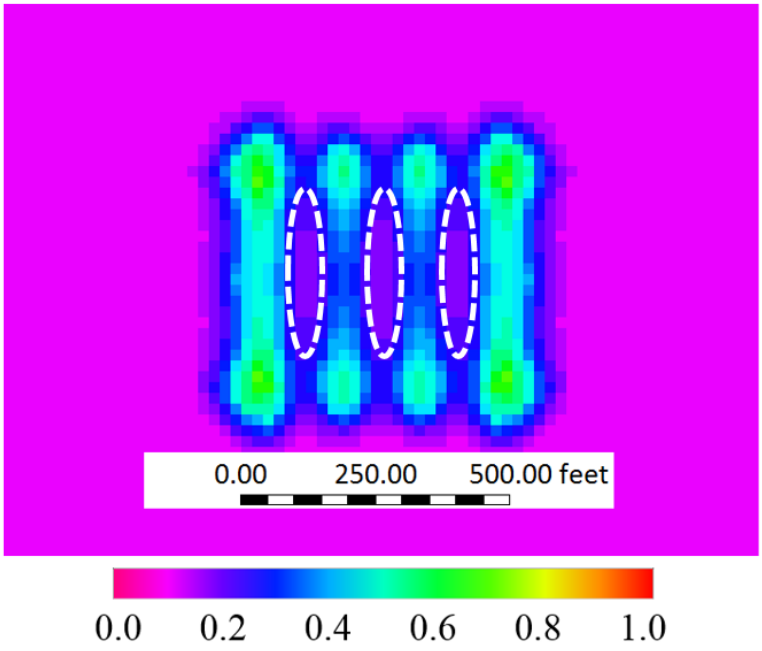

(a) Case 1

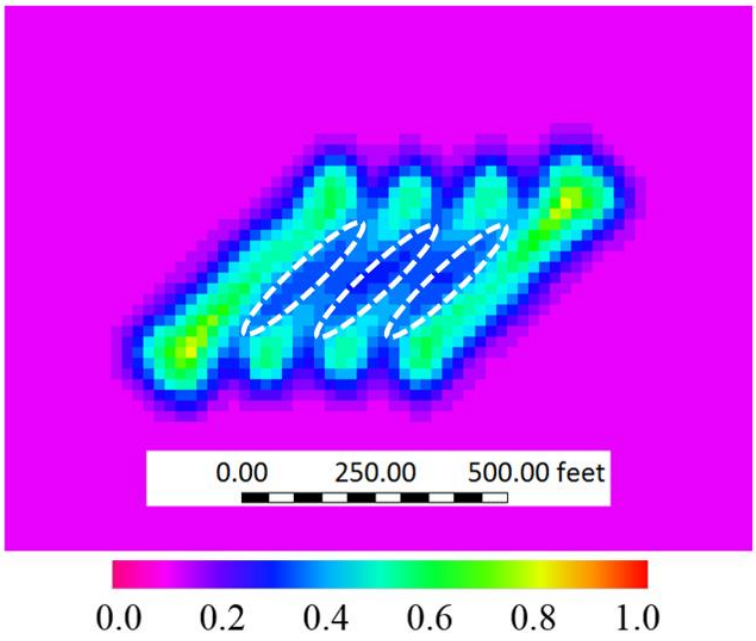

(b) Case 2

Figure 4.6: Map of global CO_2 molecule distribution after one year of injection of Huff-n-Puff treatment. Note that the main difference of CO_2 concentrations between two cases is highlighted by the oval dashed lines.

Case 3: Reoriented fractures.

Case 3 represents four non-planar fractures with outer fractures longer than inner fractures, as shown in **Figure 4.7(a)**. Each fracture is composed of two fracture segments with an orientation of 45° and 135° or 135° and 45° for upper and lower segment, respectively. The fracture half-length for outer and inner fractures is 295 ft and 125 ft, respectively. It should be noted that the total fracture length, i.e. the summation of the fracture segments, remains the same as cases 1 and 2. **Figure 4.7(b)** compares the difference of oil recovery factor between cases 1 and 3. As shown, there is a small difference of primary production.

Nevertheless, when compared to case 1, the incremental oil recovery factor of case 3 increases from 3.9% to around 4.5%. Again, this improvement is associated with the interference between the fractures. In this case, the Huff-n-Puff is more effective than case 1 because the outer fractures have a longer length and less interference with the inner fractures, as can be seen from CO_2 molecule distribution in the **Figure 4.8.**

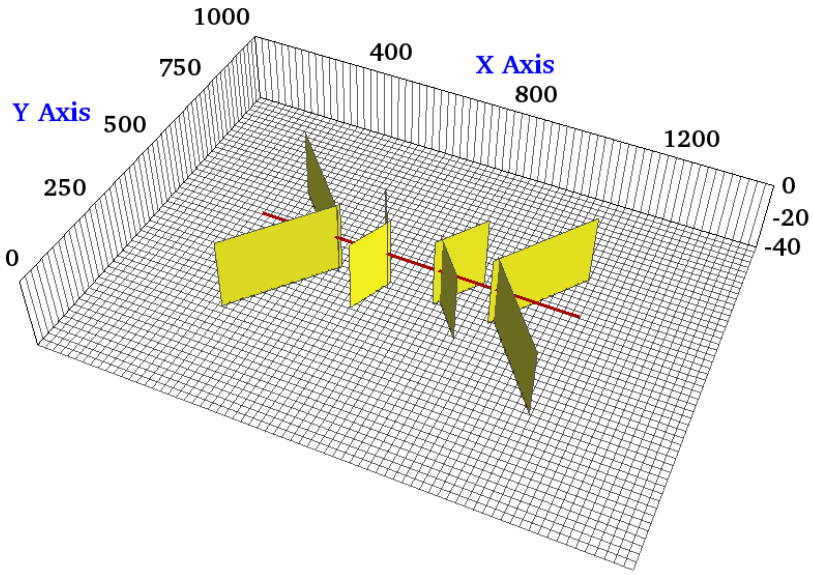

(a) Case 3: Reoriented fractures

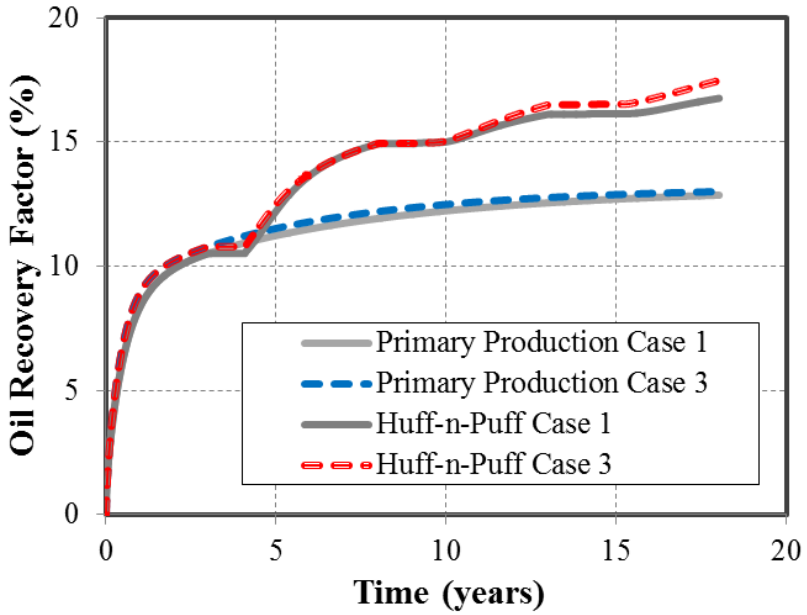

(b) Oil recovery factor curves for the primary production and Huff-n-Puff

Figure 4.7: Illustration of the fractures for case 3 and comparison of the oil recovery factors for case 1 and case 3

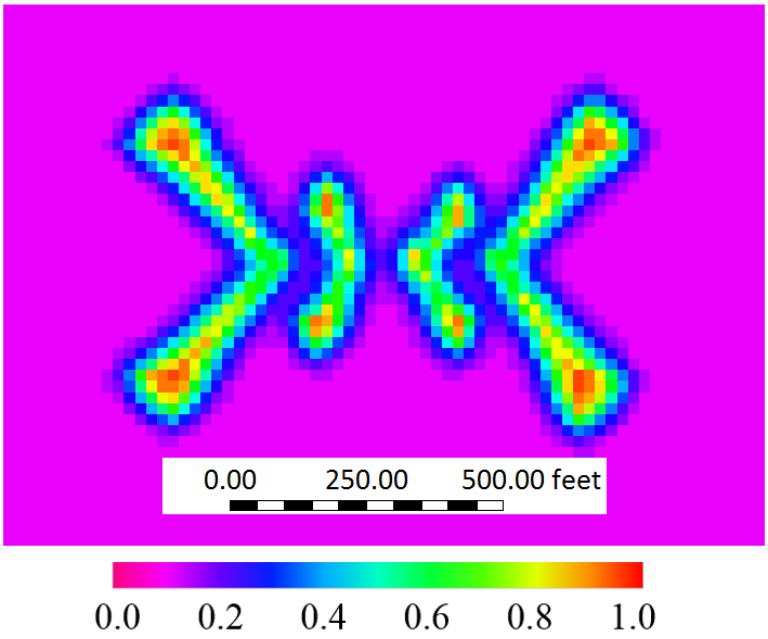

Figure 4.8: Map of global CO_2 molecule distribution after one year of injection of Huff-n-Puff treatment for case 3.

Case 4: Fracture networks.

The last case of fractures analyzed represents four systems of fracture networks created around each perforation cluster, as shown in **Figure 4.9(a)**. The fracture networks are composed of several segments that intersect each other. Similarly to previous cases, the total fracture length of all segments is equivalent to the planar fractures of case 1. Case 4 represents the more realistic fracture geometry. **Figure 4.9(b)** compares the difference of oil recovery factor between cases 1 and 4. For this case the incremental oil recovery is only 2.6%, which is lower than the other three cases evaluated.

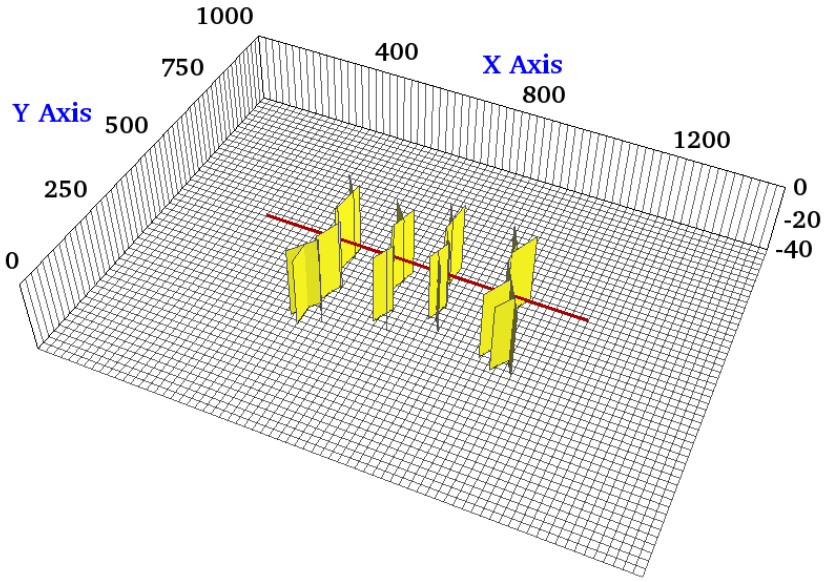

(a) Case 4: Fracture networks

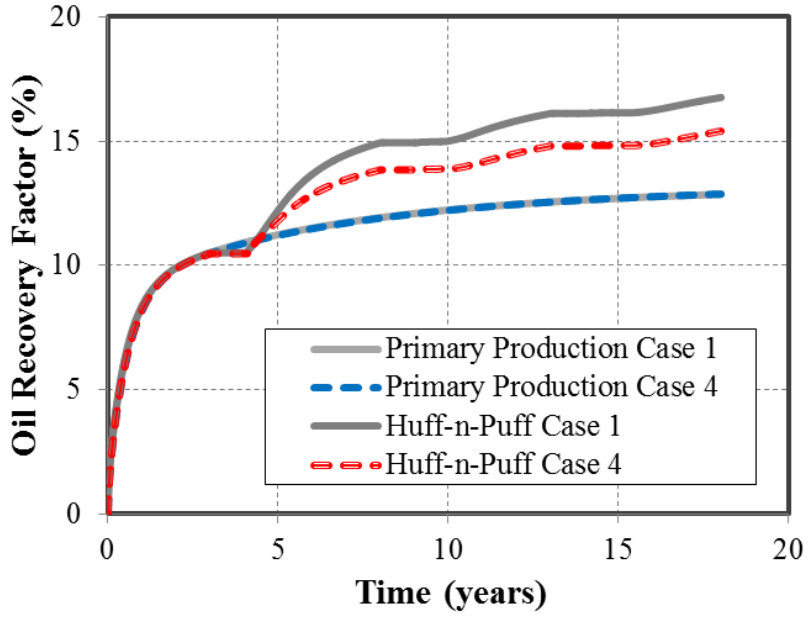

(b) Oil recovery factor curves for the primary production and Huff-n-Puff

Figure 4.9: Illustration of the fractures for case 4 and comparison of the oil recovery factors with the scenarios of reference case.

As shown in **Figure 4.10**, the Huff-n-Puff stimulated area for case 4 seems to be lower than the previous cases as a result of more serious interference between the fractures. In order to

quantitatively measure the interference degree, we calculated the CO_2-contacted area from the global CO_2 molecule distribution maps, which is defined as the area with a CO_2 mole fraction higher than 5%. The comparison of CO_2-contacted area for each case is summarized in the last column of **Table 4.4**.

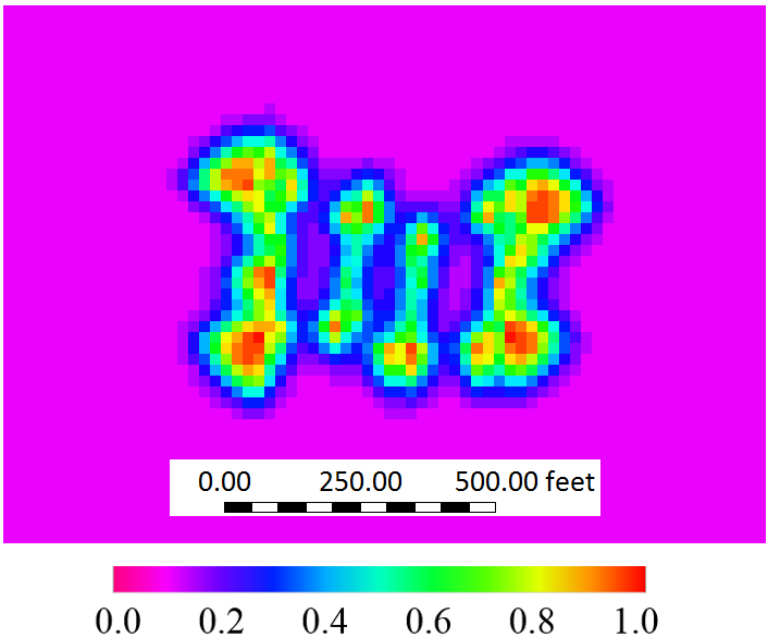

Figure 4.10: Map of global CO_2 molecule distribution after one year of injection of Huff-n-Puff treatment for case 4.

In addition, **Table 4.2** lists the oil recovery factor (RF) for primary production and the incremental RF after Huff-n-Puff for each case. The results show small differences of primary production but significant changes after Huff-n-Puff for different fracture geometries. We can notice that there is a consistent reduction in the incremental RF of CO_2 Huff-n-Puff as the fractures become shorter and closer to each other, and the CO_2-contacted area decreases as a result of the fracture interference. Case 4, which has the highest fracture complexity, has the lowest incremental oil recovery. This shows that characterizing the actual fracture geometry and accurately modeling well performance form this geometry play an important role in estimation of the additional oil

recovery after the Huff-n-Puff stimulation. The use of simple planar fractures to simplify the complex fractures might overestimate the CO_2-EOR effectiveness.

Case Number	RF Primary Production (%)	RF Huff-n-Puff (%)	Incremental RF (%)	CO_2-Contacted Area (×1000 ft^2)
Case 1	12.9	16.8	3.9	170.9
Case 2	12.8	15.7	2.9	160.9
Case 3	12.9	17.4	4.5	180.2
Case 4	12.8	15.4	2.6	152.6

Table 4.2: Summary of oil recovery factor (RF) of primary production and incremental RF after Huff-n-Puff for different cases.

4.3.2 Case Studies of CO_2 Flooding

For evaluation CO_2 flooding scenario, the same single-stage fracture geometries as CO_2 Huff-n-Puff scenario were considered, as shown in **Figure 4.11**. For these case studies, the simulation model was extended to include two horizontal wells with identical fracture geometries. The reservoir and fracture properties remain the same as those mentioned in **Tables 1** and **3**. The distance between two wells is fixed at 1,020 ft for each case. The CO_2 flooding scenario considers an initial period of primary production of 3 years for both wells. After that, one of the producing wells is converted to injector and used for CO_2 injection until the end of the production time (18 years in total). The cumulative CO_2 injection is comparable to the amount of the Huff-n-Puff scenario. The primary production simulated without CO_2 injection is used to measure the incremental oil recovery after CO_2 flooding.

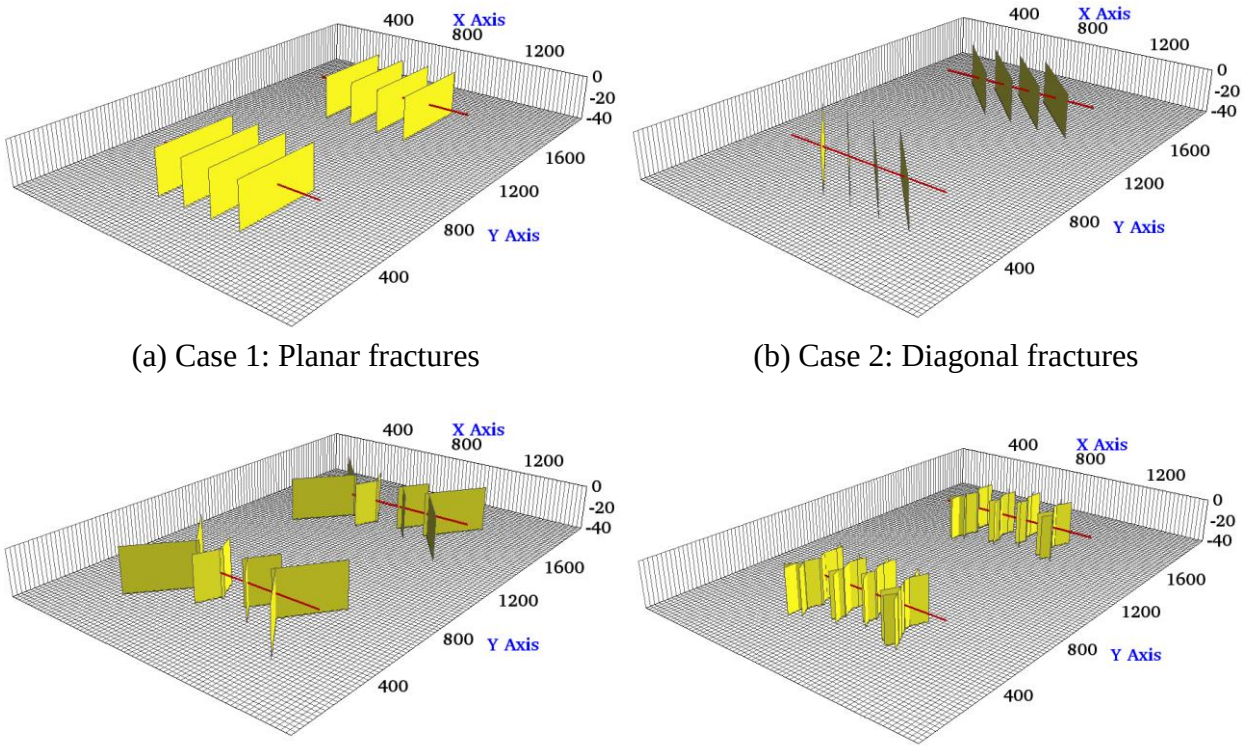

(a) Case 1: Planar fractures

(b) Case 2: Diagonal fractures

(c) Case 3: Reoriented fractures

(d) Case 4: Fracture networks

Figure 4.11: Illustration of the fracture geometries used for evaluation of CO_2 flooding scenario.

Figure 4.12 compares the oil recovery factor curves for these four cases. **Table 4.3** summarizes the oil RF of primary production and incremental RF after CO_2 flooding and CO_2-contacted area for each case at end of production. As it can be seen, the incremental RF of cases 1 and 4 is lower than that of cases 2 and 3. It can be noticed from the results that there is not a direct relationship between the increase in fracture complexity and the CO_2 flooding effectiveness. However, the incremental RFs are still in agreement to the area contacted by the CO_2 injected, even though there are some small divergences as it can be observed in cases 2 and 3. Case 2 shows a higher recovery than case 3 but it has a slightly lower CO_2 contacted area. Nonetheless, this can be expected since the average CO_2 concentration for the contacted area for case 3 is higher than case 2 (0.60 and 0.55, respectively).

For the flooding scenario a higher contacted area is due to the location of the fractures. More particularly, it is because of the dimensions of the cross sectional area covered by the fractures between the injector and producer. It can be clearly observed in the **Figure 4.11** that cases 2 and 3 have a larger extension in the x-axis direction (717 ft and 572 ft respectively), whereas cases 1 and 4 have a smaller extension (420 ft and 529 ft respectively). A longer extension of the fractures in the x-axis direction allows a higher CO_2-contacted area and therefore a higher incremental oil recoveries. For the CO_2 flooding, the fracture geometry is also a key factor affecting the estimation of the additional oil recovery. However, the inclusion of the complex fractures for the flooding scenario, unlike the Huff-n-Puff, does not necessary implies a negative effect in the incremental oil recovery.

Fracture Geometry	RF Primary Production (%)	RF Flooding (%)	Incremental RF (%)	CO_2-Contacted Area (M ft^2)
Case 1	12.93	31.81	18.88	1054.9
Case 2	12.92	35.43	22.51	1151.4
Case 3	13.04	34.79	21.75	1187.2
Case 4	12.91	32.91	20.00	1095.5

Table 4.3: Summary of oil RF of primary production and incremental RF after CO_2 flooding and CO_2-contacted area for each case.

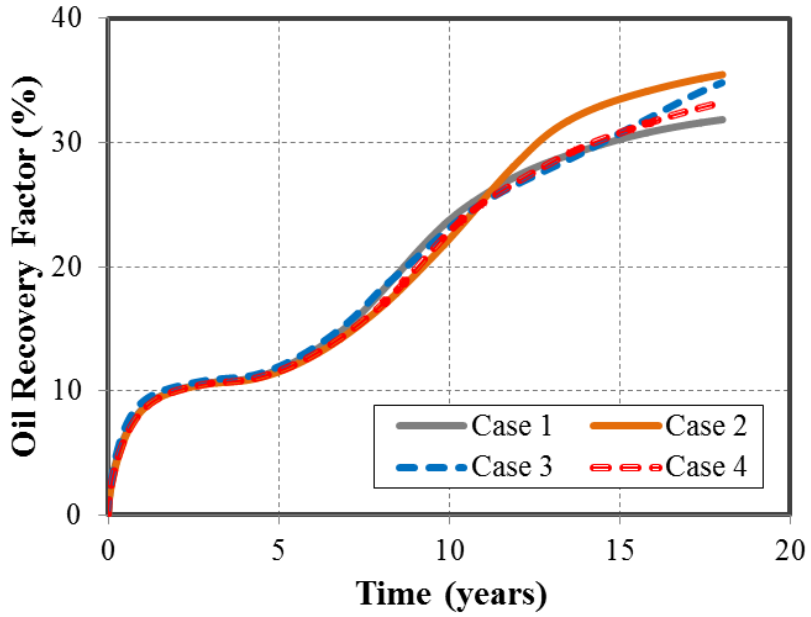

Figure 4.12: Comparison of oil recovery factor curves for four cases under CO_2 flooding scenario.

4.4 FIELD CASE STUDY

This section is devoted to analyze the influences of complex fracture geometries on well performance of CO_2 Huff-n-Puff and CO_2 flooding by building a field-scale reservoir model. Permeability values of 0.01 md and 0.1 md are considered to represent low and high permeability, which are within the range of permeability in the Bakken Formation. In addition, we also examine the effect of natural fractures on the production performance. For these purposes, the original model was extended to 5,240 ft × 2,680 ft × 40 ft (262 × 134 × 1 cells), which is able to model two horizontal wells with lateral length of 4,640 ft for each one and well spacing of 1,340 ft. Each well has 15 stages and each stage is assumed to have single effective hydraulic fracture. The fracture spacing is 290 ft. We performed both CO_2 Huff-n-Puff and CO_2 flooding simulations by considering four different geometries below:

- Planar fractures
- Non-planar fractures
- Non-planar fractures with one set of natural fractures
- Non-planar fractures with two sets of natural fractures

The first geometry evaluated, shown in **Figure 4.13(a**), only considers planar fractures, all of them have the same dimensions. The fracture half-length and fracture height are 334 ft and 40 ft, respectively. The fracture conductivity is 50 md-ft. For the second geometry, shown in **Figure 4.13(b)**, all the fractures are non-planar and have different dimensions. The fracture half-length varies from 194 to 445 ft. It should be noted that the total fractures length is kept the same for both fracture geometries. The fracture height and conductivity used are the same as the planar fractures. Both fracture geometries have the same fracture spacing of 290 ft.

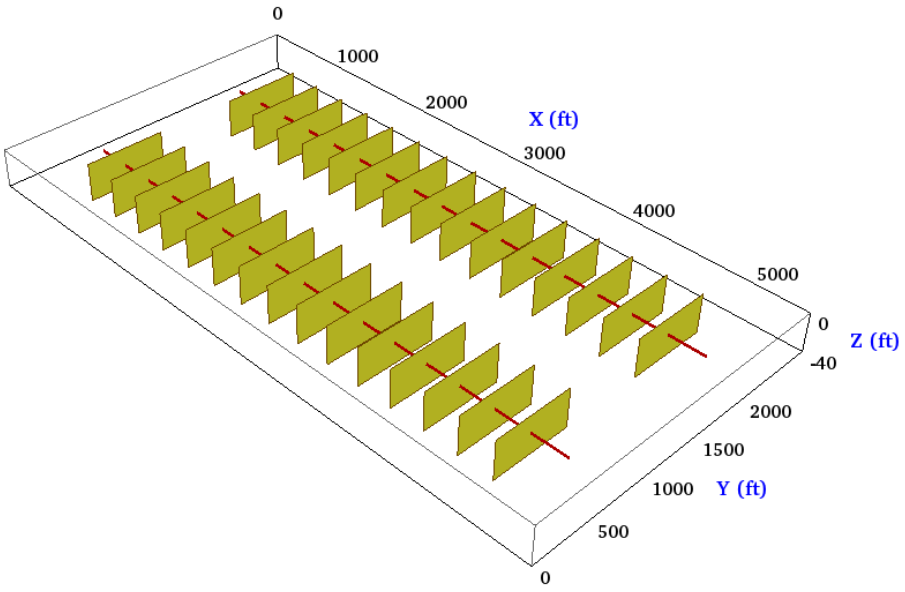

(a) Planar fractures with regular dimensions

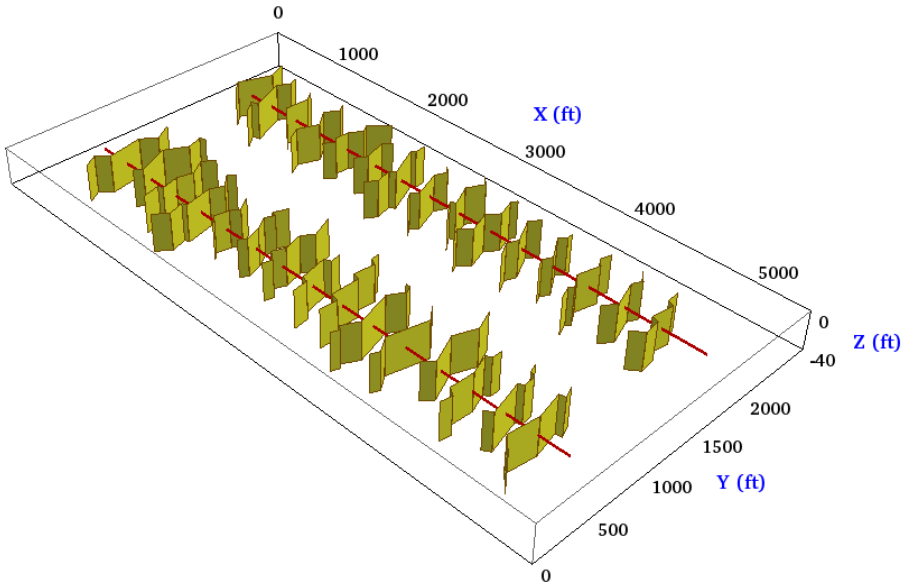

(b) Non-planar fractures with irregular dimensions

Figure 4.13: Illustration of two fracture geometries used for the field-scale CO2-EOR simulation.

Two additional cases were set in order to evaluate the impact of the natural fractures on the performance of the CO_2 Huff-n-Puff and CO_2 flooding. The first case includes a set of 300 natural fractures, which are randomly distributed with the assumption that their

orientations are parallel to the horizontal wellbore. These natural fractures have a length ranging from 100 to 200 ft, a height of 40 ft, and a fracture conductivity of 5 md-ft. The second case includes additional set of 300 natural fractures. They have the same dimensions and conductivity but the orientation trend is perpendicular to the horizontal wellbore. The illustration of the fracture sets is shown in **Figure 4.14**.

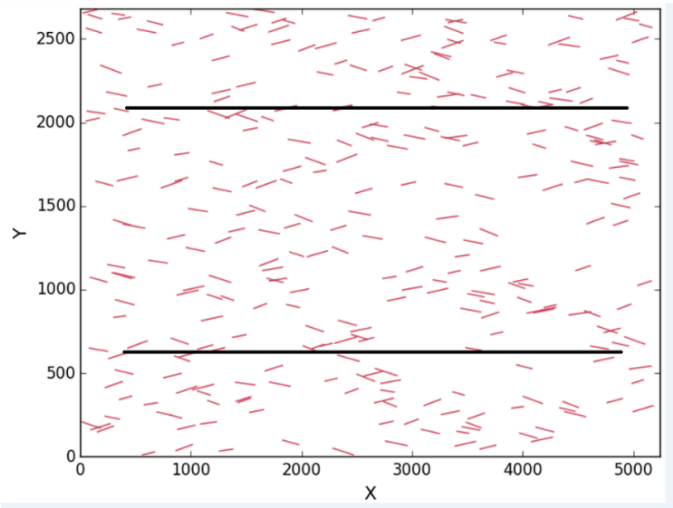

(a) One set of natural fractures parallel to the horizontal wellbores

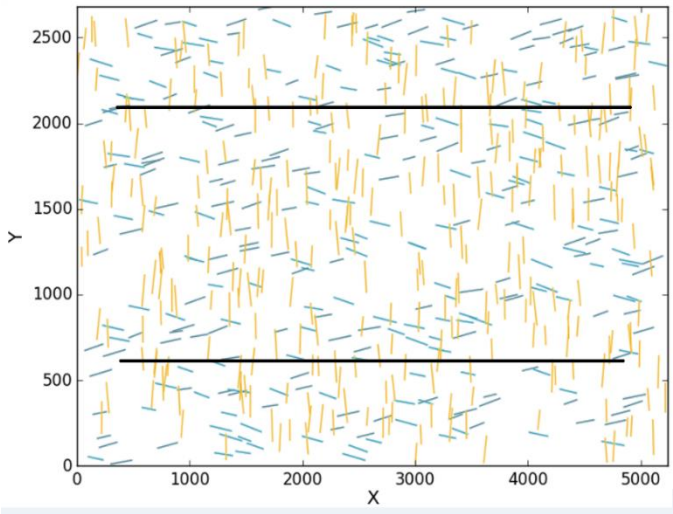

(b) Two sets of natural fractures: parallel (in blue) and orthogonal (in yellow) to the horizontal wellbores

Figure 4.14: Illustration of natural fracture sets used for the field-scale simulation.

The combination of modelling complex non-planar hydraulic fractures and natural fractures permits to model more realistic fracture networks. The two additional cases are presented in **Figure 4.15**

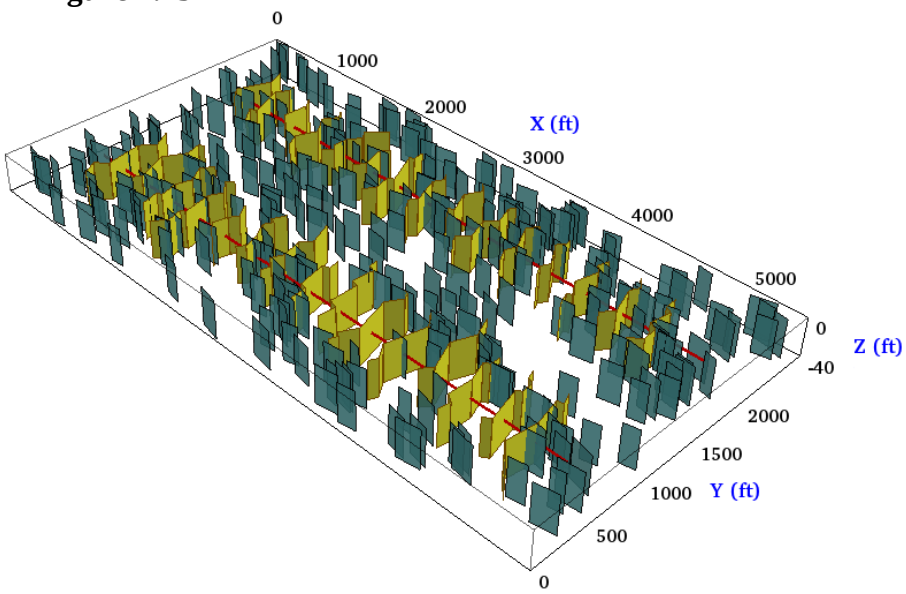

(a) One set of natural fractures parallel to the horizontal wellbore

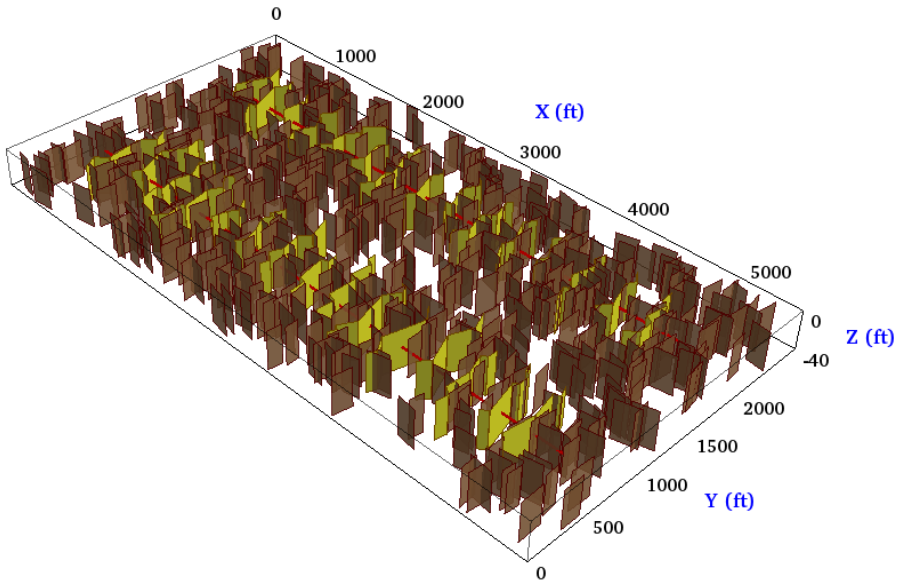

(b) Non-planar hydraulic fractures with two sets of natural fractures

Figure 4.15: Illustration of non-planar fracture geometries used for the field-scale simulation, taking into account the presence of natural fractures.

We performed the simulations for both CO_2 Huff-n-Puff and CO_2 flooding scenarios for the four cases aforementioned with two different values of matrix permeability, in order to evaluate the effect of the fracture geometry and the contribution from the natural fractures and its importance for the EOR recovery. The maximum and minimum values of matrix permeability considered for this study are 0.1 md and 0.01 md, which are in the range of tight formations.

4.4.1 CO_2 Huff-n-Puff for field-scale study

The simulations results of the CO_2 Huff-n-Puff scenario for both high and low permeabilities are shown in **Figures 4.16** and **4.17**. We can observe in **Figures 4.16(a)** and **4.17(a)** that there are no significant differences in the oil RF during primary production for four different fracture geometries regardless of high or low permeability. For the high permeability of 0.1 md, the maximum difference between four cases is less than 0.05%, and for the low permeability of 0.01 md the difference is about 0.4%. Similarly, the enhanced oil recovery at the high permeability, shown in **Figure 4.16(b),** reflects a small impact of the fracture geometries.

The incremental oil RF is about 8.3 % for the planar fractures and 7.7 % for the non-planar fractures when compared to the primary production. The previous results observed in the single stage study have shown a bigger difference because the fracture spacing used was 140 ft which is lower than the fracture spacing of 290 ft used for the field case. Then, the fracture interference decreases with increasing fracture spacing and there is only a small difference of 0.6% in the incremental oil RF between the planar and non-planar fracture geometries. In addition, the effect of natural fractures is also small. The incremental oil RF is 8.2% and 8.6% for one set and two sets of natural fractures, respectively.

On the other hand, the results at low permeability of 0.01 md, presented in **Figure 4.17(b)**, show a small difference (around 0.58%) in the incremental oil RF between the planar and non-planar geometries, but the difference becomes significant for the other two cases that include natural fractures. The incremental RF for the case with one set of natural fracture increases from 5.2% to 6.8% when compared to the non-planar fractures without natural fractures. Furthermore, the incremental RF for the case with two sets of natural fractures increases to 7.7%. Hence, the presence of natural fractures significantly impact the well performance of CO_2 Huff-n-Puff under the low permeability of 0.01 md. It can be implied that the natural fractures should be correctly included in the numerical model for simulating CO_2 Huff-n-Puff in some tight formations with low permeability and high density of natural fractures.

The previous observations can be verified by comparing CO_2 molecule distribution maps, as shown in **Figures 4.18** and **4.19**. The molecular fraction distribution maps of CO_2 presented in **Figures 4.18(a)** and **4.18(b)** show similar concentrations of CO_2 for the planar fractures and the non-planar fractures with 2 sets of natural fractures under high permeability of 0.1 md. However, it can be clearly noticed that under low permeability of 0.01 md, the non-planar fracture geometry with 2 sets of natural fractures [**Figure 4.19(a)]** has a higher concentration of CO_2 compared to the planar fractures [**Figure 4.19(b)],** especially for the values of around 0.6 displayed in cyan. Hence, the CO_2 distribution maps show that the performance of CO_2 Huff-n-Puff under the low permeability is more sensitive to the presence of natural fractures.

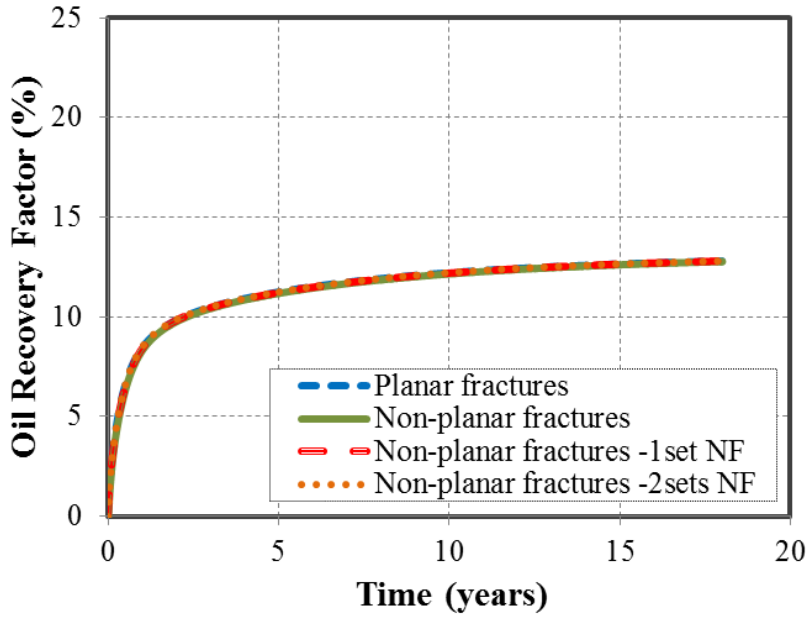

(a) Primary production under permeability of 0.1 md

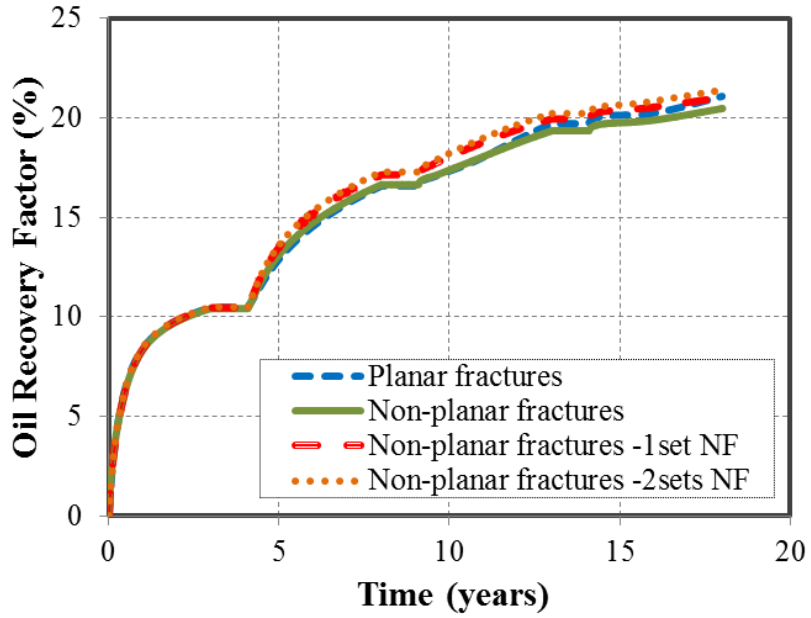

(b) CO_2 Huff-n-Puff under permeability of 0.1 md

Figure 4.16: Oil recovery factors for primary production and CO_2 Huff-n-Puff under matrix permeability of 0.1 md.

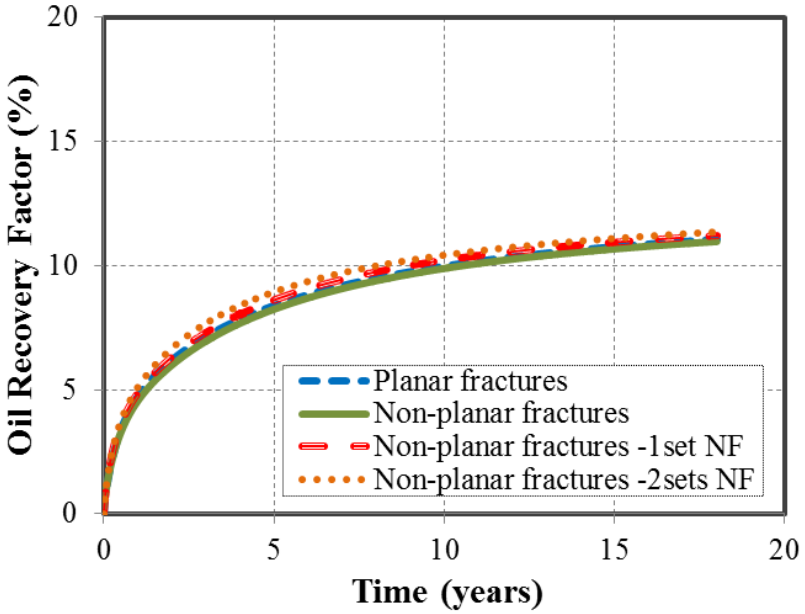

(a) Primary production under permeability of 0.01 md

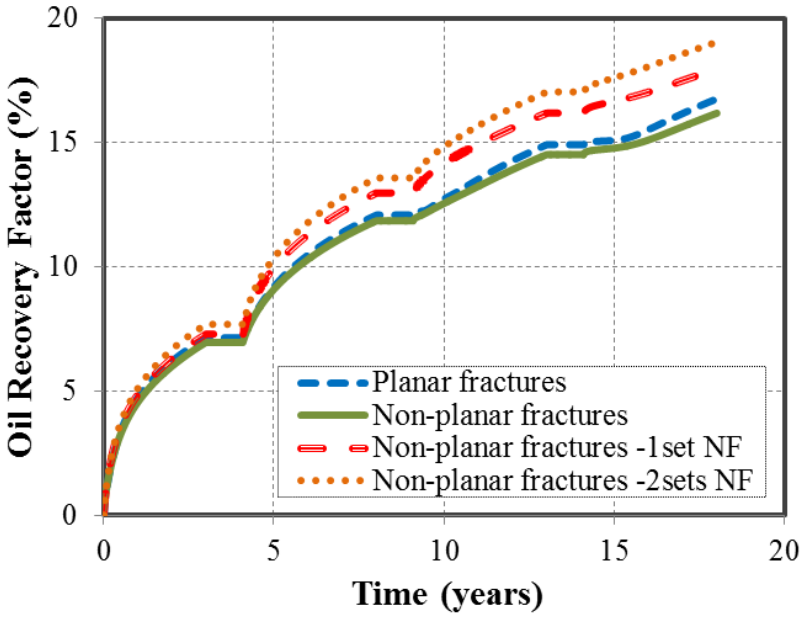

(b) CO_2 Huff-n-Puff under permeability of 0.01 md

Figure 4.17: Oil recovery factors for primary production and CO_2 Huff-n-Puff under matrix permeability of 0.01 md.

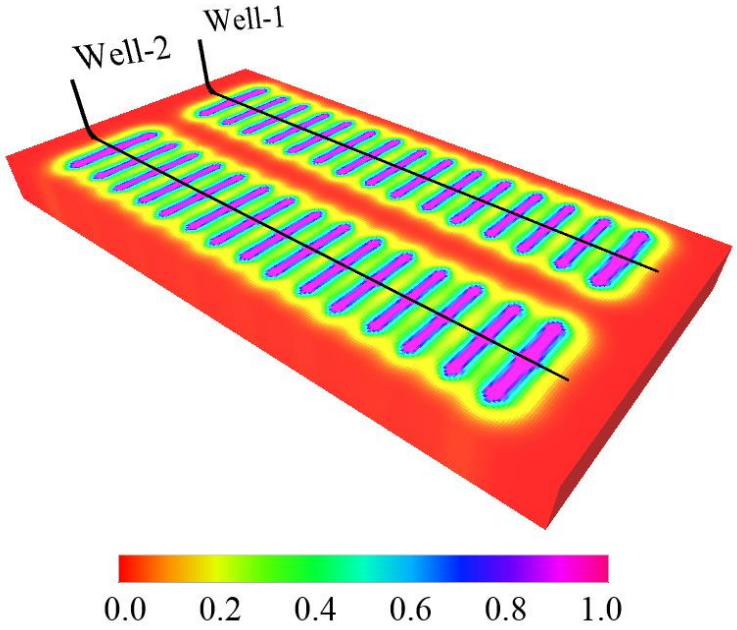

(a) Planar fractures without natural fractures under permeability of 0.1 md

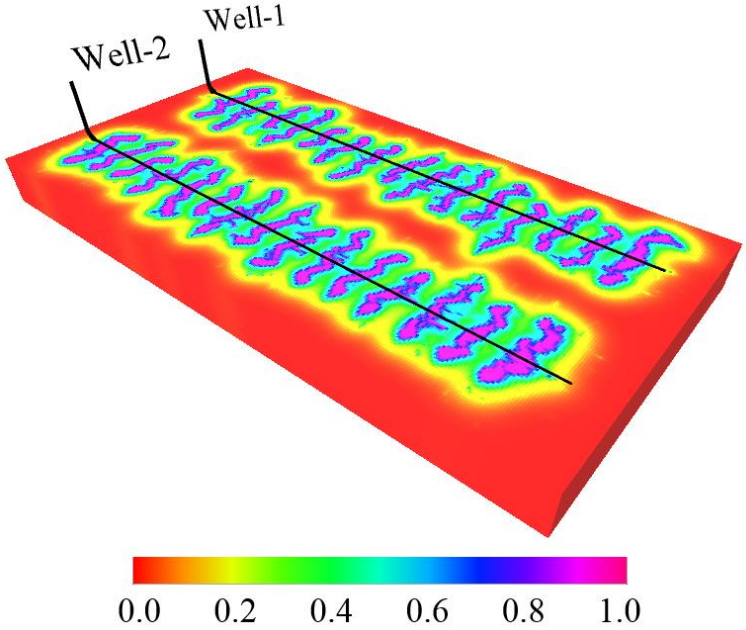

(b) Complex fracture networks with 2 sets of natural fractures under permeability of 0.1 md

Figure 4.18: Comparison of global CO_2 molecule distributions for the Huff-n-Puff scenario with and without natural fractures under high permeability after one year of CO_2 injection

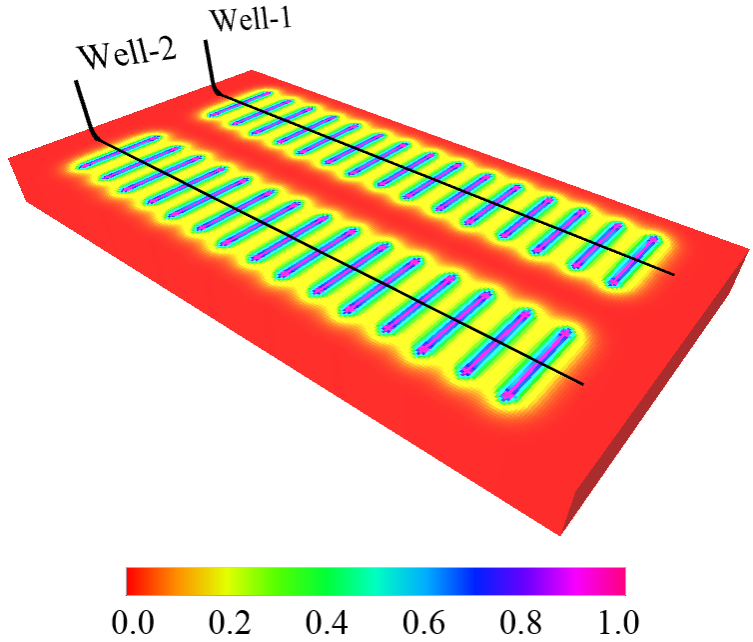

(a) Planar fractures without natural fractures under permeability of 0.01 md

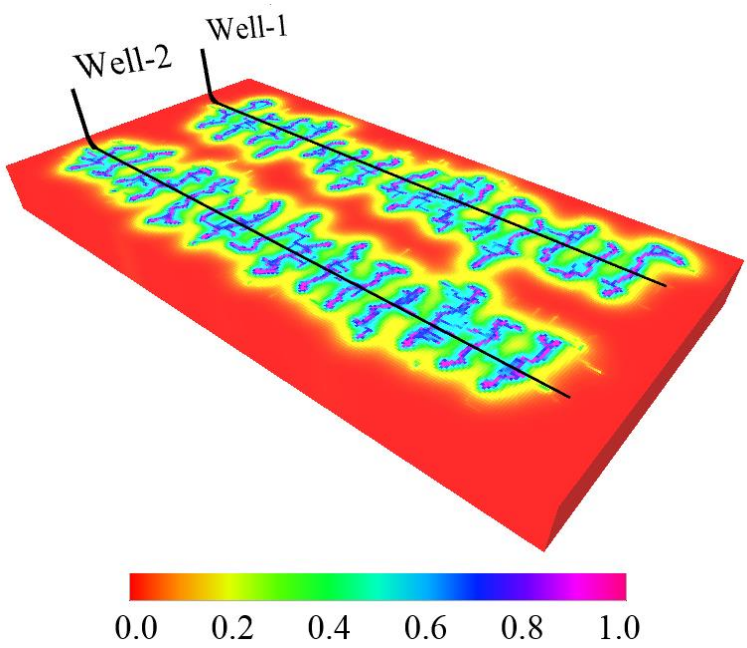

(b) Complex fracture networks with 2 sets of natural fractures under permeability of 0.01 md

Figure 4.19: Comparison of global CO_2 molecule distributions for the Huff-n-Puff scenario with and without natural fractures under low permeability after one year of CO_2 injection.

4.4.2. CO_2 flooding for field-scale study

Similarly, we performed the simulations for CO_2 flooding scenario and the results for both high and low permeabilities are shown in **Figures 4.20** and **4.21**, respectively. It can be seen that there is a small difference of primary recovery regardless of high or low permeability. **Figures 4.20(a)** and **4.20(b)** show that under the high permeability of 0.1 md, the non-planar fractures perform better than the planar fractures with an incremental oil RF of 21.2 % and 19.1 %, respectively. The effect of one set of natural fractures, which are parallel to the horizontal wellbore, is not significant and the incremental oil RF is similar to that obtained from the non-planar fractures without natural fractures (21.5% and 21.2%, respectively). Conversely, the addition of the second set of natural fractures, perpendicular to the horizontal wellbore, allows a higher incremental oil RF of 22.5%. This is because 2 sets of natural fractures improve the sweep efficiency better than the planar fractures, as shown in **Figures 4.21(a)** and **4.21(b)**.

For the low permeability of 0.01 md, **Figures 4.20(a)** and **4.20(b)** show that the flooding scenario is not favorable because the injected CO_2 cannot reach the production well (Well 1) due to the poor connectivity between two wells. The final recovery factors are lower than the primary production, which includes the production of both wells. However, it is important to notice that the non-planar fractures with 2 sets of natural fractures has a better performance compared to the other cases because the orientation of the second set of natural fractures improves the connectivity between two wells, **Figures 4.21(a)** and **4.19(b)**. The final oil RF for the case with 2 sets of natural fractures is 12%, while it is around 10.3% for the other cases.

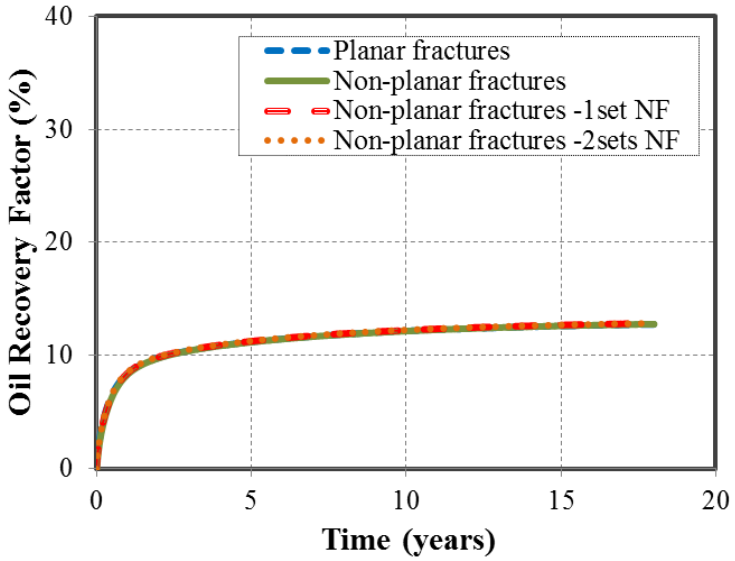

(a) Primary production under permeability of 0.1 md

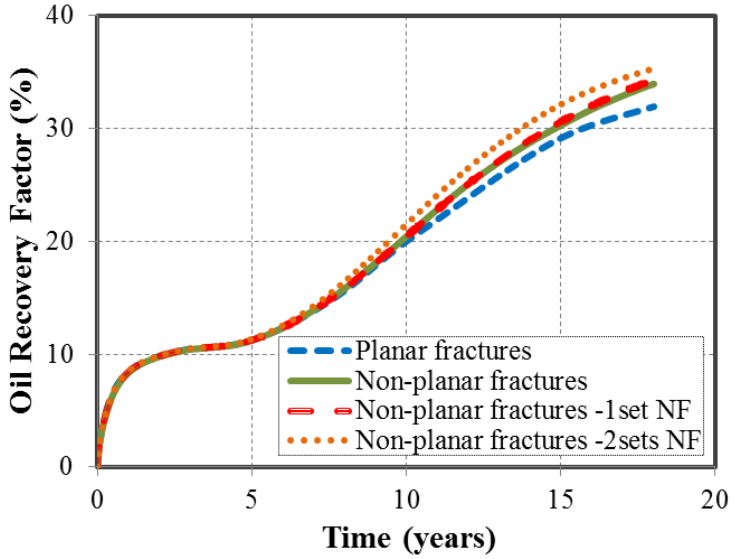

(b) CO_2 flooding permeability under permeability of 0.1 md

Figure 4.20: Oil recovery factors for primary production and CO_2 flooding under matrix permeability of 0.1 md.

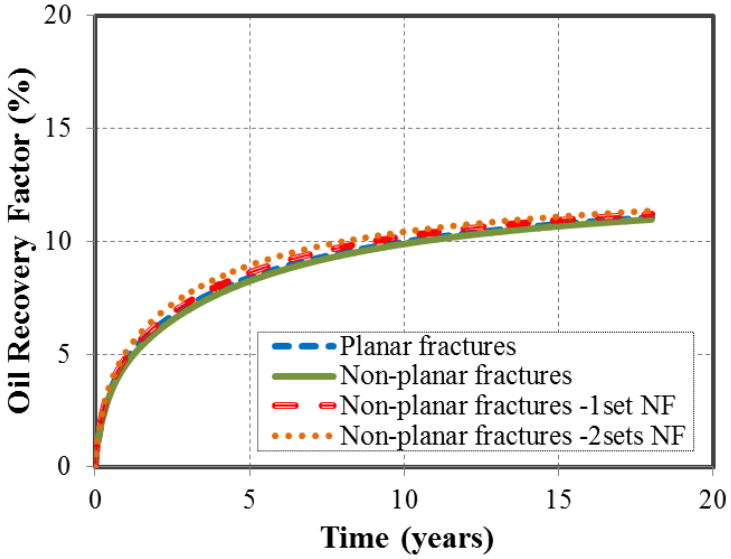

(a) Primary production under permeability of 0.01 md

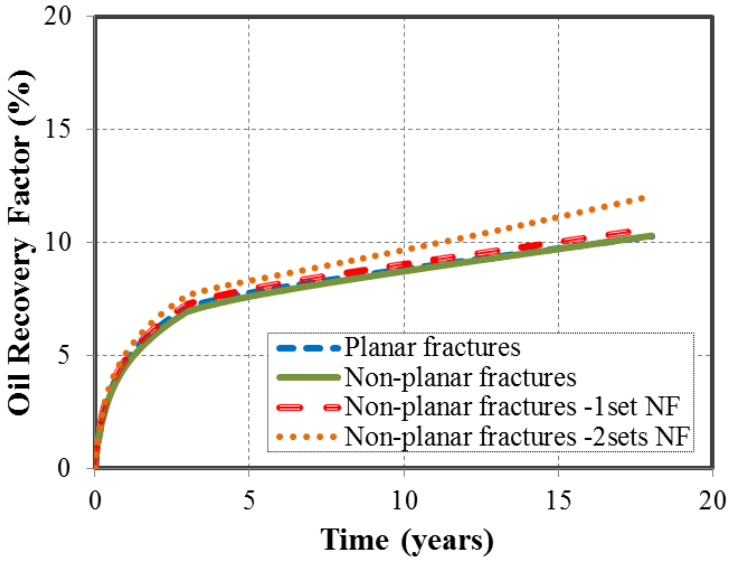

(b) CO_2 flooding under permeability of 0.01 md

Figure 4.21: Oil recovery factors for primary production and CO_2 flooding under matrix permeability of 0.01 md.

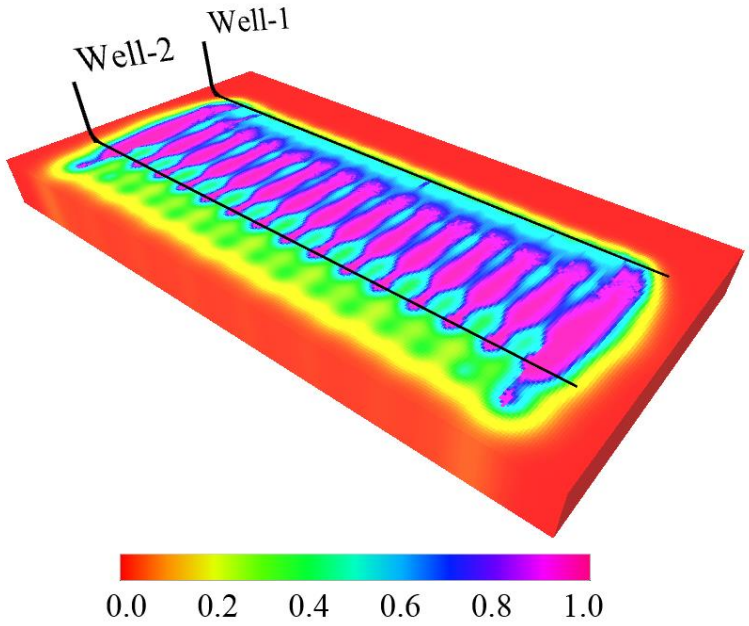

(a) Planar fractures without natural fractures, permeability: 0.1 md

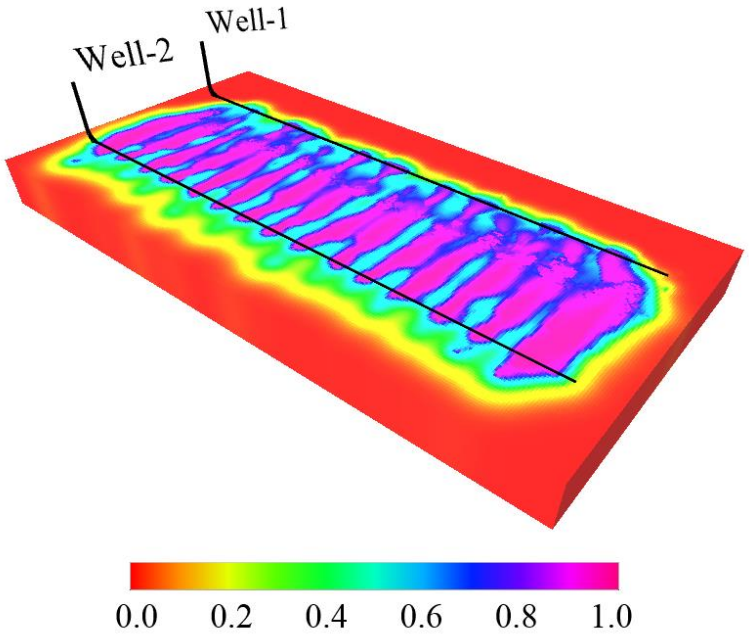

(b) Planar fractures without natural fractures, permeability: 0.01 md

Figure 4.22: Comparison of global CO_2 molecule distributions for the flooding scenario with and without natural fractures under high permeability after 15 years of CO_2 injection.

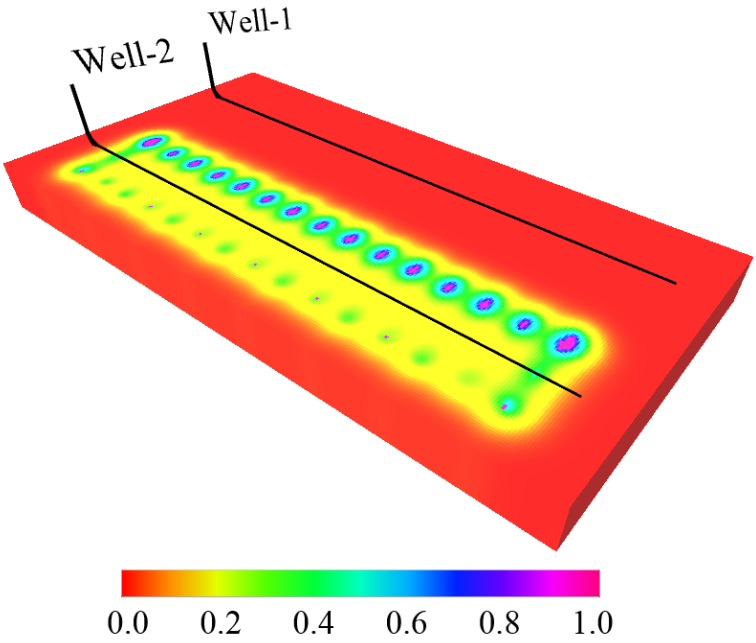

(a) Complex fracture networks with 2 sets of natural fractures, permeability: 0.1 md

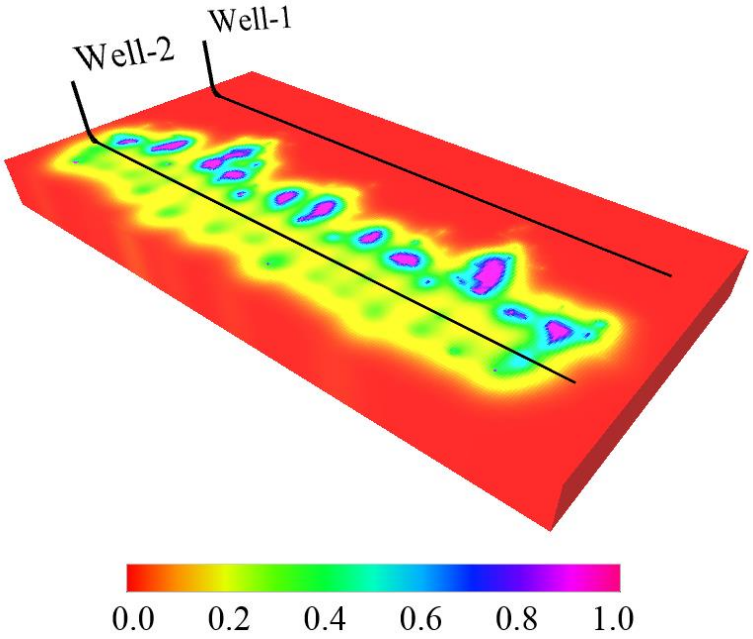

(b) Complex fracture networks with 2 sets of natural fractures, permeability: 0.01 md

Figure 4.23: Comparison of global CO_2 molecule distributions for the flooding scenario with and without natural fractures under low permeability after 15 years of CO_2 injection.

Hence, we can notice that the presence of natural fractures plays an important role in the production response of the CO_2-EOR for the cases with low permeability, and this is valid for both CO_2 injection scenarios.

Chapter 5: Conclusions and Recommendations for Future Work

5.1 CONCLUSIONS

In the first part of this study a field-scale numerical reservoir model was built to compare the well performance through CO_2 Huff-n-Puff and CO_2 flooding scenarios in the Middle Bakken Formation. The purpose of this study was to identify which scenario performs better under what reservoir and fracture conditions. We employed the DOE and RSM to perform a series of cases studies with four uncertain parameters including matrix permeability, well spacing, well pattern, and fracture half-length with a reasonable range based on the Middle Bakken Formation. The following conclusions can be drawn from this section:

- Based on sensitivity studies, the matrix permeability is the most significant parameter for the comparison of well performance between CO_2 Huff-n-Puff and CO_2 flooding, followed by well pattern and the interaction between fracture half-length and number of wells.

- The zipper well pattern performs better than the aligned well pattern regardless of CO_2 injection scenario.

- In the range of permeability from 0.001 md to 0.01md, the CO_2 Huff-n-Puff scenario performs better than CO_2 flooding scenario under the situations of appropriate number of wells (4 and 8 wells) and fracture half-length. When the number of wells and fracture half-length increase, the incremental oil recovery factor of CO_2 Huff-n-Puff increases due to the increasing contact fracture area.

- When the permeability ranges from 0.01 md to 0.1 md, the CO_2 flooding scenario performs better than CO_2 Huff-n-Puff for most situations, especially when the number

of wells is 6. An increase in number of wells does not necessarily lead to a higher incremental oil recovery factor due to the occurrence of early breakthrough of CO_2.

- The production lifetime is an important parameter to select the best injection strategy. For a shorter production time the flooding additional recovery decreases and the Huff-and-Puff injection show a higher additional recovery. For ta short production term of 8 years the injection the continuous flooding only shows a better performance for a matrix permeability higher than 0.05 md. and a well spacing of 6 wells per section or higher. For a lower number of wells per section and a lower permeability the Huff-and-Puff injection is the most suitable.

Subsequently, in the second part, a numerical compositional reservoir model was used to verify the EDFM methodology in the simulation of the CO_2 Huff-n-Puff. The verified model was used to evaluate the effects of different fracture geometries on well performance of CO_2-EOR process in the Bakken Formation for both single stage and multiple stages. For the field case study, the presence of natural fractures was considered. The following conclusions can be drawn from this study:

- The effectiveness of the CO_2 Huff-n-Puff is mainly determined by the fracture interference. Complex fracture geometries with a lower distance between the fractures are more sensitive to the fracture interference and therefore, the expected incremental oil recovery is low. As the complexity of the fracture increases the expected incremental recovery decreases. The planar fractures model is prone to overestimate the amount of additional oil recovery from CO_2 Huff-n-Puff.

- For the CO_2 flooding scenario the non-planar fractures do not show a negative effect in the EOR performance. It can improve the effectiveness of the flooding if the location

of the fractures turn into a higher contacted area, which depends on the configuration of the fractures.

- In the field-scale case study, the presence of natural fractures only represents a significant improvement of CO_2 Huff-n-Puff for the low permeability of 0.01 md. For all other cases, the oil recovery was higher if the natural fractures were present for both Huff-n-Puff and flooding scenarios, since the natural fractures allow to increase the CO_2-contacted area.

- The CO_2 flooding is not favorable for low permeability of 0.01 md due to poor connectivity between two wells, while it is suitable for high permeability of 0.1 md. The CO_2 Huff-n-Puff performs better than the CO_2 flooding for low permeability of 0.01 md.

5.2 RECOMMENDATIONS FOR FUTURE WORK

- Although the oil fluid properties cannot be considered as design parameters, their effects on the production performance of the CO_2-based EOR should be evaluated to understand the role of the fluid in the selection of the best injection strategy.

- This study can be extended to analyze the effects of different types of gas injection including N_2, CH_4, and their mixture on EOR effectiveness in tight oil formations.

- In this study the segregational effect due to gravity did not show a significant difference in the results due to a small reservoir thickness of 40 ft. However, this effect should be significant as the reservoir thickness increases, which should be investigated in our future study for some cases with a large reservoir thickness. In addition, the dipping angle of the fractures will become important for the large reservoir thickness, which also needs further research.

Bibliography

Adekunle, O.O., Hoffman, B.T., 2014. Minimum Miscibility Pressure Studies in the Bakken. Presented at the SPE Improved Oil Recovery Symposium, Tulsa, Oklahoma, USA, April 12, 2014. SPE-169077-MS. http://doi.org/10.2118/169077-MS.

Alharthy, N., Teklu, T., Kazemi, H., et al., 2015. Enhanced Oil Recovery in Liquid-Rich Shale Reservoirs: Laboratory to Field. Presented at the SPE Annual Technical Conference and Exhibition, Houston, Texas, USA, September 28, 2015. SPE-175034-MS. http://doi.org/10.2118/175034-MS.

Ajayi, B., Aso, I.I., Terry, I.J., et al., 2013. Stimulation Design for Unconventional Resource. *Oilfield Review* **25**: 34–46.

American Petroleum Institute. 2015. *Energizing America: Facts for addressing Energy Policy.* API-Digital Media.

Bardon, C., Corlay, P., Longeron, D., et al., 1994. CO_2 Huff-n-Puff Revives Shallow Light-Oil-Depleted Reservoirs. *SPE Reservoir Engineering* **9**: 92–100. SPE-22650-PA. http://doi.org/10.2118/22650-PA.

Cavalcante Filho, J.S.A., Shakiba, M., Moinfar, A., Sepehrnoori, K., 2015. Implementation of a Preprocessor for Embedded Discrete Fracture Modeling in an IMPEC Compositional Reservoir Simulator. Presented at the SPE Reservoir Simulation Symposium, Huston, Texas, USA, February 23-25. SPE-173289-MS. http://doi.org/10.2118/173289-MS

Chen, C., Balhoff, M.T., Mohanty, K.K., 2013. Effect of Reservoir Heterogeneity on Improved Shale Oil Recovery by CO_2 Huff-n-Puff. Presented at the SPE Unconventional Resources Conference-USA, The Woodlands, Texas, USA, April 10, 2013. SPE-164553-MS. http://doi.org/10.2118/164553-MS.

CMG-GEM. GEM User's Guide, Computer Modeling Group Ltd, 2015.

CMG-WinProp. WinProp User's Guide, Computer Modeling Group Ltd, 2015.

Ghaderi, S.M., Clarkson, C.R., Chen, Y., 2012. Optimization of WAG Process for Coupled CO_2 EOR-Storage in Tight Oil Formations: An Experimental Design Approach. Presented at the SPE Canadian Unconventional Resources Conference, Calgary, Alberta, Canada, November 30, 2012. SPE-161884-MS. http://doi.org/10.2118/161884-MS.

Ghaderi, S.M., Clarkson, C.R., Kaviani, D., 2011a. Investigation of Primary Recovery in Tight Oil Formations: A Look at the Cardium Formation, Alberta. Presented at the Canadian Unconventional Resources Conference, Calgary, Alberta, Canada, November 15, 2011. SPE-148995-MS. http://doi.org/10.2118/148995-MS.

Ghaderi, S.M., Clarkson, C.R., Kaviani, D., 2011b. Evaluation of Recovery Performance of Miscible Displacement and WAG Processes in Tight Oil Formations. Presented at the SPE/EAGE European Unconventional Resources Conference and Exhibition, Vienna, Austria, November 20, 2011. SPE-152084-MS. http://doi.org/10.2118/152084-MS.

Ghomian, Y., 2008. *Reservoir simulation studies for coupled CO_2 sequestration and enhanced oil recovery*. PhD Dissertation, University of Texas at Austin, Austin, Texas (May 2008).

Fisher, M.K., Heinze, J.R., Harris, C.D. et al. 2004. Optimizing Horizontal Completion Techniques in the Barnett Shale Using Microseismic Fracture Mapping. Presented at the SPE Annual Technical Conference and Exhibition, Houston, Texas, 26-29 September. SPE-90051-MS. http://doi.org/10.2118/90051-MS.

Hawthorne, S.B., Gorecki, C.D., Sorensen, J.A., et al., 2013. Hydrocarbon Mobilization Mechanisms from Upper, Middle, and Lower Bakken Reservoir Rocks Exposed to CO. Presented at the SPE Unconventional Resources Conference Canada, Calgary, Alberta, Canada, November 5, 2013. SPE-167200-MS. http://doi.org/10.2118/167200-MS.

Hoffman, B.T., Shoaib, S., 2013. CO_2 Flooding to Increase Recovery for Unconventional Liquids-Rich Reservoirs. *Journal of Energy Resources Technology* **136**: 022801.1–022801.10. http://doi.org/10.1115/1.4025843.

Holm, L. W. 1987. Evolution of the carbon dioxide flooding processes. *Journal of Petroleum Technology* **39**: 1337-1342. http://doi.org/10.2118/17134-PA

Hoteit, H., Firoozabadi, A. 2006. Compositional modeling of discrete-fractured media without transfer dunctions by the discontinuous Galerkin and mixed methods. *SPE Jouranl*. **11** (3): 341-352. SPE-90277-PA. http://doi.org/10.2118/90277-PA.

Hui, M.-H., Mallison, B. T., Fyrozjaee, M. H. et al. 2013. The upscaling of discrete fracture models for faster, coarse-scale simulations of IOR and EOR processes for fractured reservoirs. Presented at the SPE Annual Technical Conference and Exhibition, New Orleans, Louisiana, USA. September 30-2 October2. SPE-166075-MS. http://doi.org/10.2118/166075-MS

Jarrell, P.M., Fox, C.E., Stein, M.H., 2002. *Practical aspects of CO_2 flooding*, 1st printing. ed, SPE monograph series. Richardson, TX.

Kiefer, J., Wolfowitz, J., 1959. Optimum Designs in Regression Problems. *The Annals of Mathematical Statistics* **30**(2): 271-294.

Kovscek, A.R., Tang, G.-Q., Vega, B., 2008. Experimental Investigation of Oil Recovery From Siliceous Shale by CO_2 Injection. Presented at the SPE Annual Technical Conference and Exhibition, Denver, Colorado, USA, September 21, 2008. SPE-115679-MS. http://doi.org/10.2118/115679-MS.

Kurtoglu, B., Sorensen, J. A., Braunberger, J., Smith, S., and Kazemi, H. 2013. Geologic Characterization of a Bakken Reservoir for Potential CO_2 EOR. Presented at the Unconventional Resources Technology Conference, Denver, Colorado, USA, 12-14 August. SPE 168915-MS. http://doi.org/10.2118/168915-MS.

Lashgari, H. 2014. *Development of a four-phase thermal-chemical reservoir simulator for heavy oil*. PhD Dissertation, University of Texas at Austin, Austin, Texas (December 2014).

Li, L., Lee. S. 2008. Efficient field-scale simulation of black oil in naturally fractured reservoir through discrete fracture networs and homogeneized media. *SPE Reservoir Evaluation & Engineering*, **11**(4). SPE-103901-PA. http://doi.org/10.2118/103901-PA

Liu, G., Sorensen, J.A., Braunberger, J.R., et al., 2014. CO_2-Based Enhanced Oil Recovery from Unconventional Reservoirs: A Case Study of the Bakken Formation. Presented at the SPE Unconventional Resources Conference, The Woodlands, Texas, USA, April 1, 2014. SPE-168979-MS. http://doi.org/10.2118/168979-MS.

Maxwell, S. C., Weng, X., Kresse, O., and Rutledge, J. 2013. Modeling Microseismic Hydraulic Fracture Deformation. Presented at the SPE Annual Technical Conference and Exhibition, New Orleans, Louisiana, USA, 30 September-2 October. SPE 166312-MS. http://doi.org/10.2118/166312-MS.

Moinfar, A., Varavei, A., Sepehrnoori, K., Johns, R.T., 2014. Development of an Efficient Embedded Discrete Fracture Model for 3D Compositional Reservoir Simulation in Fractured Reservoirs. *SPE Journal* **19**, 289–303. SPE-154246-PA. http://doi.org/10.2118/154246-PA

Myers, R.H., Montgomery, C.D., Anderson-Cook, C., 2008. Response Surface Methodology: Process and Product Optimization Using Designed Experiments, third edition. New York: John Wiley & Sons.

Nghiem, L. X., Kohse, B. F., and Sammon, P. H. 2000. Compositional Simulation of the Vapex Process. Presented at the Canadian International Petroleum Conference, Calgary, Canada, 4-8 June. PETSOC 2000-034. http://doi.org/10.2118/2000-034

Nojabaei, B., Johns, R.T., Chu, L., 2013. Effect of Capillary Pressure on Phase Behavior in Tight Rocks and Shales. *SPE Reservoir Evaluation & Engineering* **16**, 281–289. http://dx.doi.org/10.2118/159258-PA

Ramirez Salazar, J.E., 2009. *Coupled CO_2 sequestration and enhanced oil recovery optimization using experimental design and response surface methodology*. MS Thesis, University of Texas at Austin, Austin, Texas (May 2009).

Reid, R. C., Frautsnitz, J. M., and Sherwood, T. K. 1977. *The properties of gases and liquids*. 3rd Edition, New York, McGraw-Hill.

Rubin, B., 2010. Accurate Simulation of Non Darcy Flow in Stimulated Fractured Shale Reservoirs. Presented at the SPE Western Regional Meeting, Anaheim, California, USA, May 27, 2010. SPE-132093-MS. http://doi.org/10.2118/132093-MS.

Sanchez Rivera, D., 2014. *Reservoir simulation and optimization of CO_2 huff-and-puff operations in the Bakken Shale*. MS Thesis, University of Texas at Austin, Austin, Texas (August 2014).

Sheng, J.J., 2015. Enhanced oil recovery in shale reservoirs by gas injection. *Journal of Natural Gas Science and Engineering* **22**: 252–259. http://doi.org/10.1016/j.jngse.2014.12.002.

Shoaib, S., Hoffman, B.T., 2009. CO_2 Flooding the Elm Coulee Field. Presented at the SPE Rocky Mountain Petroleum Technology Conference, Denver, Colorado, USA, April 14, 2009. SPE-123176-MS. http://doi.org/10.2118/123176-MS.

Sigmund, P.M., 1976. Prediction of Molecular Diffusion at Reservoir Conditions. Part II - Estimating the Effects of Molecular Diffusion and Convective Mixing In Multicomponent Systems. *Journal of Canadian Petroleum Technology* **15**: 53-62. http://doi.org/10.2118/76-03-07.

Sigmund, P.M., Kerr, W., MacPherson, R.E., 1984. A Laboratory and Computer Model Evaluation of Immiscible CO_2 Flooding in a Low-Temperature Reservoir. Presented at the SPE Enhanced Oil Recovery Symposium, Tulsa, Oklahoma, USA, April 15-18, 1984. SPE-12703-MS. http://doi.org/10.2118/12703-MS.

Song, C., Yang, D., 2013. Performance Evaluation of CO_2 Huff-n-Puff Processes in Tight Oil Formations. Presented at the SPE Unconventional Resources Conference Canada, Calgary, Alberta, Canada, November 5, 2013. SPE 167217-MS. http://doi.org/10.2118/167217-MS.

Sorensen, J.A., Braunberger, J.R., Liu, G., et al., 2015. Characterization and Evaluation of the Bakken Petroleum System for CO Enhanced Oil Recovery. Presented at the Unconventional Resources Technology Conference, San Antonio, Texas, USA, July 20, 2015. SPE 178659-MS. http://doi.org/10.2118/178659-MS.

Stalkup, F. I. 1987. Displacement Behavior of the Condensing/Vaporizing Gas Drive Process. Presented at the SPE Annual Technical Conference and Exhibition, Dallas, Texas, USA, 27-30 September. SPE 16715-MS. http://doi.org/10.2118/16715-MS.

Stat-Ease. Design Expert tutorial, 2015.

U.S. Energy Information Administration. 2013. *Early Release Overview*. http://www.eia.gov/forecasts/aeo/er/pdf/0383er%282013%29.pdf.

U.S. Energy Information Administration. 2015. *US Crude Oil and Natural Gas Proved Reserves, 2014*. EIA Independent Statistics and Analysis.

Wan, T., Yang, Y., Sheng J.J., 2014. Comparative Study of Enhanced Oil Recovery Efficiency by CO_2 Injection and CO_2 Huff-n-Puff in Stimulated Shale Oil

Reservoirs. Presented at AICHE annual meeting, Atlanta, Georgia, USA, November 17, 2014.

Wan, T., 2015. *Investigation of EOR performance in shale oil reservoirs by cyclic gas injection.* PhD Dissertation, Texas Tech University, Lubbock, Texas (May 2015).

Wang, X., Luo, P., Er, V., et al., 2010. Assessment of CO_2 Flooding Potential for Bakken Formation, Saskatchewan. Presented at the Canadian Unconventional Resources and International Petroleum Conference, Calgary, Alberta, Canada, January 19, 2010. SPE-137728-MS. http://doi.org/10.2118/137728-MS.

Warpinski, N. R., Mayerhofer, M. J., Vincent et al. 2009. Stimulating Unconventional Reservoirs: Maximizing Network Growth While Optimizing Fracture Conductivity. *Journal of Canadian Petroleum Technology* **48**: 39–51. SPE-114173-PA. http://doi.org/10.2118/114173-PA.

Wu, K., and Olson, J.E., 2015. Simultaneous Multi-Frac Treatments: Fully Coupled Fluid Flow and Fracture Mechanics for Horizontal Wells. *SPE Journal*, **20**: 337-346. http://doi.org/10.2118/167626-STU

Wu, R., Kresse. O., Weng, X., Cohen, C., and Gu, H., 2012. Modeling of Interaction of Hydraulic Fractures in Complex Fracture Networks. Presented at the SPE Hydraulic Fracturing Technology Conference, The Woodlands, Texas, USA, February 6-8. SPE 152052-MS. http://doi.org/10.2118/152052-MS

Xu, G., and Wong, S.W., 2013. Interaction of Multiple Non-Planar Hydraulic Fractures in Horizontal Wells. Presented at the International Petroleum Technology Conference, Beijing, China, March 26-28. IPTC-17043. http://doi.org/ 10.2523/17043-MS

Xu, Y., 2015. *Implementation and application of the embedded discrete fracture model (EDFM) for reservoir simulation in fractured reservoirs.* MS Thesis, University of Texas at Austin, Austin, Texas (December 2015).

Yu, W., Lashgari, H., Sepehrnoori, K., 2014. Simulation Study of CO_2 Huff-n-Puff Process in Bakken Tight Oil Reservoirs. Presented at the SPE Western North American and Rocky Mountain Joint Meeting, Denver, Colorado, USA, April 17, 2014. SPE-169575-MS. http://doi.org/10.2118/169575-MS.

Yu, W., Sepehrnoori, K., 2014. An Efficient Reservoir-Simulation Approach to Design and Optimize Unconventional Gas Production. *Journal of Canadian Petroleum Technology* **53**(2): 109-121. http://dx.doi.org/10.2118/165343-PA.

Yu, W., 2015. *Developments in Modeling and Optimization of Production in Unconventional Oil and Gas Reservoirs*. PhD Dissertation, University of Texas at Austin, Austin, Texas (May 2015).

Yu, W., Lashgari, H.R., Wu, K., et al., 2015. CO_2 Injection for Enhanced Oil Recovery in Bakken Tight Oil Reservoirs. *Fuel* **159**: 354–363. http://doi.org/10.1016/ j.fuel.2015.06.092.